COPERNICUS
MARINE ENVIRONMENT MONITORING SERVICE

QUALITY INFORMATION DOCUMENT

North West European Shelf Production Centre NWSHELF_MULTIYEAR_PHY_004_009

Issue: 5.2

Contributors: Richard Renshaw, Sarah Wakelin, Inga Golbeck, Enda O'Dea

Approval date by the CMEMS product quality coordination team: 01/12/2021

CHANGE RECORD

When the quality of the products changes, the QuID is updated and a row is added to this table. The third column specifies which sections or sub-sections have been updated. The fourth column should mention the version of the product to which the change applies.

Issue	Date	§	Description of Change	Author	Validated By
1.0	January 2014	All	Creation of the document for V4.0	Sarah Wakelin	Ed Blockley
2.0	December 2014	All	Addition of biological product assessment (BIO_004_011)	Robert McEwan	Ed Blockley
2.1	February 2015	All	Revision after acceptance V5		Ed Blockley
2.2	13/03/2015	I.2, II	Warning remarks after evidence of 004_011 interannual nutrient drifts		Ed Blockley
2.3	01/05/2015	all	Change format to fit CMEMS graphical rules		L. Crosnier
3.0	21/01/2016	all	Update for V2 (time series extension to 2014 and addition of MLD)	Sarah Wakelin, Jon Tinker	Marina Tonani
3.0	01/04/2016	all	Revision after V2 AR	Marina Tonani	Marina Tonani
4.0	06/08/2018	all	New version for Copernicus V4	Richard Renshaw, Sarah Wakelin, Enda O'Dea, Jon Tinker, Marina Tonani	Ina Lorkowsky
4.1	26/02/2019	V	Text added explaining reanalysis extensions beyond 2016	Richard Renshaw	
4.2	19/04/2019	III,V	Text added to explain updates of reanalysis beyond 2017	Richard Renshaw	Marina Tonani
5.0	04/09/2020		Update for V5 reanalysis	Richard Renshaw Sarah Wakelin Inga Golbeck Enda O'Dea	Marina Tonani

Issue	Date	§	Description of Change	Author	Validated By
5.1	15/02/2021	all	RAN extension to June 2020 Add interim product INT	Richard Renshaw Sarah Wakelin	Marina Tonani
5.2	03/09/2021		Update MME (temperature & salinity) Add hourly verification	Tabea Rebekka Panteleit Richard Renshaw	Marina Tonani

Table of contents

I EXECUTIVE SUMMARY

I.1 Products covered by this document

NWSHELF_MULTIYEAR_PHY_004_009: The physical part of a North-West European Shelf Reanalysis (version 5) performed at ~7 km resolution, with monthly interim updates. Comparisons are made to the previous North-West European Shelf reanalysis NORTHWESTSHELF_REANALYSIS_PHYS_004_009, version 4.

I.2 Summary of the results

The quality of the NWS reanalysis simulation NWSHELF_MULTIYEAR_PHY_004_009 version 5 (V5) from 01/01/1993 to 31/12/2019 has been assessed by comparison with observations. Results from the previous version of the reanalysis (V4) covering 01/01/1992 to 31/12/2018, are included for validation purposes.

Results for V5 relative to V4 are a mix of positive and negative. For temperature (IV.1), the generally cold bias of V4 for the Norwegian Sea has been reduced, and for the deeper ocean South of 50°N the warm bias of V4 becomes a slightly cold bias in V5. The cold bias in the southern Irish Sea and the warm bias in the southern North Sea are both larger. For salinity (IV.2), the fresh bias above 80 m in the Norwegian Sea that occurred in V4 persists in V5. However, V5 has improved on the isolated regions of fresh biases west of 10°W that occurred in V4.

The results for the AMM7 V5 reanalysis are summarised below.

Temperature: V5 biases are generally smaller than ±0.5°C at all depths over the North West Shelf. Off the Shelf, biases are similarly small except for in the Norwegian Sea, where cold biases up to 2°C are seen between 30 and 300 m depth, and below 2000 m in the Bay of Biscay, where temperatures are up to 1.5°C too warm. Correlations between V5 and mooring data are generally greater than 0.98, with V5 representing the annual temperature cycle well.

Salinity: In the top 30 m biases are generally of magnitude less than ±0.5 PSU whilst below 30 m depth they are less than ±0.1 PSU. In the Norwegian Trench and the Irish and Celtic Seas, V5 is typically too saline. In the Norwegian Sea surface and near-surface waters are too fresh.

Currents: Comparison with climatology at 15 m depth shows that the reanalysis simulation reproduces major current systems in the region. Hourly surface currents show good agreement with radar data.

Tidal analysis: The M2 constituent of tidal elevation has RMSD (root mean square difference) of 10.6 cm for amplitude and 14° for phase. The amplitude is underestimated in the Irish Sea and off the coast of southern England, but over-estimated in large tidal areas such as the Bristol Channel and other parts of the coast of the UK. The phase error is largest in the Southern Bight and German Bight, south coast of England and through the North Channel between Scotland and Northern Ireland.

Mixed layer depth: Over the North-West Shelf, biases overall are typically less than 0.5m and RMS differences average ~15 m. V5 MLD is generally too deep in Winter, too shallow in Summer, compared to observations. The V5 MLDs show good spatial agreement with observations on seasonal timescales, capturing the deep permanent thermocline off-shelf in winter and spring and the transition to seasonal MLD for summer. In the deeper ocean, V5 MLD consistently underestimates that from observations.

Sea Surface Height: Sea level is provided as part of this reanalysis product but is not extensively validated here. The reason for excluding sea level is that it is not possible to produce a meaningful sea level trend product from this reanalysis because the model mean sea level is a product of the open boundary conditions. There are two distinct model data sources used for open boundary conditions each with their own reference sea level, internal model drifts and distinct long term trends. Thus, it would be inappropriate to infer any long term sea level trend from the reanalysis as the signal will be dominated by the differences in the forcing datasets.

I.3 Estimated Accuracy Numbers

Variable	Location	RMS difference	Mean bias
SST	Full domain	0.57°C	-0.05°C
SST	Continental shelf	0.50°C	-0.07°C
Temperature 0-5 m	Full domain	0.45°C	-0.06°C
Temperature 5-30 m	Full domain	0.61°C	-0.09°C
Temperature 30-80 m	Full domain	0.64°C	-0.10°C
Temperature 80-300 m	Full domain	0.49°C	-0.12°C
Temperature 300-800 m	Full domain	0.72°C	-0.11°C
Temperature 800-2000 m	Full domain	0.53°C	-0.04°C
Temperature > 2000 m	Full domain	0.52°C	0.25°C
SSS	Continental shelf	1.20	-0.14
Salinity 0-5 m	Full domain	1.59	0.24
Salinity 5-30 m	Full domain	0.82	0.07
Salinity 30-80 m	Full domain	0.19	0.00
Salinity 80-300 m	Full domain	0.07	-0.01
Salinity 300-800 m	Full domain	0.05	0.00
Salinity 800-2000 m	Full domain	0.08	0.01
Salinity > 2000 m	Full domain	0.09	0.05
Mixed layer depth	Full domain	100.2 m	-21.9 m
Mixed layer depth	Continental shelf	16.8 m	-0.4 m

Temperature and salinity data for 1993-2019 are compared to in-situ observations from World Ocean Database (WOD, https://www.nodc.noaa.gov/OC5/WOD/pr_wod.html) that have been binned to the model grid to give a daily 3D field for comparison. Mixed layer depth data for 1993-2019 are compared to MLD profiles calculated from EN4 (Good et al. 2013) temperature and salinity profiles, version 4.2.2.

II PRODUCTION SYSTEM DESCRIPTION

Production centre's name: Met Office, UK

Production system name: North West European Shelf Reanalysis physics (CMEMS name: NWSHELF_MULTIYEAR_PHY_004_009)

Description

The North West shelf reanalysis was produced using the Forecasting Ocean Assimilation Model 7 km Atlantic Margin model (FOAM AMM7) which uses version 3.6 of the Nucleus for European Modelling of the Ocean (NEMO) ocean model code (Madec et al, 2016) with observations assimilated using version 6 of NEMOVar (Mogensen et al, 2012).

The model is located on the European North-West continental Shelf (NWS), from 40°N, 20°W to 65°N, 13°E, on a regular lat-lon grid with 1/15° latitudinal resolution and 1/9° longitudinal resolution (approximately 7 km square). The model domain is shown in Figure 1 partitioned into shallow (on shelf) and deeper (off shelf) waters. Although the domain extends beyond the shelf to include some of the adjacent North-East Atlantic, the focus of this system is on the shelf itself and the deep water is primarily included to ensure there is appropriate cross-shelf exchange. Thus a hybrid s-sigma terrain following coordinate system (following Siddorn and Furner, 2013) with 51 levels is employed in order to retain vertical resolution on the shelf. To reduce horizontal pressure gradient errors over extreme topography the scheme includes a z-S hybrid as described in Madec et al. (1996). The loss of vertical resolution at these points is more than compensated for by reduced errors in the horizontal pressure gradient term. A key feature of the bathymetry dividing the shelf from the deep ocean is the shelf slope, running south to north from Portugal to Norway. Associated with the shelf slope is the important "Joint Effect of Baroclinicity And bottom Relief" (JEBAR, Huthnance, 1984) which drives a poleward shelf slope current. The shelf slope itself varies in width and steepness. It is particularly steep along the Iberian slope to the west of Portugal and the Cantabrian slope to the north of Spain. The combination of very steep bathymetry and sigma coordinates requires special treatment for modelling horizontal pressure gradients, which is done using a Pressure Jacobian formulation. Bathymetry was supplied by North-West Shelf Operational Oceanographic System (NOOS) partners, who have processed GEBCO 1 arc-minute data together with a variety of other local data sources. The bathymetry was further interpolated in-house to fit with the model grid.

In order to make analysis and visualization easier for users, the products are delivered on 24 geopotential (z-level) vertical levels based upon the ICES standard depths. Gridpoints near to the model boundaries will be strongly affected by the model boundary conditions. For this reason, products are provided for the interior of the domain only. The outermost 10 gridpoints and points East of 10°E on the Baltic boundary are masked.

Tidal forcing is included both on the open boundary conditions via a Flather radiation boundary condition (Flather, 1976) and through the inclusion of the equilibrium tide. The external elevation and depth mean velocity was determined from 15 tidal constituents taken from a tidal model of the north-east Atlantic (Flather, 1981).

With the exception of the Baltic Sea, the model was forced at its open boundaries by temperature, salinity, sea surface height and currents taken from global ocean analyses from GloSea (MacLachlan et al., 2014), version 13. Baltic boundary conditions (temperature, salinity and currents) were taken from BALTICSEA_REANALYSIS_PHY_003_011. Baltic boundary conditions weren't available for the last 6 months of 2019, and so values from 2018 were used.

The interim monthly updates take Atlantic boundary conditions from an interim version of the GloSea version 13 reanalysis. Baltic boundary conditions come from the near-real-time Baltic reanalysis BALTICSEA_ANALYSISFORECAST_PHY_003_006.

Freshwater input was provided by a daily timeseries of river discharge, nutrient loads (nitrate, phosphate, silicate, ammonia), alkalinity (total alkalinity, bioalkalinity, dissolved organic carbon), and oxygen from 1991-2017. Timeseries data are produced from an updated version of the river datasets used in Lenhart et al. (2010) combined with climatology of daily discharge data from the Global River Discharge Data Base (Vörösmarty et al., 2000) and from data prepared by the Centre for Ecology and Hydrology as used by Young and Holt (2007). Values for 2017 were re-used for 2018 and 2019 as recent data wasn't available.

Surface forcing of hourly precipitation, wind stress, pressure and radiative fluxes were taken from the ECMWF ERA5 reanalysis (Hersbach et al., 2020), or from the ERA5T near-real-time extension for interim updates. These fluxes were then processed through the CORE bulk forcing algorithms (Large and Yeager, 2004; Large and Yeager 2009) before being applied to the model. The inverse barometer effect of atmospheric pressure gradients on the sea surface height was also included. The light attenuation scheme is the RGB scheme within NEMO.

A non-linear free surface was implemented using a variable volume layer method. The short time scales associated with tidal propagation and the free surface require a time splitting approach, splitting modes into barotropic and baroclinic components. The bottom boundary condition includes a log layer representation and a k-epsilon turbulence scheme is implemented with a generic length scale (Umlauf and Burchard, 2003). The model uses a non-linear free surface, and an energy and entrophy conserving form of the momentum advection. It uses free slip boundary conditions. The tracer equations use a TVD advection scheme (Zalesak, 1979). For tracer diffusion a Laplacian diffusion scheme on geopotential surfaces is applied, whereas for momentum diffusion a mixed Laplacian/bilaplacian scheme is used, with the Laplacian operator applied on geopotential surfaces and the bilaplacian on model surfaces.

For the reanalysis, assimilation of Sea Surface Temperature (SST) and in situ temperature and salinity profiles was performed using a 3DVar algorithm. Calculation of the assimilation increments was done using an adapted version of the NEMOVAR (Mogensen et al, 2012) system. Assimilation proceeded in three steps. Firstly, a one day model forecast was performed, within which observations were compared to model output at the nearest time-step; this is a First Guess at Appropriate Time (FGAT) system. In the second stage, observation minus model differences were converted to SST increments by minimising a 3DVar cost function. In minimising this function seasonally varying estimates of the observation representativity error variance (assumed uncorrelated) and background error variance were used. The total observation error variance was obtained by adding an estimate of the measurement error variance of each observation to the representativity error variance. Information from observations was spread horizontally according to lengthscales that are inversely proportional to the potential vorticity gradient and have a maximum value of 130 km. In the final stage the analysis was produced by rerunning the model for the same day with the increments added onto the model fields using the Incremental Analysis Update (IAU, Bloom et al., 1996) method.

Satellite observations of SST were taken from the ESA CCI database (Merchant et al., 2014). For AVHRR, level 2 data was taken from ESA CCI version 1.0. For ATSR, level 3 data was used, from version 1.0 until end of 2010 and from version 1.1 after that. GHRSST data (http://www.ghrsst.org) from the

AMSRE and SEVIRI instruments were assimilated from August 2006, with the AMSRE instruments failing in November 2011.

In-situ SST data were assimilated throughout the entire reanalysis run, using ICOADS (see http://icoads.noaa.gov/).

In situ observations of sub-surface temperature and salinity were taken from the EN4 database (Good et al, 2013). The reanalysis was run as one continuous stream.

For the interim monthly updates, in situ and satellite SST data are taken from the same sources as for the analysis forecast system NWSHELF_ANALYSISFORECAST_PHY_LR_004_001. This is the Global Telecommunications System (GTS) for in situ, and GHRSST (www.ghrsst.org) level 3 for the satellite SST.

In this document, the reanalysis product NWSHELF_MULTIYEAR_PHY_004_009 (labelled as NEMO-reanalysis, or AMM7 V5) is assessed for 01/01/1993 to 31/12/2019. In addition, the previous version of this reanalysis, covering 01/01/1992 to 31/12/2018, is evaluated for comparison (here labelled V4).

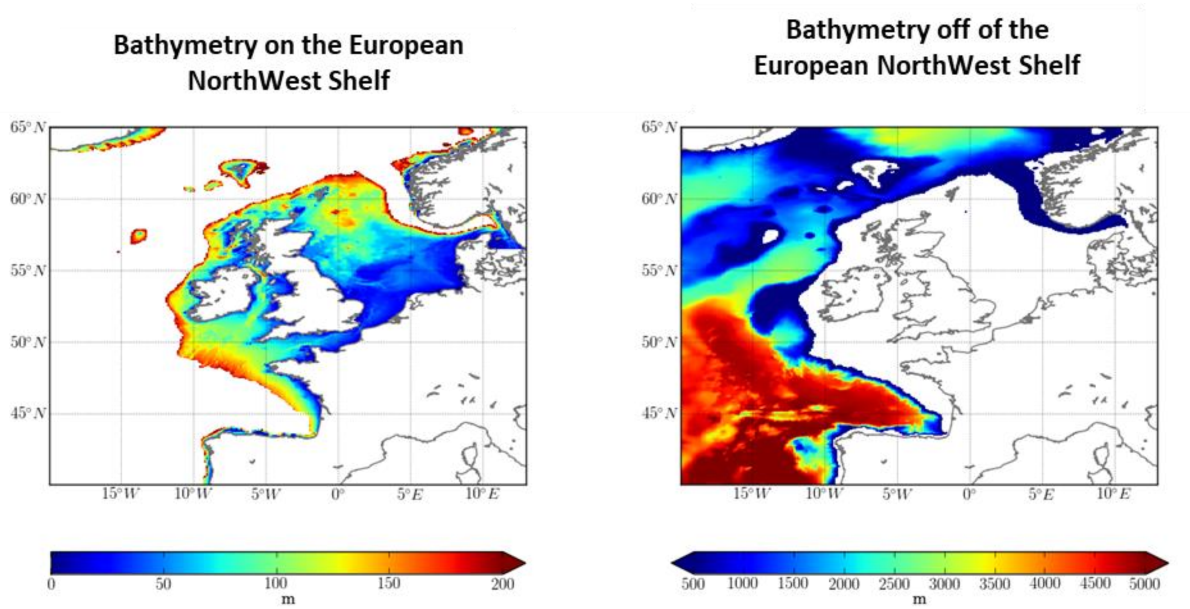

Figure 1: FOAM AMM7 bathymetry (m) showing (left) the domain on the European NorthWest Shelf (defined here as total depth less than 200 m) and (right) the domain off the shelf.

Changes from the previous reanalysis

The major differences from the previous North West European Shelf Reanalysis V4, as described in QuID vn4.2 are:

- Update of the NEMOVAR code base from v3 to v6
- Use of hourly ERA5 atmospheric forcing, replacing ERA-Interim 3-hourly
- Update bias correction scheme for satellite SST against in situ
- Coupled physical/biogeochemical reanalysis (NEMO/ERSEM)
- Updated rivers dataset (V4 used a climatology)
- Use of baroclinic boundary conditions (V4 used barotropic)
- Use of latest version Baltic reanalysis for boundary conditions
- Period updated to be 1993 to one year behind present

III VALIDATION FRAMEWORK

The products assessed are temperature, salinity, currents, tidal elevation, mixed layer depth, and section transports.

The model temperature and salinity fields are compared with in-situ observations from the World Ocean Database 2018 (WOD, https://www.nodc.noaa.gov/OC5/WOD/pr_wod.html), averaged through vertical layers; with satellite observations of surface temperature and salinity; and with mooring data time series at Cypris (Isle of Man), the Western Channel Observatory (L4, E1) and from the CMEMS database (product INSITU_NWS_NRT_OBSERVATIONS_013_036). Validation is also done with the multi-model ensemble of multi-year products (MME MYP), a CMEMS internal product

Maps of time-averaged near surface (15 m deep) model currents are compared to NOAA AOML drifter climatology (http://www.aoml.noaa.gov/phod/dac/drifter_climatology.html) and volume fluxes through the NOOS sections in the North Sea are compared to published values, where available.

Harmonic constants of tidal elevations for the main tidal constituents are compared to observed values.

Table 1: Summary of metrics and observations used in the assessment (continues overleaf).

Variable	Description	Observations	Class	Metrics
temperature	Time integrated means at depth levels; averages through depth layers; time series at mooring locations	WOD in-situ data, satellite SST, moorings at Cypris and the Western Channel Observatory (L4, E1) and CMEMS moorings. Also the MME MYP ensemble mean. HadIOD in situ SST for validation of hourly fields.	1, 2, 3 & 4	maps, time series, correlation, biases, RMS differences
salinity	Time integrated means at depth levels; averages through depth layers; time series at mooring locations	WOD in-situ data, moorings at Cypris and the Western Channel Observatory (L4, E1) and CMEMS moorings. Also the MME MYP ensemble mean. EN4 profiles for hourly salinity.	1, 2, 3 & 4	maps, time series, correlation. biases, RMS differences
currents	Near surface (15 m) zonal and meridional current climatologies. Radar data for hourly surface currents.	NOAA AOML drifter climatology;	1	maps
Tidal constants	Maps and statistics of errors	Tide gauge data from the British Oceanographic Data Centre and the National Oceanographic Centre	1	RMS errors
Mixed layer depth	Daily and hourly Kara MLD	MLD from EN4 temperature and salinity profiles.	1,4	Maps, RMS and percent difference

IV VALIDATION RESULTS

IV.1 Temperature

The reanalysis temperature is validated against four datasets covering different time and space scales:

1. Contemporary temperature observations from World Ocean Database (WOD, https://www.nodc.noaa.gov/OC5/WOD/pr_wod.html) are used to calculate mean reanalysis biases. For dates before 2018, data from the 2013 release of the WOD are used so that a direct comparison with the V4 analysis is possible. After 2018, WOD 2018 data are used.
2. SST data from satellite (CMEMS: product SST_GLO_SST_L4_REP_OBSERVATIONS_010_011).
3. High frequency (daily to monthly) observations at fixed point moorings.
4. MME MYP ensemble mean.

The interim monthly updates are assessed against satellite SST and against mooring data.

Hourly SST is assessed against HadIOD in situ observations (Atkinson et al, 2014).

IV.1.1 World Ocean Database

For each observation in the WOD, daily mean model data for the corresponding day are interpolated to the location of the measurement. The resulting data are binned onto the model grid to give a daily 3D error field. This method prevents observation datasets at high spatial and temporal resolution (e.g. measured by gliders) from disproportionately influencing the validation compared to other data sources (e.g. CTD casts).

The resulting model – observation biases are averaged into layers for the time periods 1993-2018 for V4 (Figure 2) and 1993-2019 for V5 (Figure 3). In V4, temperatures were generally too cold in the Norwegian Sea in the 30-80 m and 80-300 m layers, and these biases are reduced in V5. In the same two layers, in the deep ocean south of 50°N, V4 was too warm; in V5, the 30-80 m layer is slightly cool (~0.1°C on average) and the mean biases in the 80-300 m layer are close to zero. Below 800 m in the deep ocean south of 50°N V4 was generally too cold; in V5, biases are generally between -0.5°C and 0.5°C in the 800-2000 m layer and up to 1.5°C too warm below 2000 m. In the North Sea around 55°N, V4 was cool in the 5-30 m layer and warm in the 30-80 m layer and these biases increase slightly in magnitude in V5. The cold bias in the 30-80 m layer in the southern Irish Sea, increases (to between 1 and 3°C) in V5.

Mean biases (Figure 4) and root-mean-square differences (RMSD, Figure 5) averaged over the reanalysis region and for different depth ranges have high monthly variability (left columns), partly due to different numbers of observations per month, but neither V4 nor V5 show a trend in the differences with time (central columns). In depths shallower than 800 m, V5 has a larger cold bias than V4. Between 800 and 2000 m the V5 cold bias is less than that of V4 and, below 2000 m, V5 is warm bias whereas V4 was cold. Above 80m, temperature biases are greater in the winter than during the summer. However, RMSD are larger during the summer, with V5 greater than V4 between 5 and 80 m.

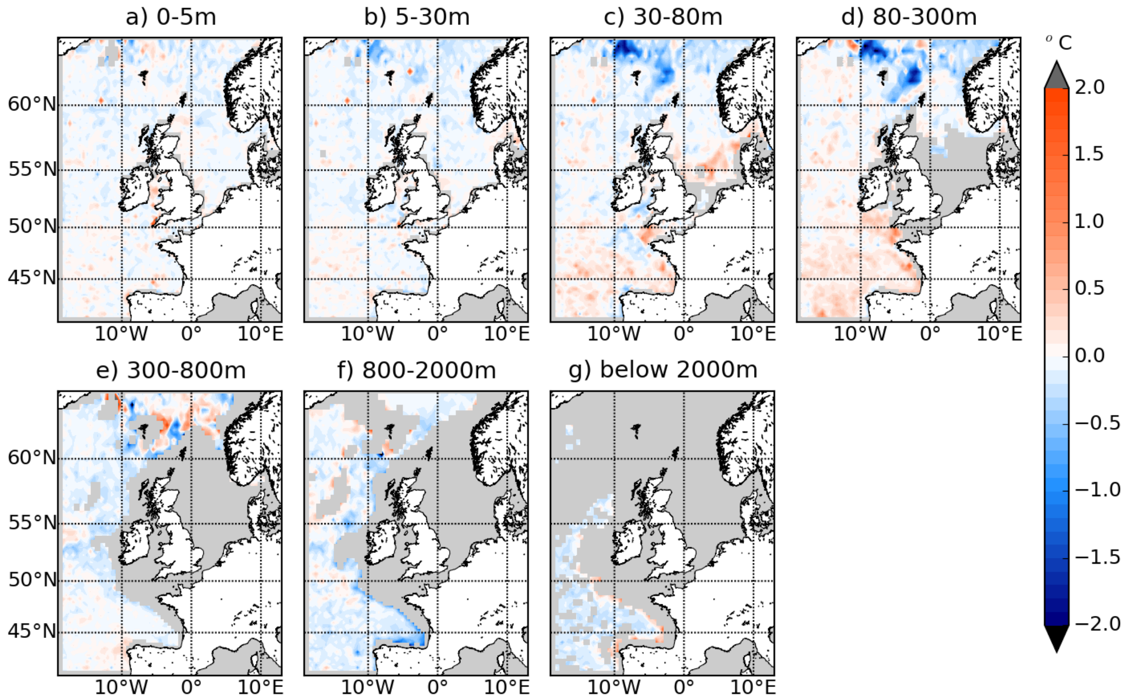

Figure 2: Mean biases between co-located V4 temperatures and WOD observations in different layers for 1993-2018.

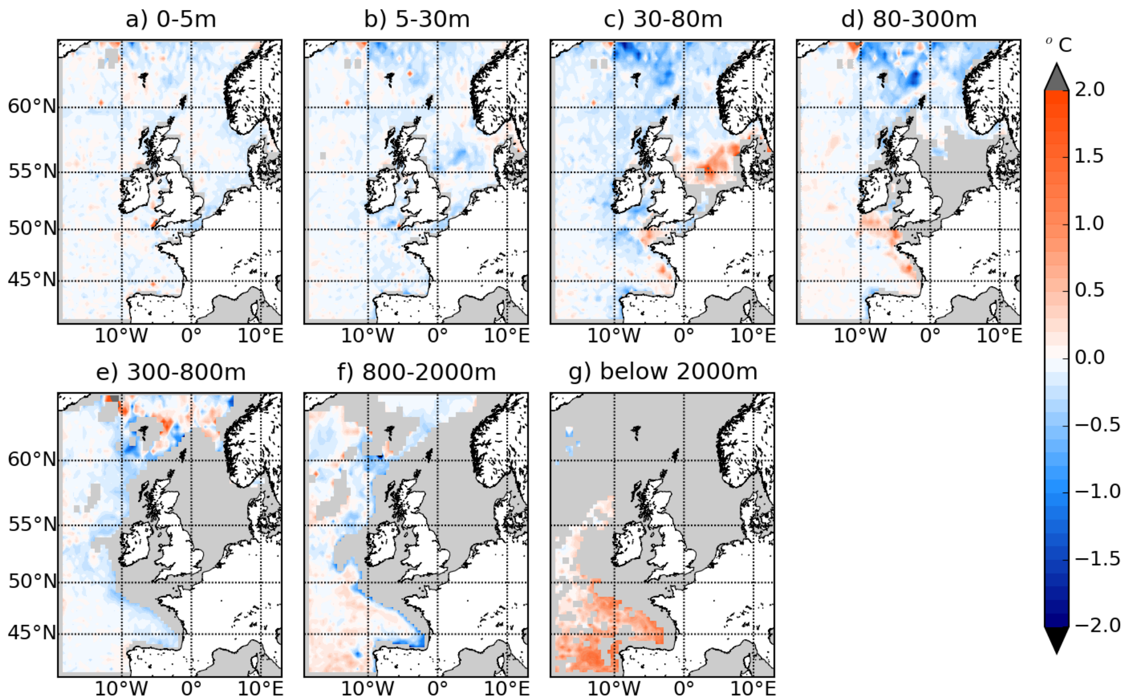

Figure 3: Mean biases between co-located V5 temperatures and WOD observations in different layers for 1993-2019.Areas shaded light grey are below the sea bed or outside of the AMM7 domain (for instance the Baltic and Mediterranean Seas).

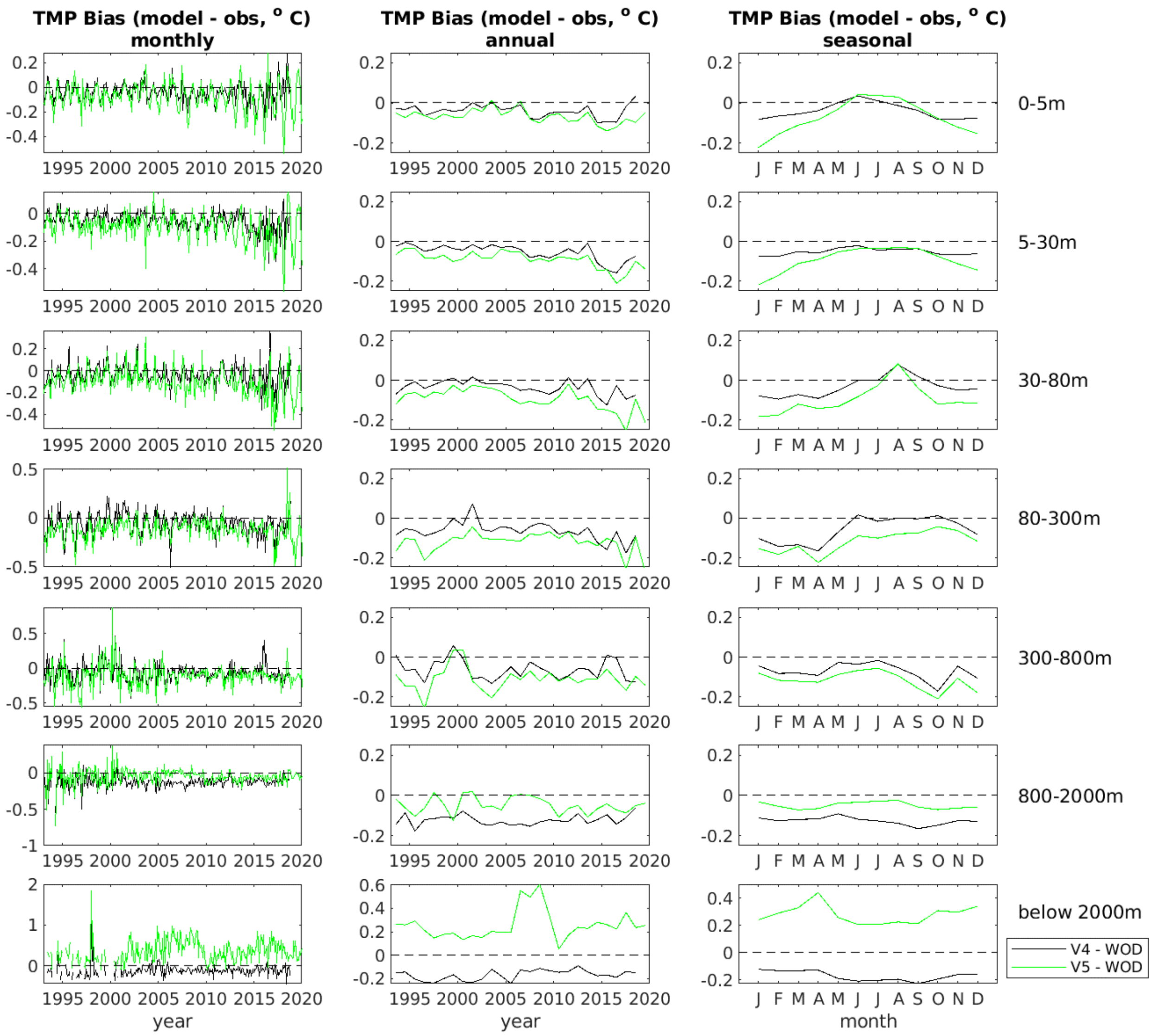

Figure 4: Mean biases (model – observed) for model temperature compared to WOD observations, averaged over different depth layers for the model domain. The left column shows monthly mean biases, the central column is annual mean biases, and the right column is seasonal biases. Annual and seasonal biases are calculated from monthly biases weighted according to the number of observations per month.

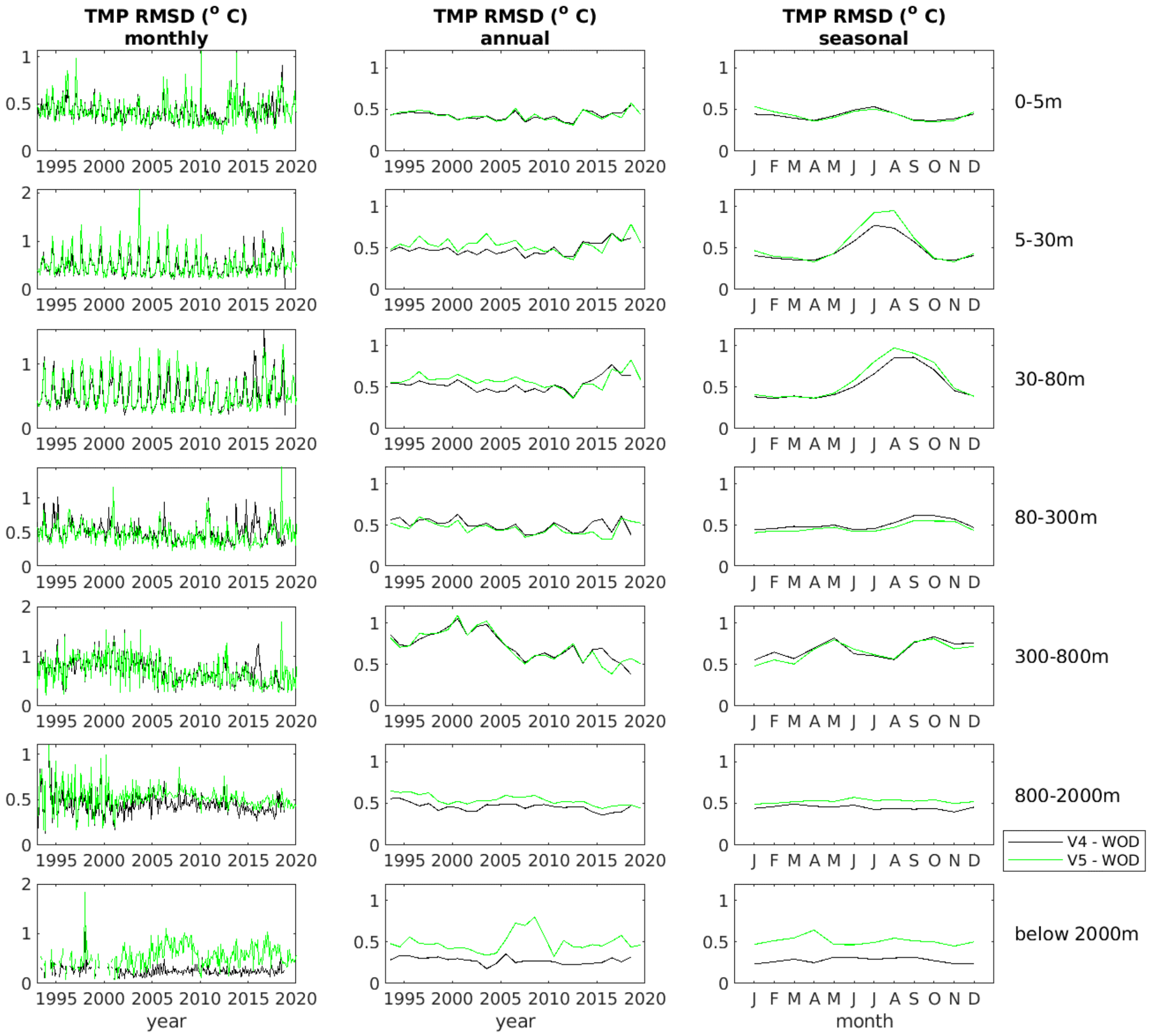

Figure 5: Root-mean-square differences (RMSD) for model temperature compared to WOD observations, averaged over different depth layers for the model domain. The left column shows monthly RMSD, the central column is annual means of the monthly RMSD, and the right column is seasonal RMSD. Annual and seasonal RMSD are calculated from monthly RMSD weighted according to the number of observations per month.

Validation of hourly SST against Hadiod in situ observations (Figure 6) shows RMS differences slightly larger than for monthly and annual means, as expected. The peaks at the synoptic hours (00,06,12,18Z) are due to increased number of observations, and spatial coverage, at these times.

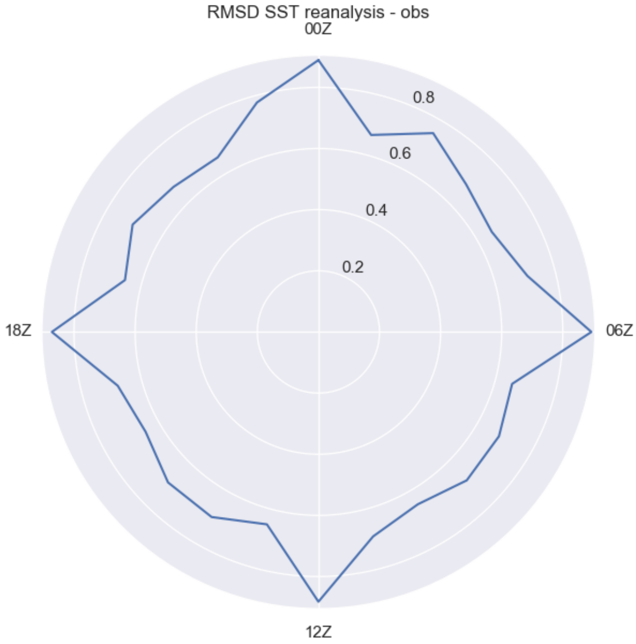

Figure 6 RMSD surface temperature (K), reanalysis minus HadIOD in situ observations, plotted against time of day

IV.1.2 Satellite SST

Daily mean SST from the V5 reanalysis are compared to daily satellite temperature from the CMEMS product SST_GLO_SST_L4_REP_OBSERVATIONS_010_011 (Figure 7) for 1993 to 2018. This Level 4 (gridded) product derives from the same Level 2 satellite SSTs that were assimilated in the reanalysis. On the European continental shelf and in the Norwegian Sea, V5 is on average cold bias compared to the satellite data, however, to the south and west of the shelf, V5 is slightly warm bias. Except near coasts, in the Norwegian Sea, Faroe-Shetland channel and Norwegian Trench, RMS differences are generally less than 0.5°C. The domain-mean SST is on average cold bias, but with warm biases in the summer; there is an increase in the cold bias and its seasonality from the second half of 2012. Domain-mean RMS differences are generally less than 0.5°C. Spatial correlation each day is mostly greater than 0.97. There is a similar spatial pattern to SST biases during spring, autumn and winter (Figure 8); in the summer the bias changes from cold to warm to the north and west of Scotland, in the Norwegian Sea and in some coastal regions.

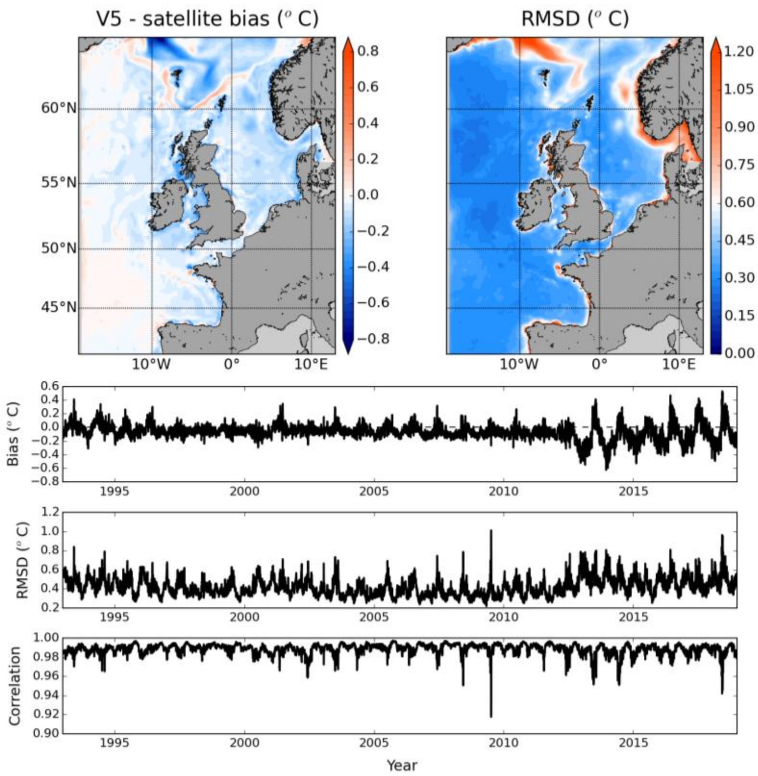

Figure 7: Top left: V5 – satellite SST bias; top right: RMSD for V5 compared to satellite SST; bottom three panels are time series of 1) V5 – satellite bias, 2) RMSD and 3) spatial correlation of the monthly mean V5 and satellite SST for 1993 to 2018.

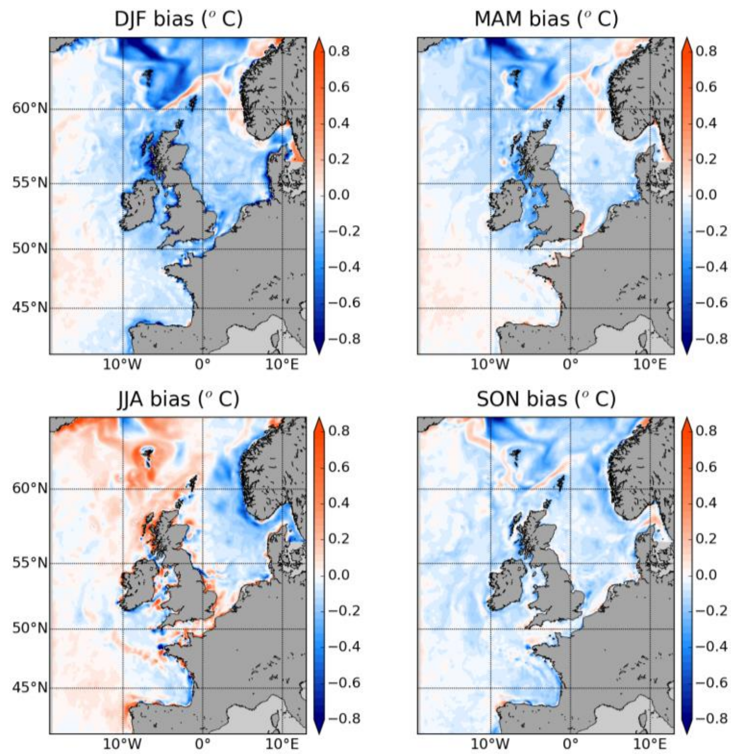

Figure 8: Seasonal biases of V5 – satellite SST for 1993 to 2018 in winter (DJF: December, January, February), spring (MAM: March, April, May), summer (JJA: June, July, August) and autumn (SON: September, October, November).

IV.1.3 Mooring data

The V5 reanalysis temperatures are compared to time series of observations from three sources:

1. water column data from Cypris Station (4.833°W, 54.092°N) from the Isle of Man Long-term Environmental Time Series from 1984 to 2009, collected at between weekly and monthly intervals, downloaded from the British Oceanographic Data Centre (BODC),
2. water column data from locations E1 (4.367°W, 50.033°N) and L4 (4.217°W, 50.250°N) in the Western Channel Observatory collected by Plymouth Marine Laboratory at between weekly and monthly intervals and downloaded from http://www.pangaea.de; data are available for 1984, 1985 and 2002 to 2011 for E1 (Smyth et al., 2012) and 1988 to 2011 for L4 (Smyth et al., 2011). Data for 2012-2014 were downloaded from http://www.westernchannelobservatory.org.uk These and the Cypris Station data are not assimilated in the reanalysis.
3. mooring time series data from INSITU_NWS_NRT_OBSERVATIONS_013_036 which were downloaded from http://marine.copernicus.eu/. Many of these observations will have been assimilated in the reanalysis and so aren't independent data.

Locations of the mooring points are shown in Figure 9.

For comparison with the observation time series, V5 temperatures are extracted co-located with the date and location of each observation. The Cypris, E1 and L4 data are observed at frequencies of less than 1 day and are compared to the daily mean temperature of the model on the day of observation. The CMEMS time series are generally recorded more than once per day and so, for each day, all observations recorded are averaged to make a daily mean for comparing to the model. The CMEMS datasets have quality control flags and only data flagged as "good data" are used; additionally any observations that are clearly in error (i.e. out of range or obviously different from the rest of the data) are removed.

V5 is generally in good agreement with the L4 temperature time series (Figure 10), except that from 2000 to 2003 winter SST is too high. V5 is on average between 0.10 and 0.31°C too warm, with RMSD less than 0.8°C and correlation greater than 0.97 (Table 2). The agreement at E1 is also good (Figure 11) although the water column is potentially under-stratified in the model during the summers of 2007 and 2008, shown by higher temperatures at 70 m depth compared to observations, and winter minima in 2013 are too cold at all levels. V5 is generally too cold near surface and too warm at depth, with RMSD less than 0.85°C and correlation greater than 0.95 (Table 2). At Cypris, winter minima are too cold at all depths in 2001 and 2009 (Figure 12). V5 is on average too cold, with RMSD less than 0.64°C and correlation of 0.99 at all depths (Table 2).

For the CMEMS mooring temperatures, data assimilation has ensured a good fit to the observations at most locations (Figure 13). There are some differences where the observations appear to be in error (not flagged in the data file) and have apparently not been used in the assimilation (e.g. at the start of 2009 at station 32 and early 1995 at station 25). Time-mean biases are generally between -0.4 and 0.2°C, with correlation between V5 and mooring time series generally higher than 0.98 (Table 2). RMSD are generally less than 0.6°C and are below 1°C for all but six mooring time series. Exceptions occur at station 14 (GL_TS_MO_62444) on the coast of northern France, at station 56 (NO_TS_MO_Ijmuiden) in the Netherlands and at four stations to the west of Denmark: stations 40 (NO_TS_MO_Borkum), 47 (NO_TS_MO_FINO3FerryBox at 17 m depth), 54 (NO_TS_MO_Hoernum) and 64 (NO_TS_MO_Sylt). For two of these stations (47 and 64), there are large differences between V5 and the mooring data (in mid-2014 at station 47, and at the end of 2012 at station 64). However, in the case of station 64, the mooring temperatures seem unusually high in 2012 compared to other years and so could be bad data.

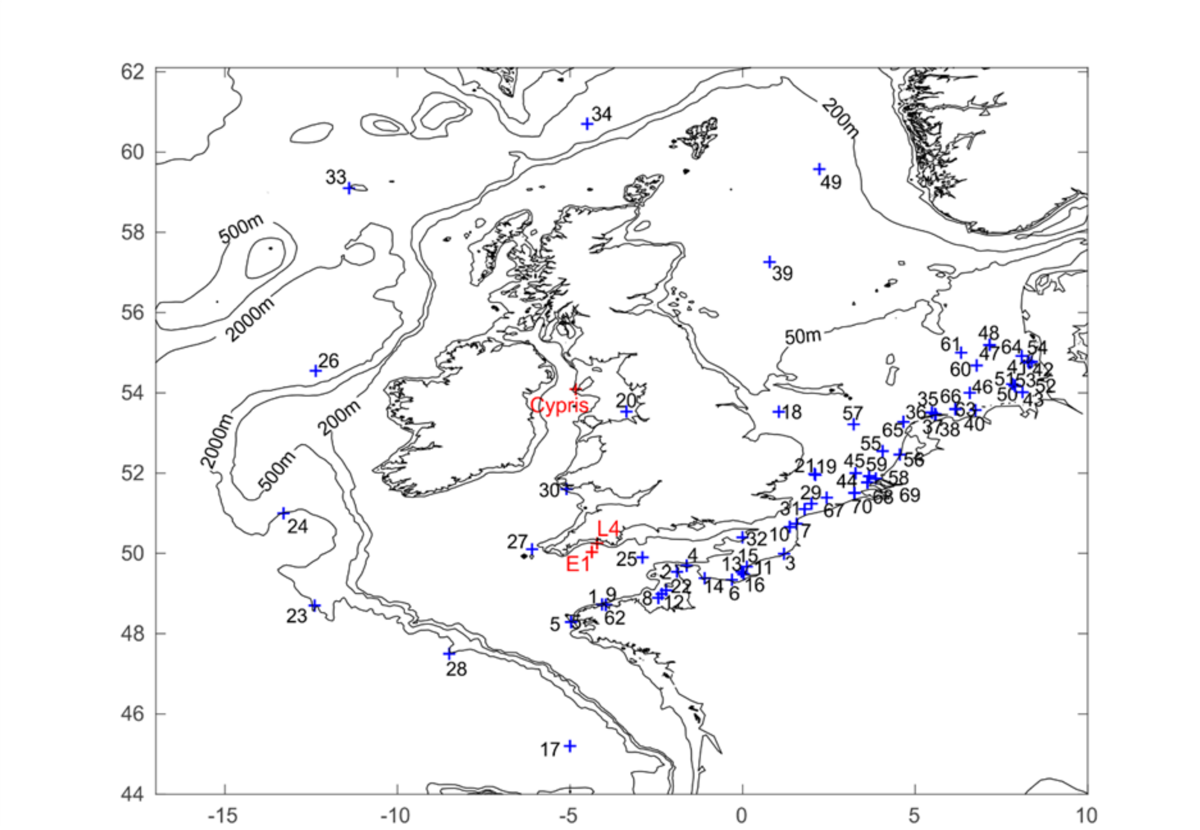

Figure 9: Locations of the moorings: CMEMS mooring points are in blue; Cypris on the Isle of Man and E1 and L4 Western Channel Observatory sites are in red.

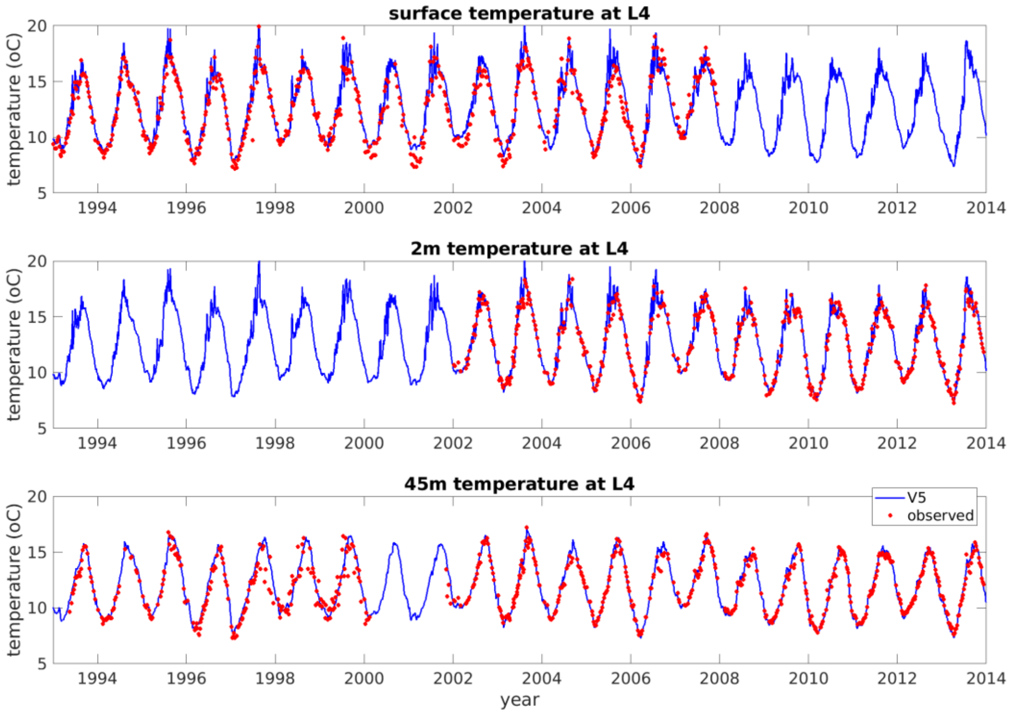

Figure 10: Comparison of daily mean V5 temperatures with L4 observations at the surface and at 2 m and 45 m depth.

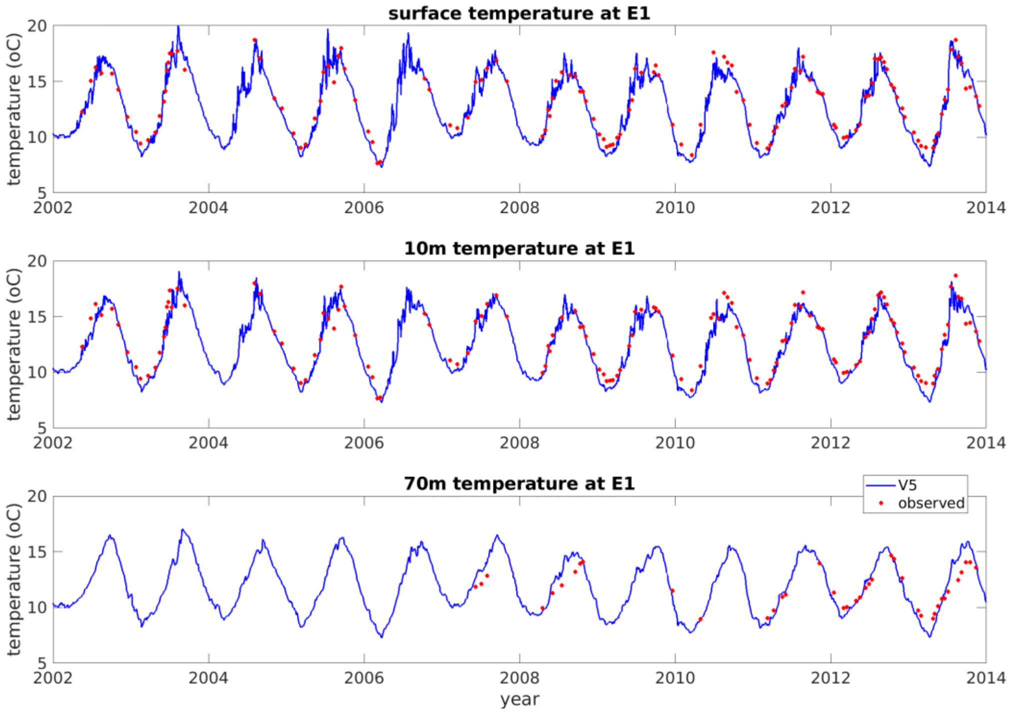

Figure 11: Comparison of daily mean V5 temperatures with E1 observations at the surface and at 10 m and 70 m depth.

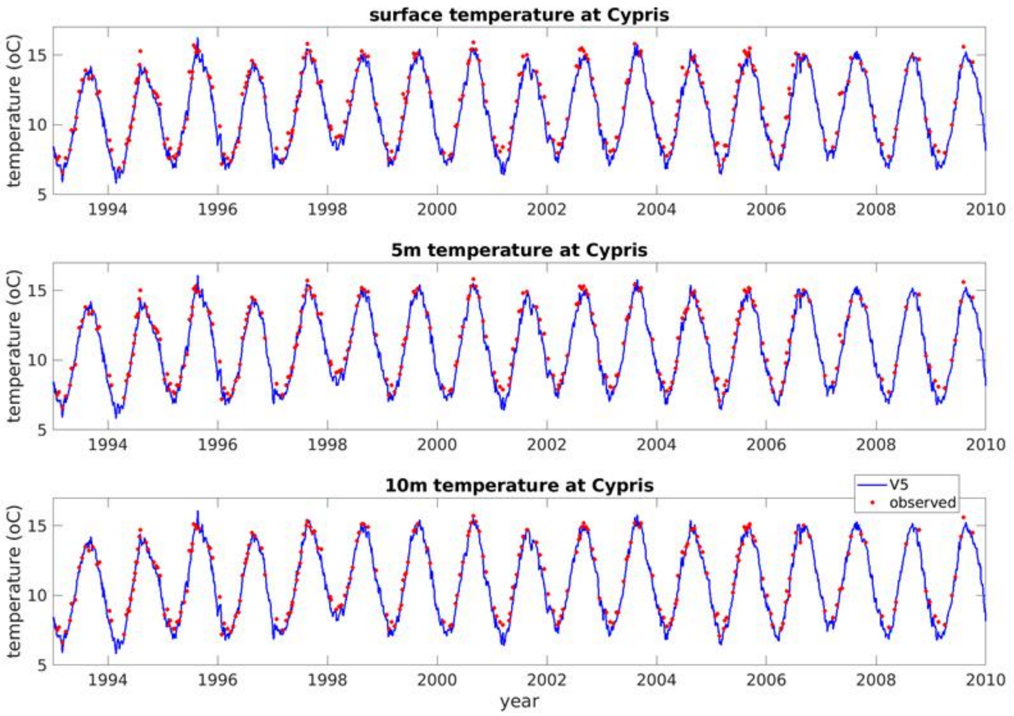

Figure 12: Comparison of daily mean V5 temperatures with Cypris observations at the surface and at 5 m and 10 m depth.

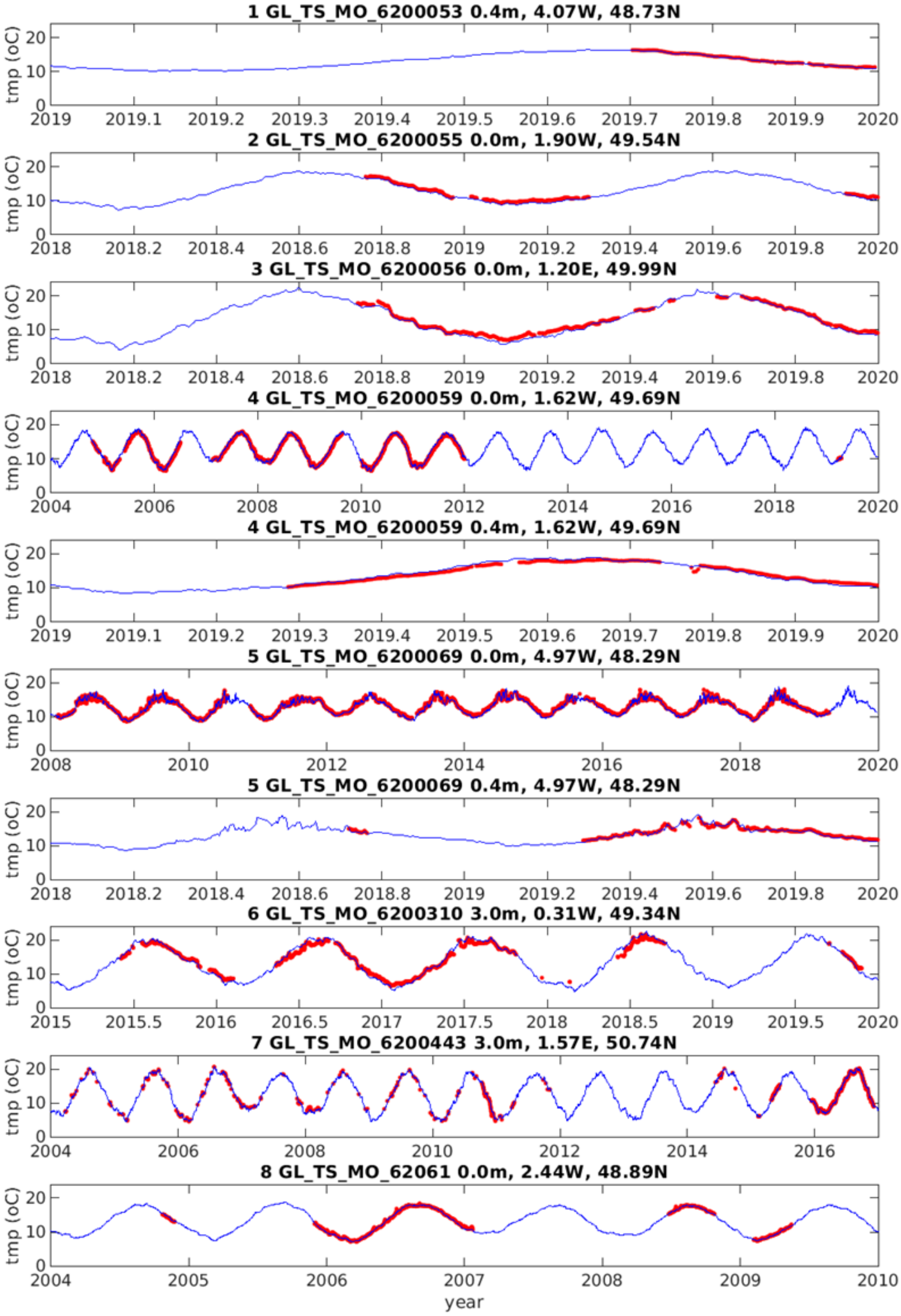

Figure 13: Comparison of daily mean V5 temperatures with CMEMS observations. The titles contain: numbers referring to locations in Figure 9, names from the CMEMS data files and depths, longitudes and latitudes of the observations. The blue line is V5 and the red dots are observations.

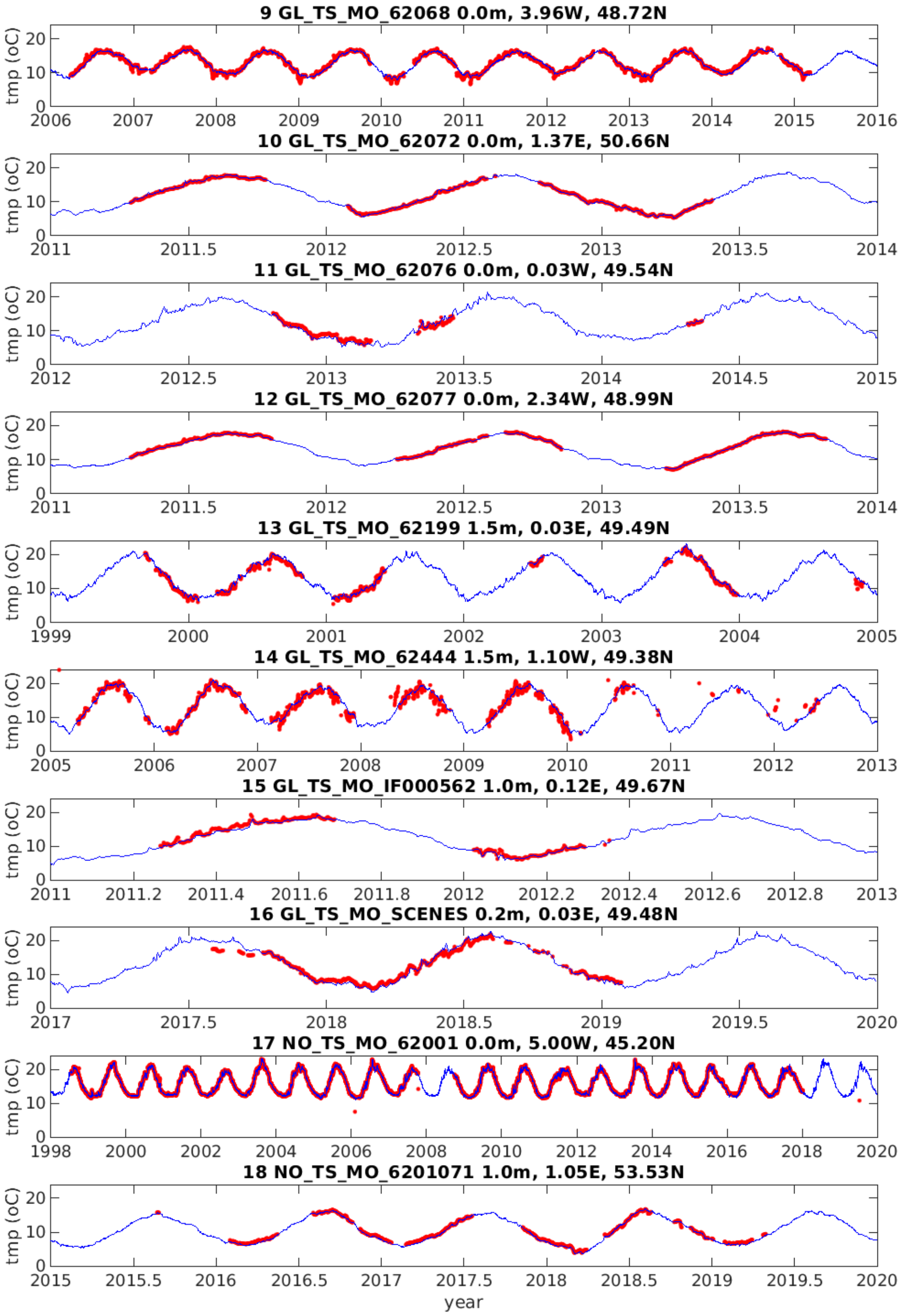

Figure 13, continued.

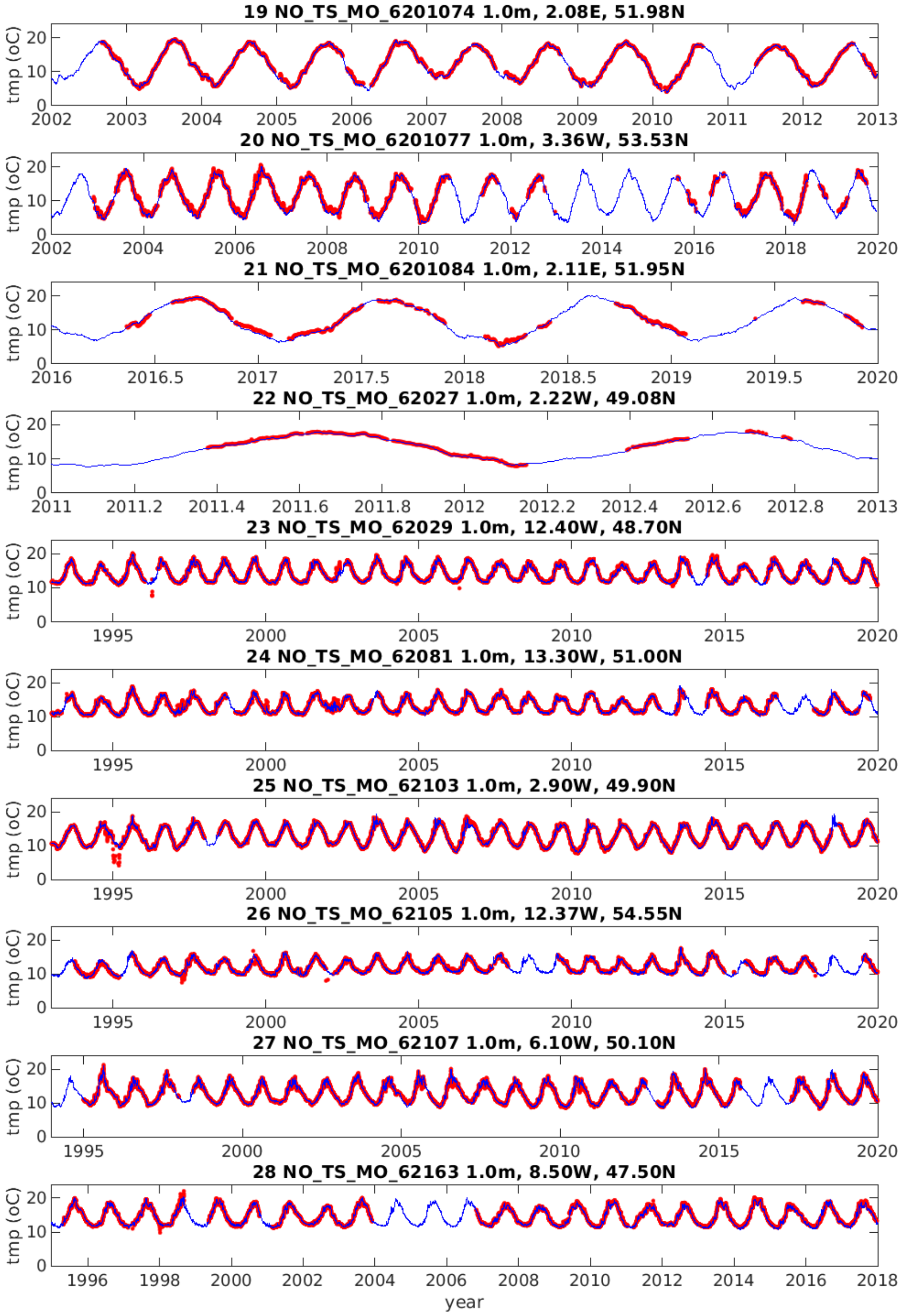

Figure 13, continued.

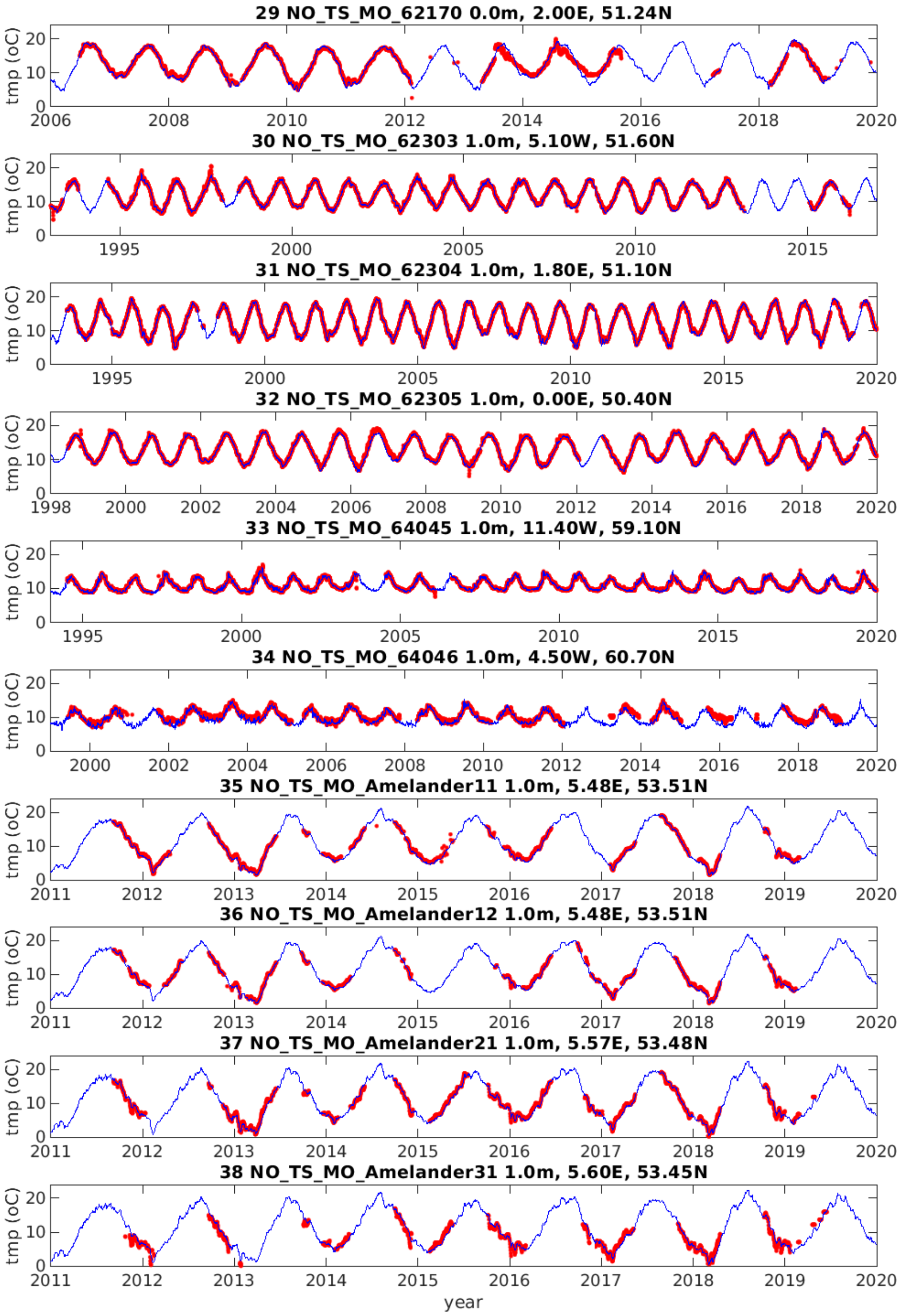

Figure 13, continued.

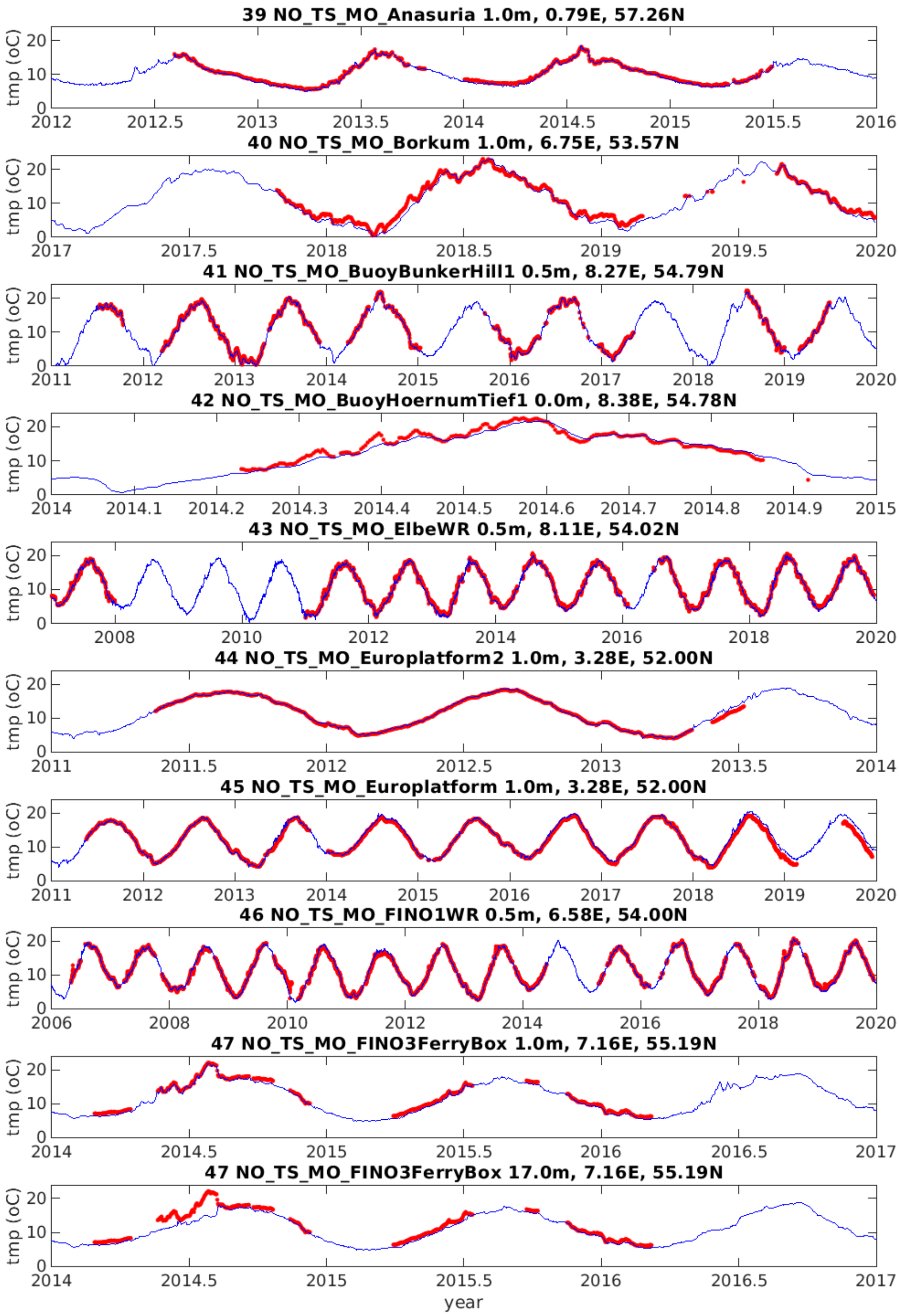

Figure 13, continued.

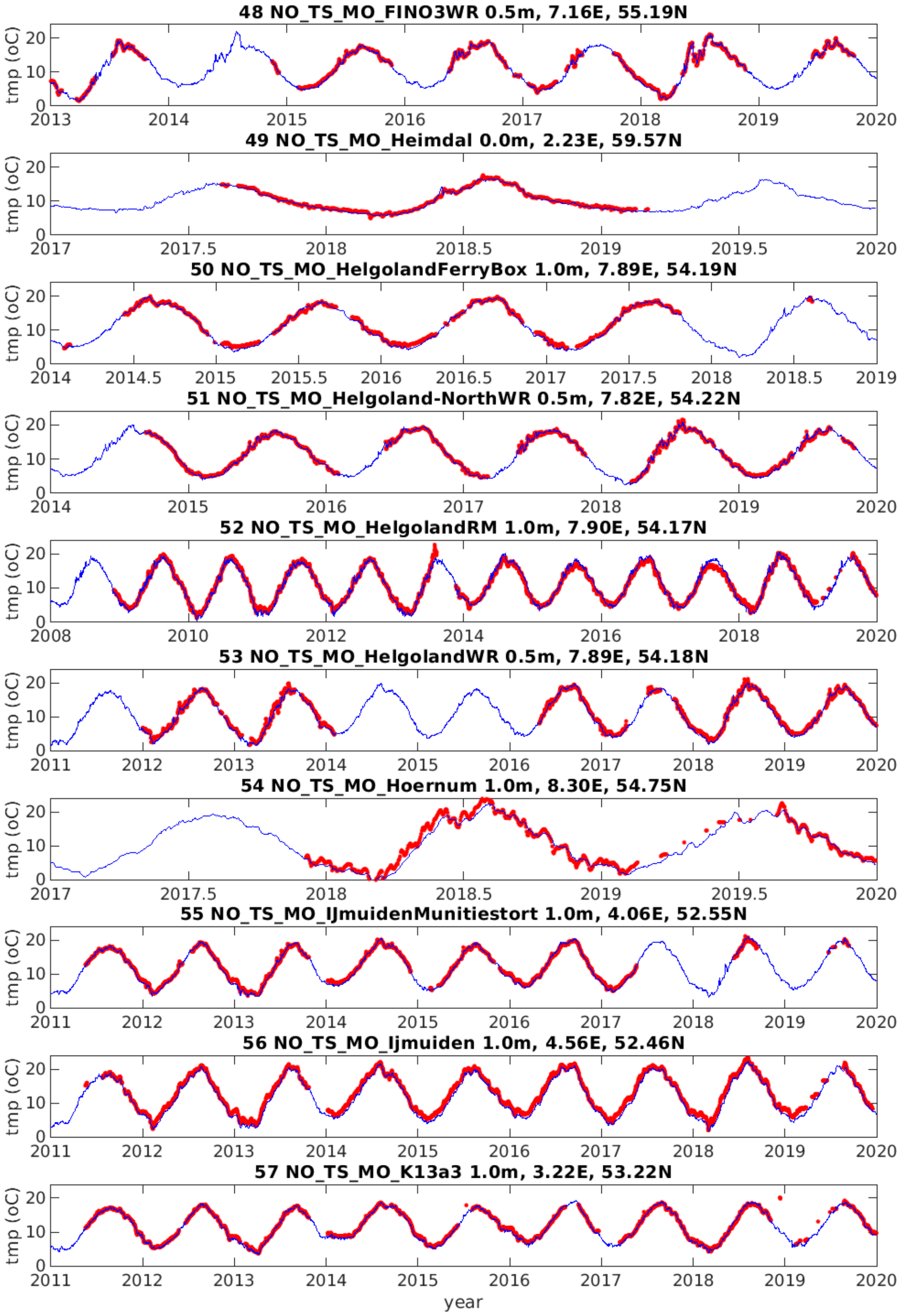

Figure 13, continued.

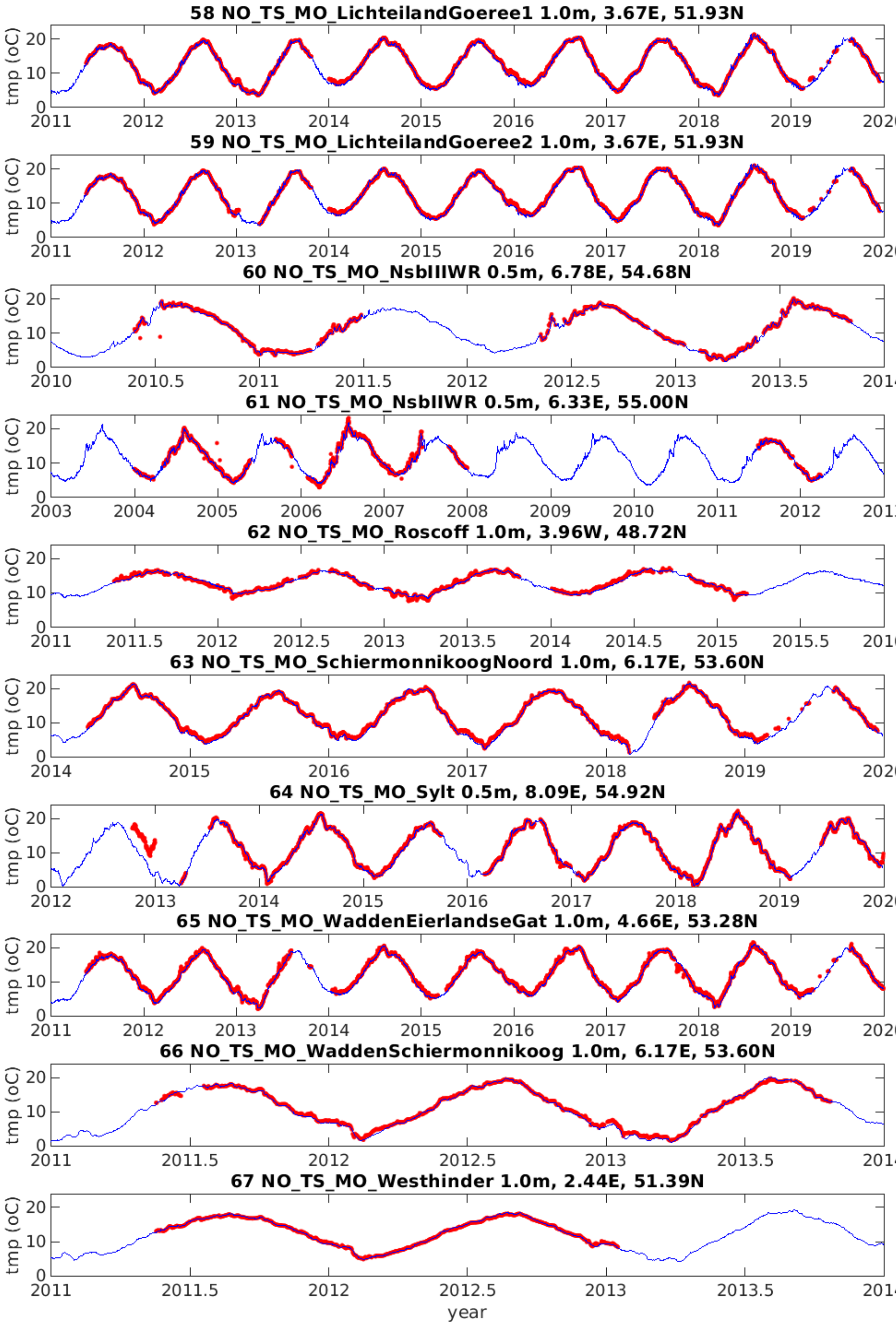

Figure 13, continued.

Table 2: Mean bias (V5 – observation), root-mean-square difference (RMSD) and correlation coefficient for E1, L4, Cypris and the CMEMS moorings daily mean temperatures compared to V5 (continues overleaf).

no	mooring name	longitude	latitude	depth (m)	mean bias (°C)	RMSD (°C)	corre-lation
-	L4	4.22°W	50.25°N	0.0	0.31	0.80	0.97
-	L4	4.22°W	50.25°N	2.0	0.10	0.47	0.99
-	L4	4.22°W	50.25°N	45.0	0.16	0.59	0.97
-	E1	4.37°W	50.03°N	0.0	-0.21	0.75	0.97
-	E1	4.37°W	50.03°N	10.0	-0.44	0.84	0.97
-	E1	4.37°W	50.03°N	70.0	0.25	0.85	0.95
-	Cypris	4.83°W	54.09°N	0.0	-0.46	0.64	0.99
-	Cypris	4.83°W	54.09°N	5.0	-0.37	0.51	0.99
-	Cypris	4.83°W	54.09°N	10.0	-0.28	0.44	0.99
1	GL_TS_MO_6200053	4.07°W	48.73°N	0.4	-0.10	0.16	1.00
2	GL_TS_MO_6200055	1.90°W	49.54°N	0.0	-0.60	0.62	1.00
3	GL_TS_MO_6200056	1.20°E	49.99°N	0.0	-0.62	0.76	1.00
4	GL_TS_MO_6200059	1.62°W	49.69°N	0.0	0.16	0.59	0.99
4	GL_TS_MO_6200059	1.62°W	49.69°N	0.4	0.17	0.64	0.98
5	GL_TS_MO_6200069	4.97°W	48.29°N	0.0	-0.18	0.54	0.98
5	GL_TS_MO_6200069	4.97°W	48.29°N	0.4	-0.14	0.47	0.97
6	GL_TS_MO_6200310	0.31°W	49.34°N	3.0	0.15	0.88	0.99
7	GL_TS_MO_6200443	1.57°E	50.74°N	3.0	0.02	0.39	1.00
8	GL_TS_MO_62061	2.44°W	48.89°N	0.0	-0.08	0.28	1.00
9	GL_TS_MO_62068	3.96°W	48.72°N	0.0	-0.03	0.47	0.98
10	GL_TS_MO_62072	1.37°E	50.66°N	0.0	0.04	0.26	1.00
11	GL_TS_MO_62076	0.03°W	49.54°N	0.0	-0.34	0.83	0.97
12	GL_TS_MO_62077	2.34°W	48.99°N	0.0	-0.08	0.19	1.00
13	GL_TS_MO_62199	0.03°E	49.49°N	1.5	0.44	0.68	0.99
14	GL_TS_MO_62444	1.10°W	49.38°N	1.5	0.15	1.30	0.95
15	GL_TS_MO_IF000562	0.12°E	49.67°N	1.0	-0.34	0.57	1.00
16	GL_TS_MO_SCENES	0.03°E	49.48°N	0.2	-0.03	0.90	0.99
17	NO_TS_MO_62001	5.00°W	45.20°N	0.0	-0.08	0.32	1.00
18	NO_TS_MO_6201071	1.05°E	53.53°N	1.0	-0.26	0.39	1.00
19	NO_TS_MO_6201074	2.08°E	51.98°N	1.0	-0.12	0.37	1.00
20	NO_TS_MO_6201077	3.36°W	53.53°N	1.0	-0.33	0.70	0.99
21	NO_TS_MO_6201084	2.11°E	51.95°N	1.0	-0.26	0.53	1.00
22	NO_TS_MO_62027	2.22°W	49.08°N	1.0	-0.16	0.25	1.00
23	NO_TS_MO_62029	12.40°W	48.70°N	1.0	-0.10	0.27	0.99
24	NO_TS_MO_62081	13.30°W	51.00°N	1.0	-0.04	0.25	0.99
25	NO_TS_MO_62103	2.90°W	49.90°N	1.0	-0.10	0.33	0.99
26	NO_TS_MO_62105	12.37°W	54.55°N	1.0	-0.06	0.35	0.98

no	mooring name	longitude	latitude	depth (m)	mean bias (°C)	RMSD (°C)	corre-lation
27	NO_TS_MO_62107	6.10°W	50.10°N	1.0	-0.03	0.34	0.99
28	NO_TS_MO_62163	8.50°W	47.50°N	1.0	-0.09	0.30	0.99
29	NO_TS_MO_62170	2.00°E	51.24°N	0.0	-0.06	0.86	0.98
30	NO_TS_MO_62303	5.10°W	51.60°N	1.0	-0.11	0.34	1.00
31	NO_TS_MO_62304	1.80°E	51.10°N	1.0	-0.11	0.37	1.00
32	NO_TS_MO_62305	0.00°E	50.40°N	1.0	-0.19	0.41	0.99
33	NO_TS_MO_64045	11.40°W	59.10°N	1.0	-0.06	0.31	0.98
34	NO_TS_MO_64046	4.50°W	60.70°N	1.0	-0.50	0.86	0.92
35	NO_TS_MO_Amelander11	5.48°E	53.51°N	1.0	-0.39	0.55	1.00
36	NO_TS_MO_Amelander12	5.48°E	53.51°N	1.0	-0.28	0.49	1.00
37	NO_TS_MO_Amelander21	5.57°E	53.48°N	1.0	-0.19	0.62	0.99
38	NO_TS_MO_Amelander31	5.60°E	53.45°N	1.0	0.09	0.97	0.96
39	NO_TS_MO_Anasuria	0.79°E	57.26°N	1.0	-0.27	0.38	1.00
40	NO_TS_MO_Borkum	6.75°E	53.57°N	1.0	-0.76	1.14	1.00
41	NO_TS_MO_BuoyBunkerHill1	8.27°E	54.79°N	0.5	-0.19	0.43	1.00
42	NO_TS_MO_BuoyHoernumTief1	8.38°E	54.78°N	0.0	-0.36	0.93	0.98
43	NO_TS_MO_ElbeWR	8.11°E	54.02°N	0.5	-0.30	0.58	1.00
44	NO_TS_MO_Europlatform2	3.28°E	52.00°N	1.0	0.09	0.42	1.00
45	NO_TS_MO_Europlatform	3.28°E	52.00°N	1.0	0.41	0.78	0.99
46	NO_TS_MO_FINO1WR	6.58°E	54.00°N	0.5	-0.12	0.50	1.00
47	NO_TS_MO_FINO3FerryBox	7.16°E	55.19°N	1.0	-0.56	0.64	1.00
47	NO_TS_MO_FINO3FerryBox	7.16°E	55.19°N	17.0	-1.25	1.92	0.95
48	NO_TS_MO_FINO3WR	7.16°E	55.19°N	0.5	-0.17	0.38	1.00
49	NO_TS_MO_Heimdal	2.23°E	59.57°N	0.0	-0.23	0.46	0.99
50	NO_TS_MO_HelgolandFerryBox	7.89°E	54.19°N	1.0	-0.33	0.59	1.00
51	NO_TS_MO_Helgoland-NorthWR	7.82°E	54.22°N	0.5	-0.05	0.40	1.00
52	NO_TS_MO_HelgolandRM	7.90°E	54.17°N	1.0	-0.09	0.77	0.99
53	NO_TS_MO_HelgolandWR	7.89°E	54.18°N	0.5	-0.41	0.69	1.00
54	NO_TS_MO_Hoernum	8.30°E	54.75°N	1.0	-0.67	1.21	0.99
55	NO_TS_MO_IJmuidenMunitiestort	4.06°E	52.55°N	1.0	-0.18	0.49	1.00
56	NO_TS_MO_Ijmuiden	4.56°E	52.46°N	1.0	-1.00	1.11	1.00
57	NO_TS_MO_K13a3	3.22°E	53.22°N	1.0	-0.20	0.53	0.99
58	NO_TS_MO_LichteilandGoeree1	3.67°E	51.93°N	1.0	-0.23	0.47	1.00
59	NO_TS_MO_LichteilandGoeree2	3.67°E	51.93°N	1.0	-0.19	0.47	1.00
60	NO_TS_MO_NsbIIIWR	6.78°E	54.68°N	0.5	-0.19	0.55	1.00
61	NO_TS_MO_NsbIIWR	6.33°E	55.00°N	0.5	-0.21	0.51	1.00
62	NO_TS_MO_Roscoff	3.96°W	48.72°N	1.0	-0.05	0.43	0.99
63	NO_TS_MO_SchiermonnikoogNoord	6.17°E	53.60°N	1.0	-0.33	0.58	1.00
64	NO_TS_MO_Sylt	8.09°E	54.92°N	0.5	-0.35	1.30	0.98

no	mooring name	longitude	latitude	depth (m)	mean bias (°C)	RMSD (°C)	corre-lation
65	NO_TS_MO_WaddenEierlandseGat	4.66°E	53.28°N	1.0	-0.31	0.52	1.00
66	NO_TS_MO_WaddenSchiermonnikoog	6.17°E	53.60°N	1.0	-0.25	0.53	1.00
67	NO_TS_MO_Westhinder	2.44°E	51.39°N	1.0	-0.02	0.24	1.00

IV.1.4 Multi-Model Ensemble mean

The MME MYP V5 is a weighted ensemble mean of monthly temperature and salinity fields of three CMEMS reanalysis products from the GLO MFC (GLORYS12), IBI MFC (IBIRYS) and NWS MFC (AMM7 V5). The weights for each ensemble member are calculated using the KLIWAS North Sea climatology (https://icdc.cen.uni-hamburg.de/en/knsc-hydrographic.html), a gridded set of yearly and monthly mean hydrographic and surface meteorological data (1993 – 2012), and the CMEMS MultiOBS product MULTIOBS_GLO_PHY_REP_015_002 (2013 – 2019). The MME MYP is available as a CMEMS internal product since 3rd July 2020.

The temperature fields of AMM7 V5 at 0, 10, 30, 75, 300, 750 and 2000 m depths are compared to the MME MYP ensemble mean temperature (Figure 13). AMM7 V5 is generally warmer near the surface (0 and 10 m) with colder bias in coastal regions. For depth between 30 and 750 m a colder bias with warmer biases in some regions on-shelf and along the Western model boundary can be observed. In the region around the Faeroe Islands, AMM7 V5 shows a large cold bias for 75 and 300 m. Below 30 m, areas of slightly positive bias increase with increasing depth (75, 300, 750 m). At 2000 m, AMM7 V5 is generally warmer by more than ~0.5°C. Along the bottom, AMM7 V5 is warmer in most regions, except along bathymetrically distinct areas, such as the Northwest Shelf edge, the Norwegian Trench and the region around the Faeroe Islands, which all show colder AMM7 V5 values than the ensemble mean.

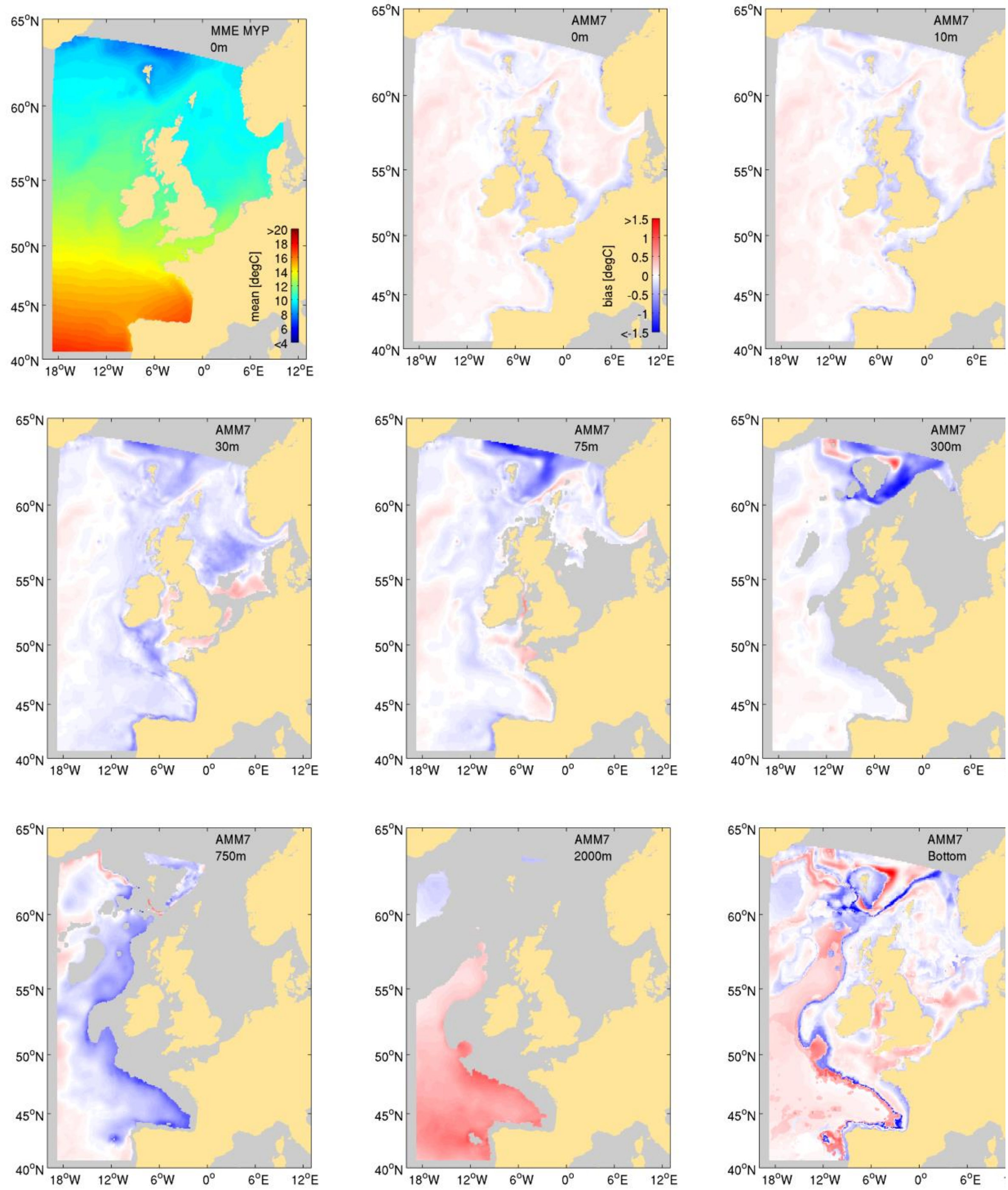

Figure 14: Bias (AMM7 V5 – MME MYP) between AMM7 V5 temperature (1993-2018) and the MME MYP V4 mean at different depth levels. The upper left panel shows the MME MYP V4 mean at the surface. The lower right panel shows the bias at the bottom.

The monthly mean biases show seasonal changes, and the variability increases slightly in 2013 – 2018 for 0 m and 10 m (Figure 14). Highest positive biases occur in June, July and August for these depths, while lowest biases in 30 m depth occur in August and September. In 1998 and 2004 two outliers with high negative biases occur in depth layers until 750 m. In 0 and 10 m depth the negative biases occur in the beginning and end of 1998 and 2004 whereas in higher depths the negative biases occur during the summer months July and August.

Generally, AMM7 V5 underestimates the temperature relative to the ensemble most of the time for depth between 30 m and 750 m. Without the outliers the bias near the surface (0 m, 10 m) varies between +0.23°C and -0.49°C and for depths 30 m and 75 m between +0.11°C and –0.51°C. At 300 and 750 m, the bias is almost always negative, varying between +0.02°C and -0.73°C. For deep layers (2000 m), AMM7 V5 exceeds the ensemble temperature by 0.16 – 0.8 °C and at the bottom layer the bias varies between 0.14°C and -0.3°C.

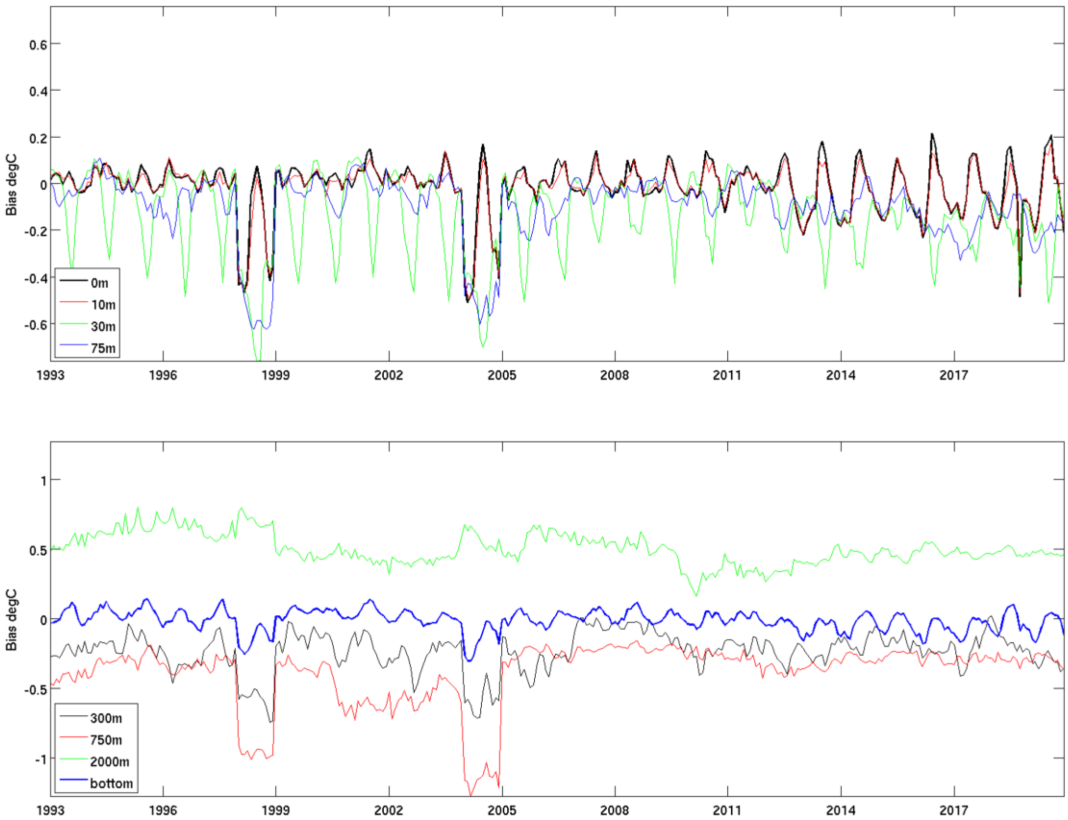

Figure 15: Monthly mean biases (AMM7 V5 – MME MYP V5) for model temperature compared to the MME MYP V5 mean, for different depth layers averaged over the model domain. Note, that the ordinates have different values in both panels.

IV.1.5 Temperature for Interim updates

Quality of interim is compared against satellite SST product and against mooring data.

Figure 16 shows bias and RMSD for INT surface temperature (Jul-Dec 2020) against the satellite product SST_GLO_SST_L4_NRT_OBSERVATIONS_010_001. There is a slight warm bias except for in the eastern North Sea. RMSD values are generally less than 0.4K on the continental shelf, consistent with the RAN EAN of 0.5K.

Figure 17 shows time series of observed and INT temperature at various depths for selected moorings. Table 3 shows these as statistics of bias, RMSD and correlation. The match to observations is generally good and is comparable to statistics in Table 2 for the reanalysis.

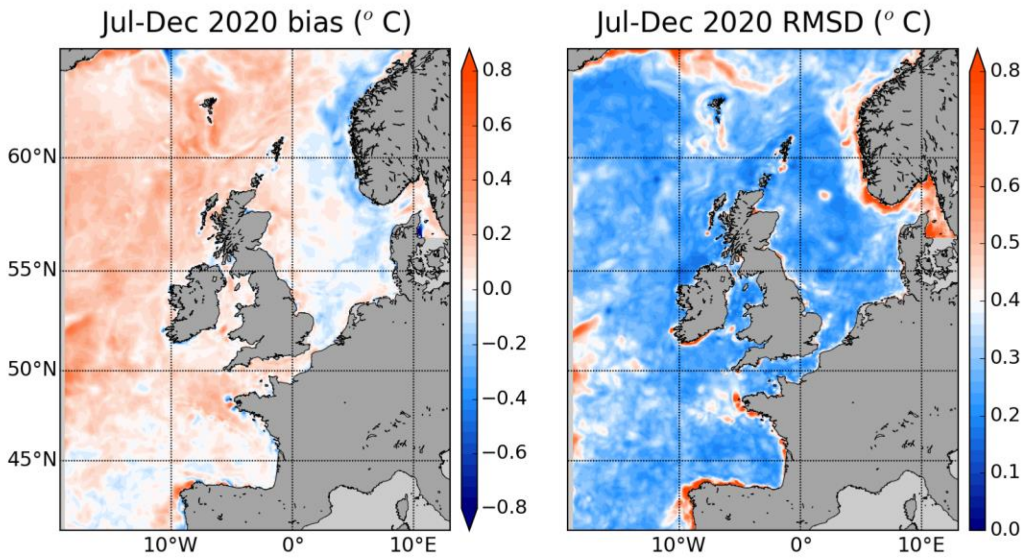

Figure 16: Left: V5-INT – satellite SST bias; right: RMSD for V5-INT compared to satellite SST. Compared to daily values from the satellite product SST_GLO_SST_L4_NRT_OBSERVATIONS_010_001/METOFFICE-GLO-SST-L4-NRT-OBS-SST-V2.

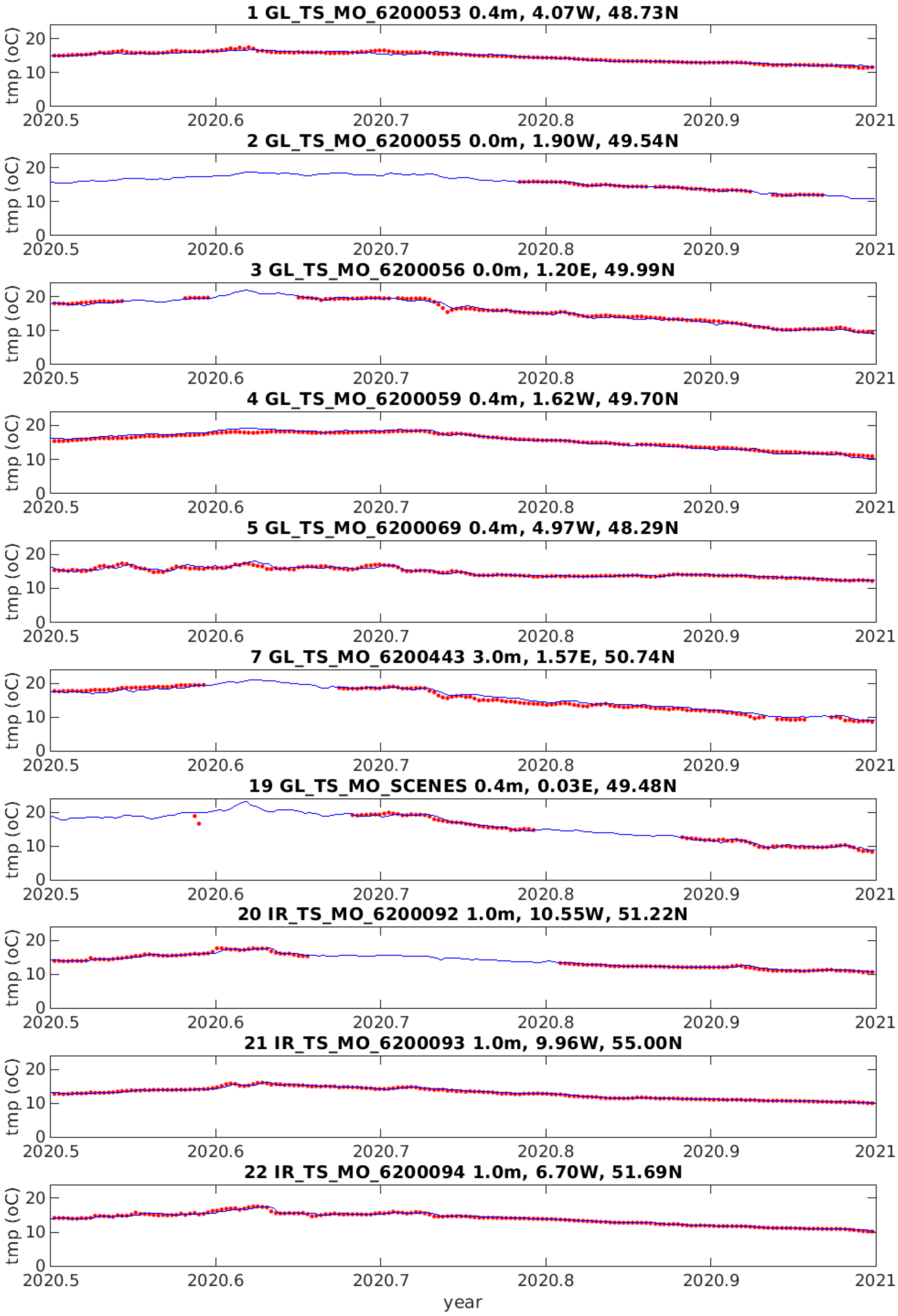

Figure 17: Comparison of daily mean V5-INT temperature with CMEMS observations. The titles contain names from the CMEMS data files and depths, longitudes and latitudes of the observations. The blue line is V5-INT and the red dots are observations. Only CMEMS observations with "good data" quality flags are included.

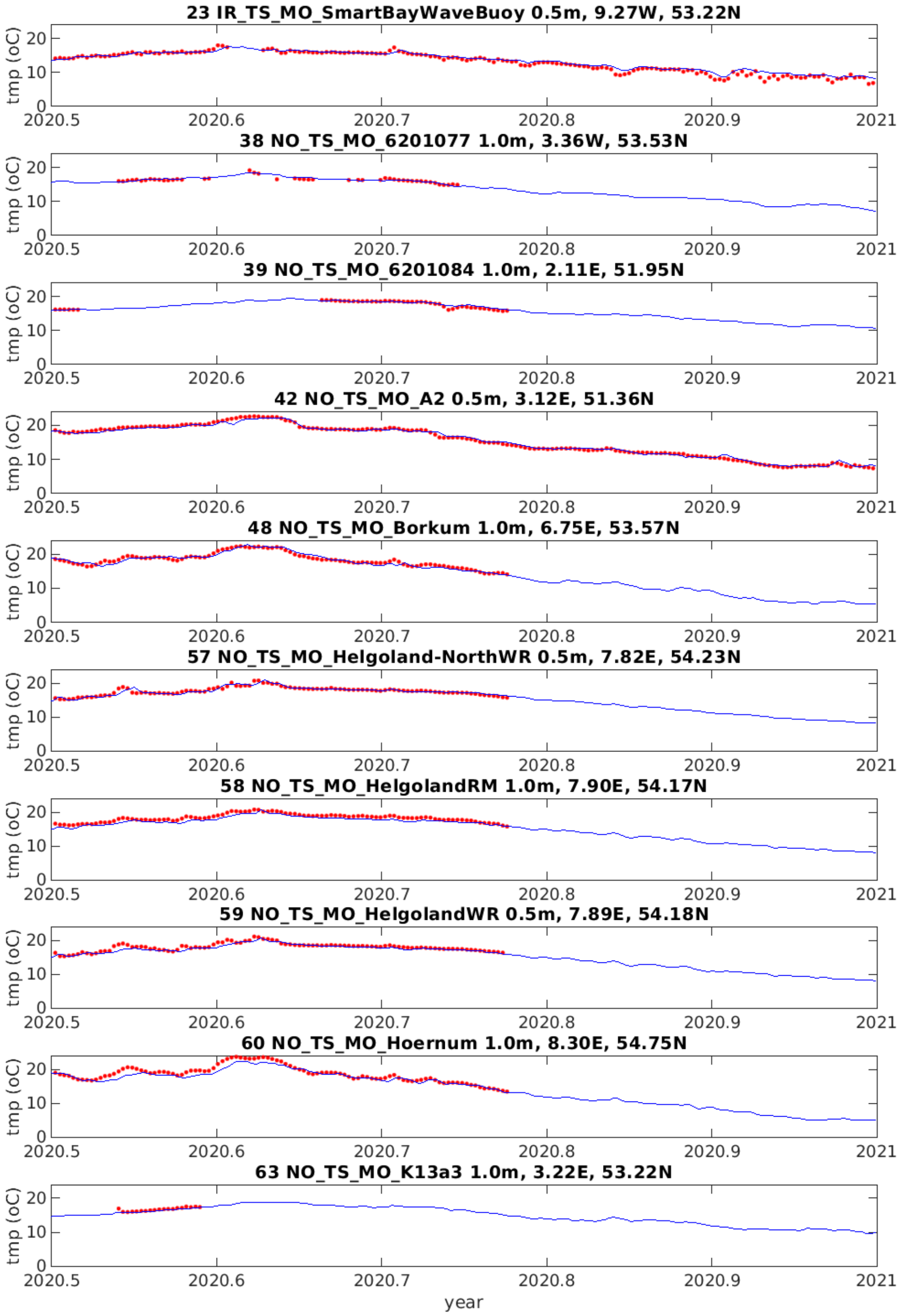

Figure 17: continued

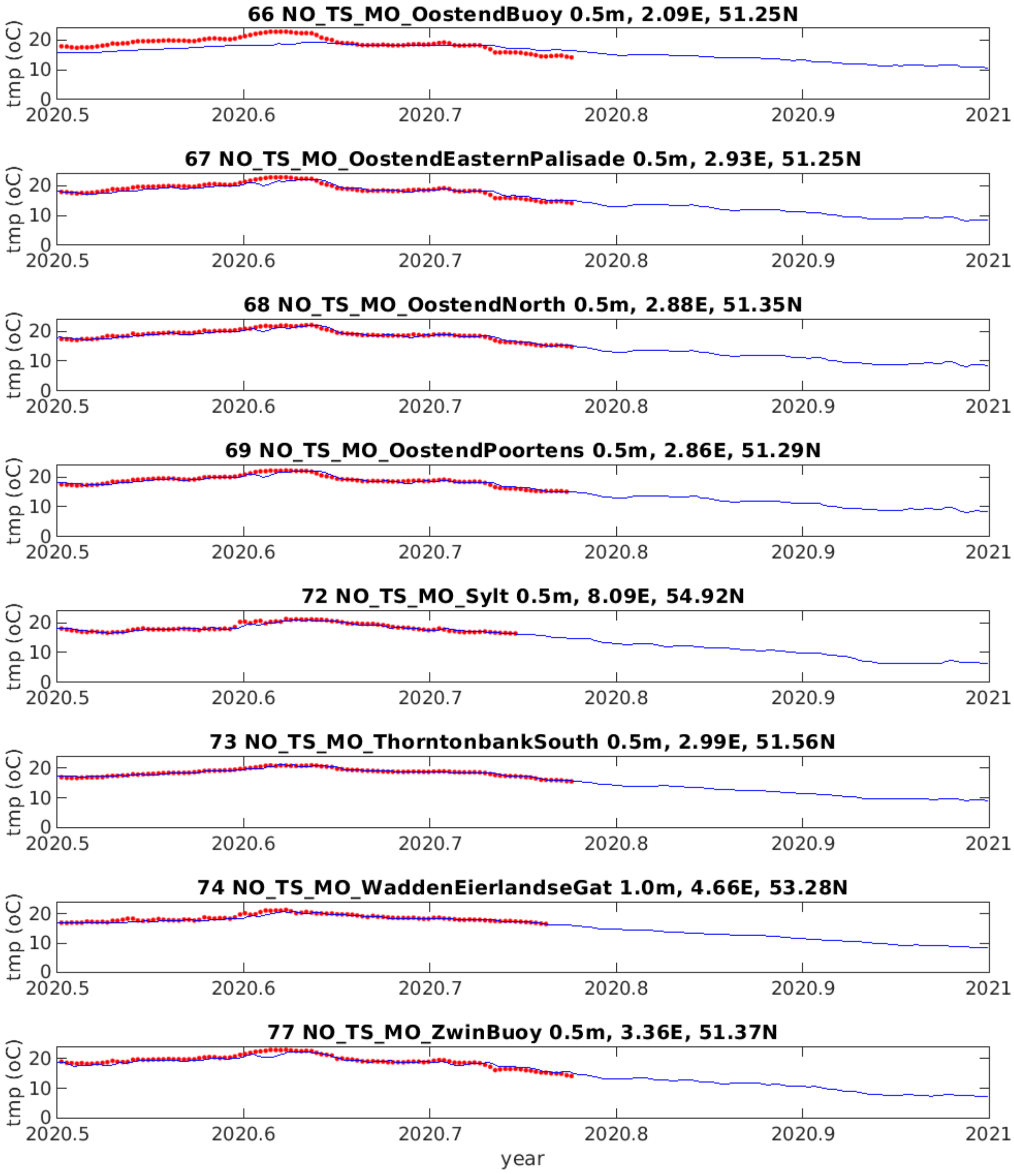

Figure 17: continued

Table 3: Mean bias (V5-INT – observation), root-mean-square difference (RMSD) and correlation coefficient for the CMEMS moorings daily mean temperatures compared to V5-INT.

no	mooring name	longitude	latitude	depth (m)	mean bias (°C)	RMSD (°C)	correl-ation
1	GL_TS_MO_6200053	4.07°W	48.73°N	0.4	-0.07	0.32	0.98
2	GL_TS_MO_6200055	1.90°W	49.54°N	0.0	-0.09	0.12	1.00
3	GL_TS_MO_6200056	1.20°E	49.99°N	0.0	-0.24	0.43	1.00
4	GL_TS_MO_6200059	1.62°W	49.70°N	0.4	0.09	0.52	0.99
5	GL_TS_MO_6200069	4.97°W	48.29°N	0.4	0.05	0.29	0.98
7	GL_TS_MO_6200443	1.57°E	50.74°N	3.0	0.20	0.54	0.99
19	GL_TS_MO_SCENES	0.03°E	49.48°N	0.4	-0.04	0.47	0.99
20	IR_TS_MO_6200092	10.55°W	51.22°N	1.0	0.05	0.12	1.00
21	IR_TS_MO_6200093	9.96°W	55.00°N	1.0	0.03	0.09	1.00
22	IR_TS_MO_6200094	6.70°W	51.69°N	1.0	0.01	0.12	1.00
23	IR_TS_MO_SmartBayWaveBuoy	9.27°W	53.22°N	0.5	0.28	0.64	0.99
38	NO_TS_MO_6201077	3.36°W	53.53°N	1.0	-0.01	0.33	0.93
39	NO_TS_MO_6201084	2.11°E	51.95°N	1.0	0.03	0.31	0.97
42	NO_TS_MO_A2	3.12°E	51.36°N	0.5	-0.12	0.38	1.00
48	NO_TS_MO_Borkum	6.75°E	53.57°N	1.0	-0.16	0.47	0.98
57	NO_TS_MO_Helgoland-NorthWR	7.82°E	54.23°N	0.5	-0.02	0.32	0.97
58	NO_TS_MO_HelgolandRM	7.90°E	54.17°N	1.0	-0.73	0.78	0.98
59	NO_TS_MO_HelgolandWR	7.89°E	54.18°N	0.5	-0.39	0.52	0.96
60	NO_TS_MO_Hoernum	8.30°E	54.75°N	1.0	-0.68	0.85	0.98
63	NO_TS_MO_K13a3	3.22°E	53.22°N	1.0	-0.17	0.29	0.91
66	NO_TS_MO_OostendBuoy	2.09°E	51.25°N	0.5	-1.22	2.11	0.62
67	NO_TS_MO_OostendEasternPalisade	2.93°E	51.25°N	0.5	-0.22	0.62	0.98
68	NO_TS_MO_OostendNorth	2.88°E	51.35°N	0.5	-0.18	0.38	0.99
69	NO_TS_MO_OostendPoortens	2.86°E	51.29°N	0.5	-0.12	0.40	0.98
72	NO_TS_MO_Sylt	8.09°E	54.92°N	0.5	-0.15	0.32	0.98
73	NO_TS_MO_ThorntonbankSouth	2.99°E	51.56°N	0.5	-0.03	0.21	0.99
74	NO_TS_MO_WaddenEierlandseGat	4.66°E	53.28°N	1.0	-0.29	0.38	0.98
77	NO_TS_MO_ZwinBuoy	3.36°E	51.37°N	0.5	-0.31	0.67	0.97

IV.2 Salinity

The reanalysis salinity is validated against three datasets covering different time and space scales:

1. Contemporary salinity observations from World Ocean Database (WOD, https://www.nodc.noaa.gov/OC5/WOD/pr_wod.html).
2. High frequency (hourly to daily to monthly) observations at fixed point moorings.
3. MME MYP ensemble mean.

IV.2.1 World Ocean Database

Reanalysis is compared against observations as for temperature above. The resulting data are binned onto the model grid to give a daily 3D error field. This method prevents observed data sets at high spatial and temporal resolution (e.g. measured by gliders) from unduly influencing the validation compared to other data sources (e.g. CTD casts). The resulting model – observation biases are averaged into layers for the time periods 1993-2018 for V4 (Figure 18) and 1993-2019 for V5 (Figure 19). The majority of these observations will have been assimilated, as there will be overlap with the EN4 observation dataset used in the reanalysis. The V5 biases are generally less than 0.1. The fresh bias above 80 m in the Norwegian Sea that occurred in V4 persists in V5. However, V5 has improved on the isolated regions of fresh biases west of 10°W that occurred in V4. V5 is too salty in the Irish and Celtic Seas and shallower than 30 m in the Norwegian Trench with increased biases from V4. The Bay of Biscay deeper than 2000 m is also too salty in V5.

Mean biases (Figure 20) and root-mean-square differences (RMSDs, Figure 21) averaged over the reanalysis region and for different depth ranges show high monthly variability above 5 m depth in both V4 and V5 (left columns). Above 2000 m depth, the mean biases and RMSDs are similar in V4 and V5. However, isolated error spikes in the V4 reanalysis (e.g. at the end of November 2015) are not present in V5. Below 2000 m, V5 has a mean bias of 0.05, which larger than that of V4. There is no trend in the annual mean biases or RMSD (Figure 20 and Figure 21, middle columns), V5 RMSD are smaller than V4 between 80 and 800 m, but larger than V4 outside of this depth range. Biases above 30 m are highest during the summer; between 30 and 300 m RMSD are smaller during the summer (right columns).

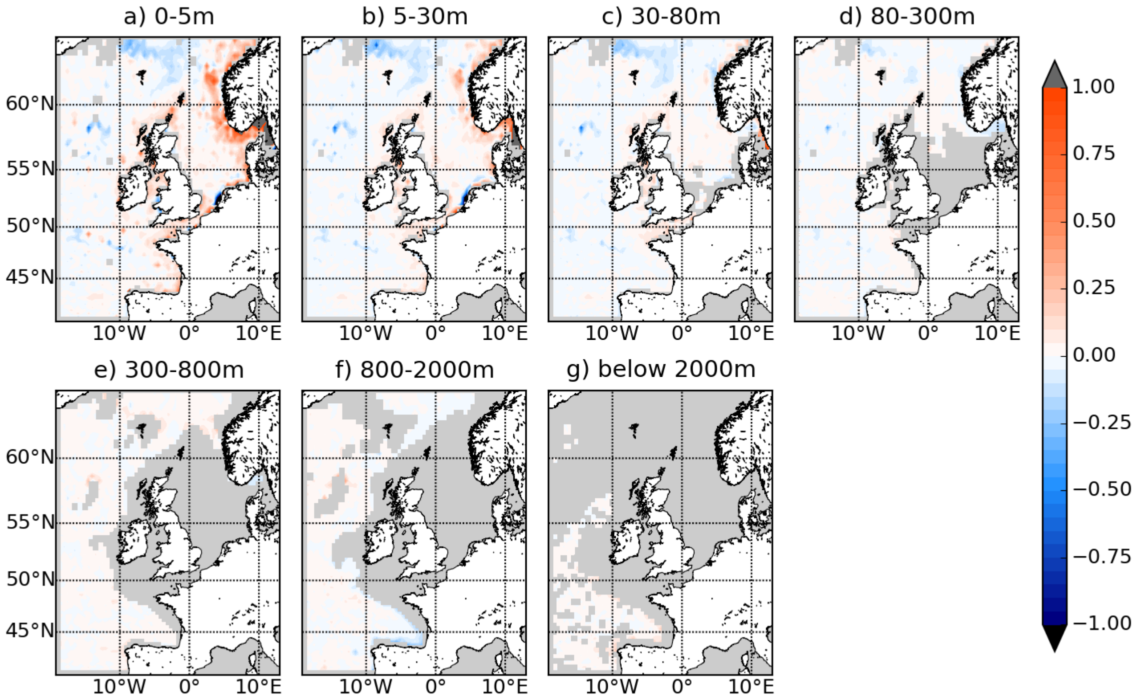

Figure 18: Mean biases between co-located V4 salinities and WOD observations in different layers for 1993-2018. Regions coloured very dark grey have mean bias greater than 1. Regions in light grey are below the sea bed.

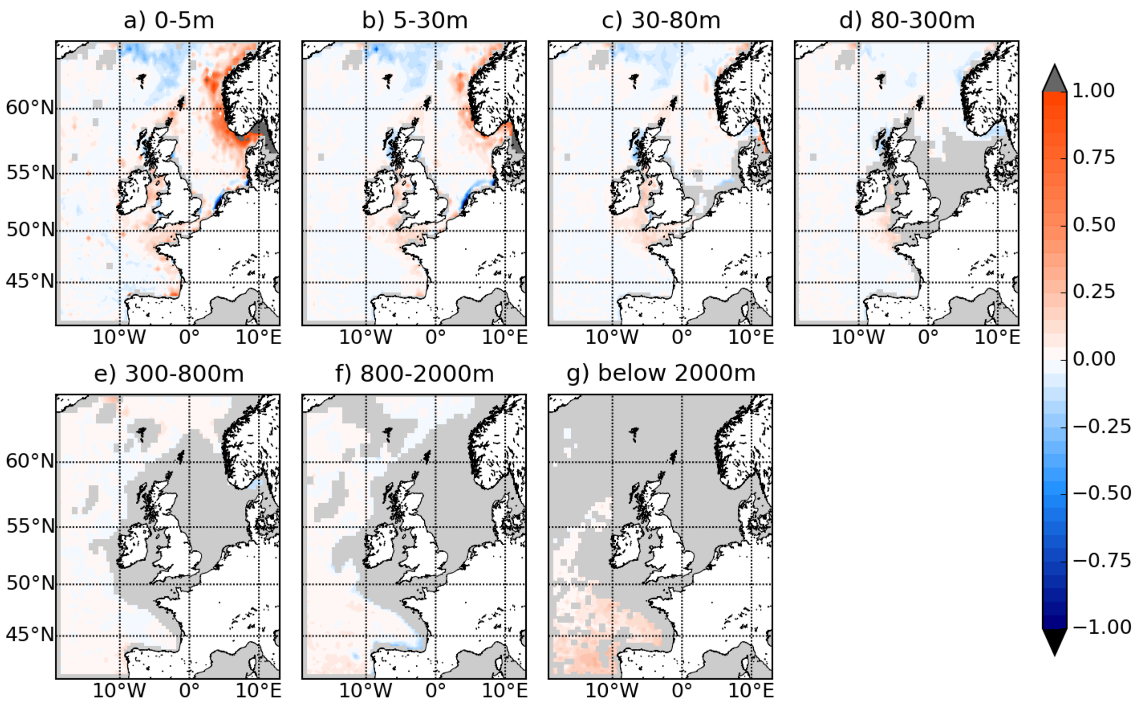

Figure 19: Mean biases between co-located V5 salinities and WOD observations in different layers for 1993-2019. Regions coloured very dark grey have mean bias greater than 1. Regions in light grey are below the sea bed.

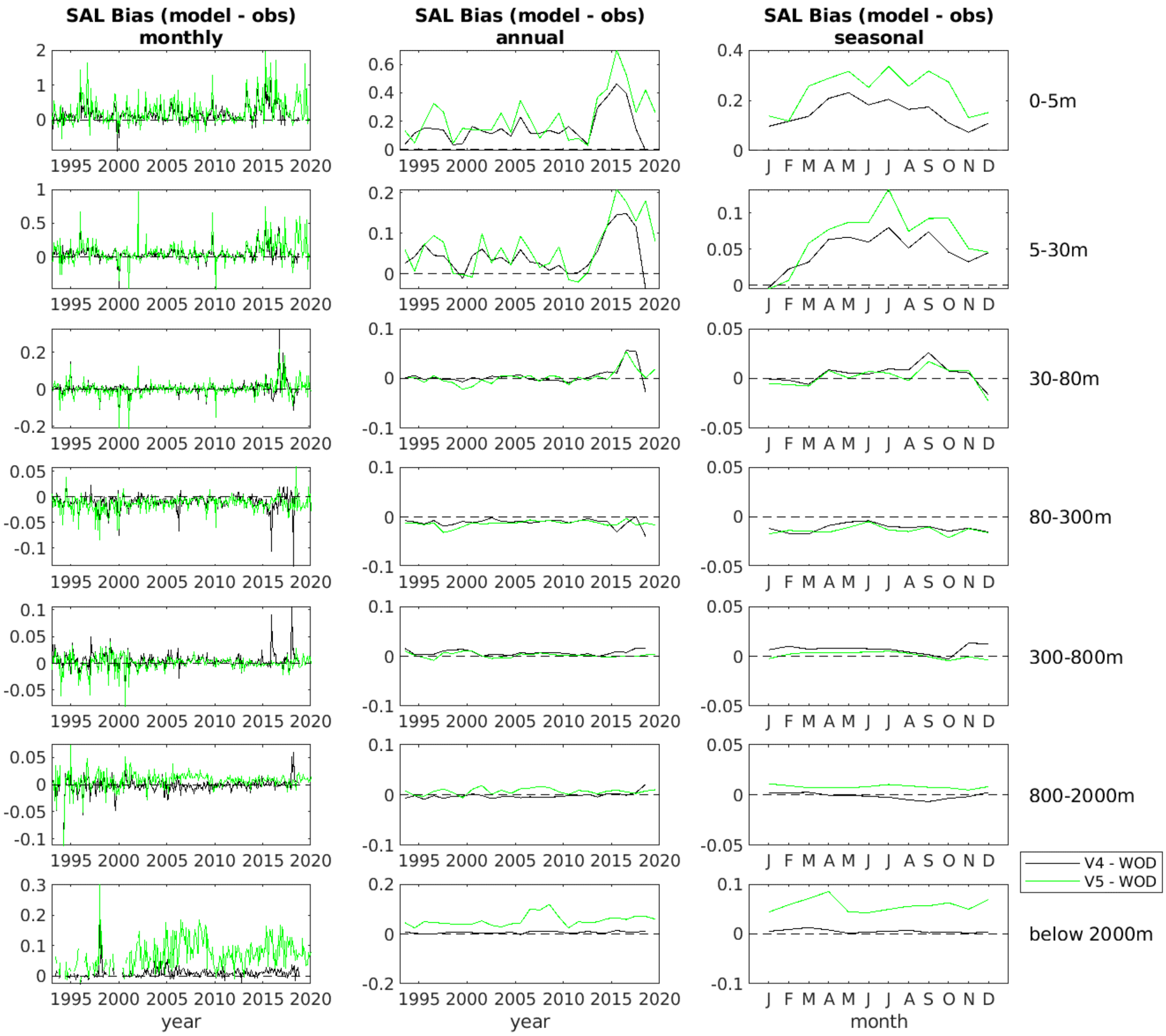

Figure 20: Mean biases (model – observed) for model salinity compared to WOD observations, averaged over different depth layers for the model domain. The left column shows monthly mean biases, the central column is annual mean biases, and the right column is seasonal biases. Annual and seasonal biases are calculated from monthly biases weighted according to the number of observations per month.

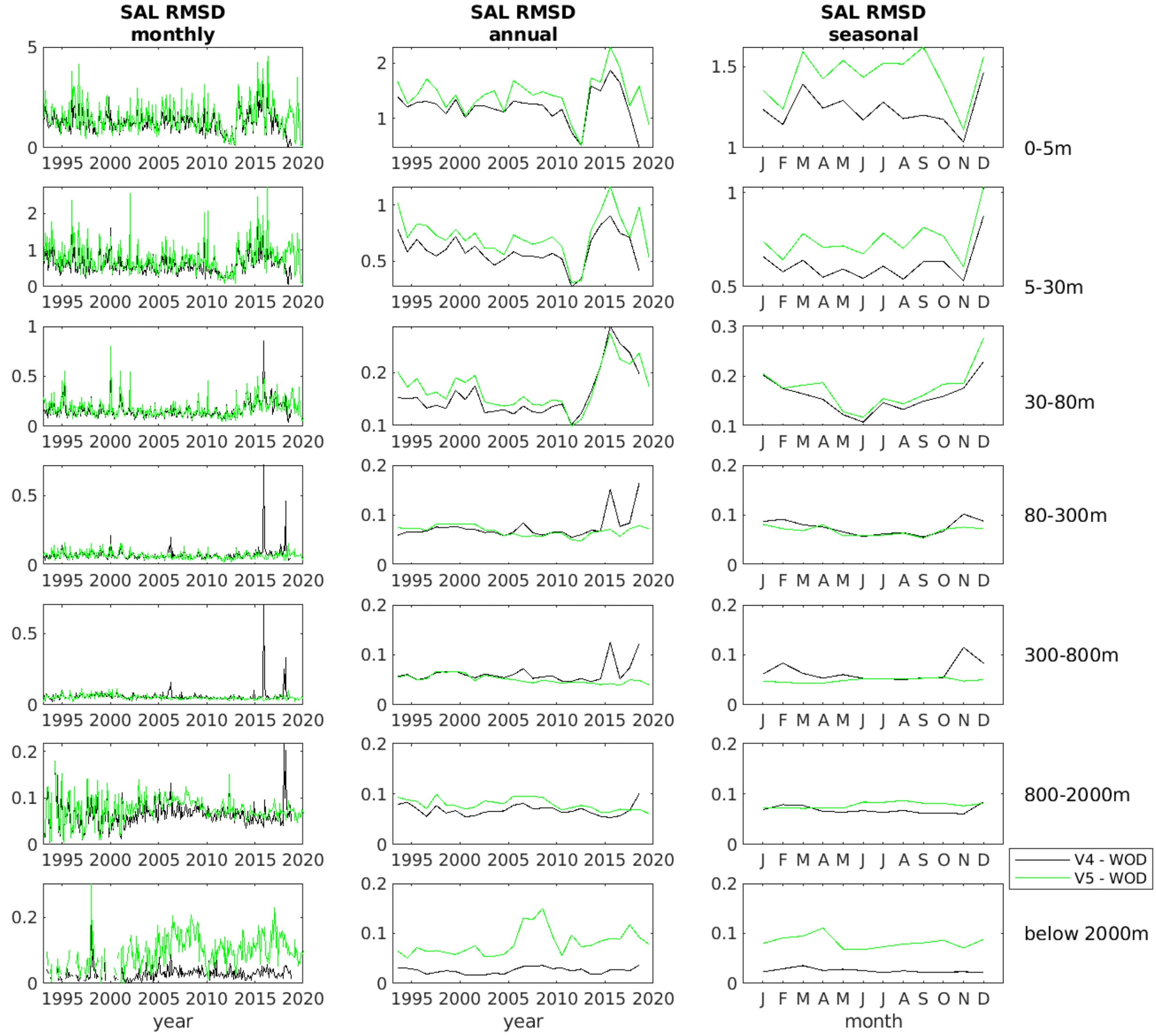

Figure 21: Root-mean-square differences (RMSD) for model salinity compared to WOD observations, averaged over different depth layers for the model domain. The left column shows monthly RMSD, the central column is annual means of the monthly RMSD, and the right column is seasonal RMSD. Annual and seasonal RMSD are calculated from monthly RMSD weighted according to the number of observations per month.

IV.2.2 Mooring data

The V5 reanalysis is compared to time series of observations from L4, E1, Cypris and the CMEMS mooring dataset, described in section IV.1.3. Locations of the datasets are shown in Figure 9. The L4, E1 and Cypris data wasn't assimilated in the reanalysis. Many of the CMEMS moorings will have been assimilated. Only 15 of the CMEMS files contained salinity data. For comparison with the observation time series, V5 salinities are extracted co-located with the date and location of each observation. The Cypris, E1 and L4 data are observed at frequencies of less than 1 day and are compared to the daily mean salinity of the model on the day of observation. The CMEMS time series are generally recorded more than once per day and so for each day all observations recorded are averaged to make a daily mean for comparing to the model. The CMEMS datasets have quality control flags and only data flagged as "good data" are used; additionally any observations that are clearly in error (i.e. out of range or obviously different from the rest of the data) are removed.

At L4, at the surface and 2 m depth, V5 does not capture the variability of the observed salinity (Figure 22). At 45 m deep, the L4 data is less variable and V5 gives a good approximation to the mean value (bias is 0.1) but does not describe completely the monthly to annual variability. RMS differences vary from 0.14 at 45 m depth to 0.35 at the surface (Table 4). The best correlation (0.47) between V5 and the mooring time series is at 2 m depth.

At E1, V5 is on average too fresh at all levels (Figure 23 and Table 4). The variability is of similar magnitude to the observation but does not capture the monthly to annual variability. The best correlation (0.24) between V5 and the mooring time series is at 70 m depth.

From 1994 onwards, surface salinity at Cypris station (Figure 24) shows good agreement between V5 and observations both in mean values and variability. V5 is on average 0.12 too salty and highly correlated (r=0.87) with the mooring time series.

Comparison between V5 salinity and CMEMS mooring observations is shown in Figure 25. There is potentially bad data in the CMEMS files that is not flagged. V5 has RMSDs of less than 1 (Table 4) for six of the mooring time series: stations 18 (NO_TS_MO_6201071), 19 (NO_TS_MO_6201074), 20 (NO_TS_MO_6201077), 21 (NO_TS_MO_6201084) and 47 (NO_TS_MO_FINO3FerryBox, 1 and 17 m depths). The largest RMSD (4.22) is for station 69 (NO_TS_MO_Haringvliet10) at 1 m depth, where V5 has much larger variability than observed and is on average too fresh by 3.55. Correlations between daily mean observed salinity and V5 at the CMEMS moorings range between -0.5 and 0.80 showing good agreement between monthly to annual signals at some moorings but poor agreement at others.

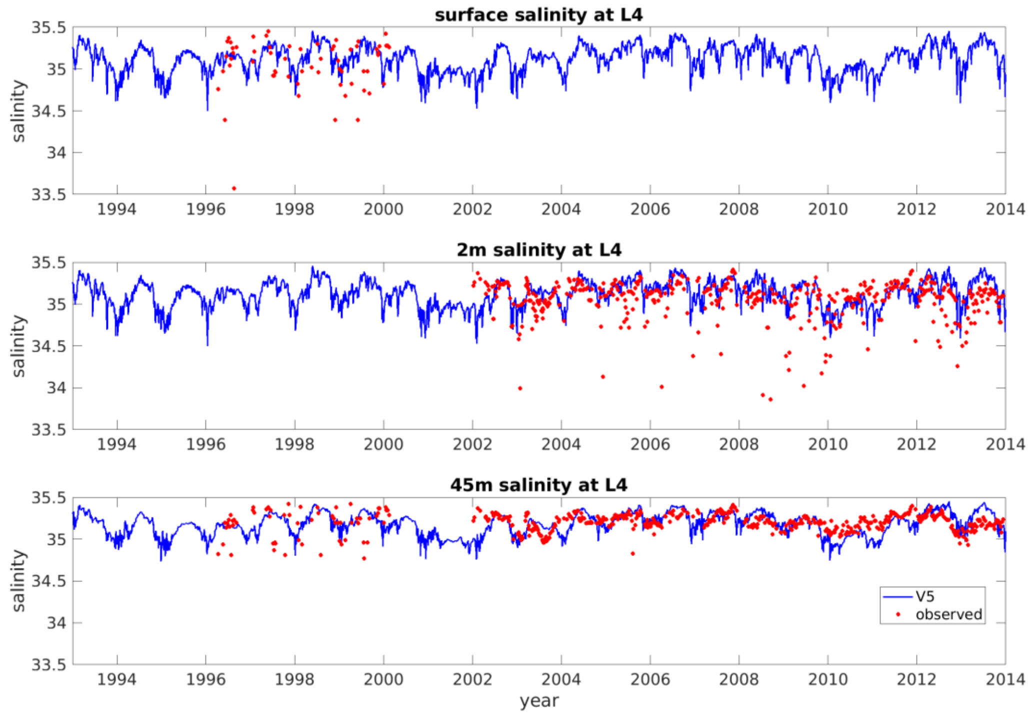

Figure 22: Comparison of daily mean V5 salinities with L4 observations at the surface and at 2 m and 45 m depth.

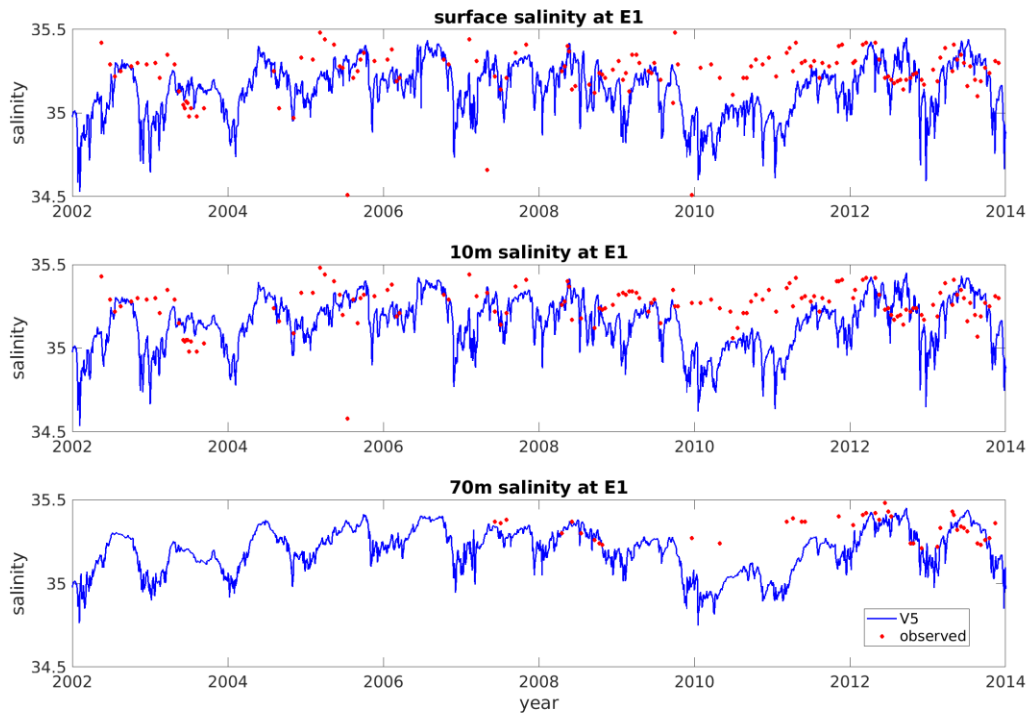

Figure 23: Comparison of daily mean V5 salinities with E1 observations at the surface and at 10 m and 70 m depth.

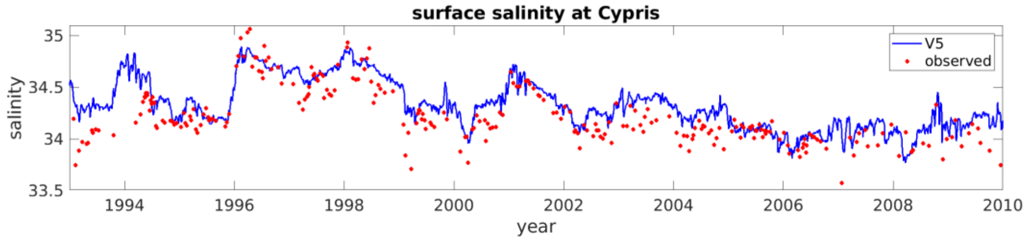

Figure 24: Comparison of daily mean V5 salinities with Cypris observations at the surface.

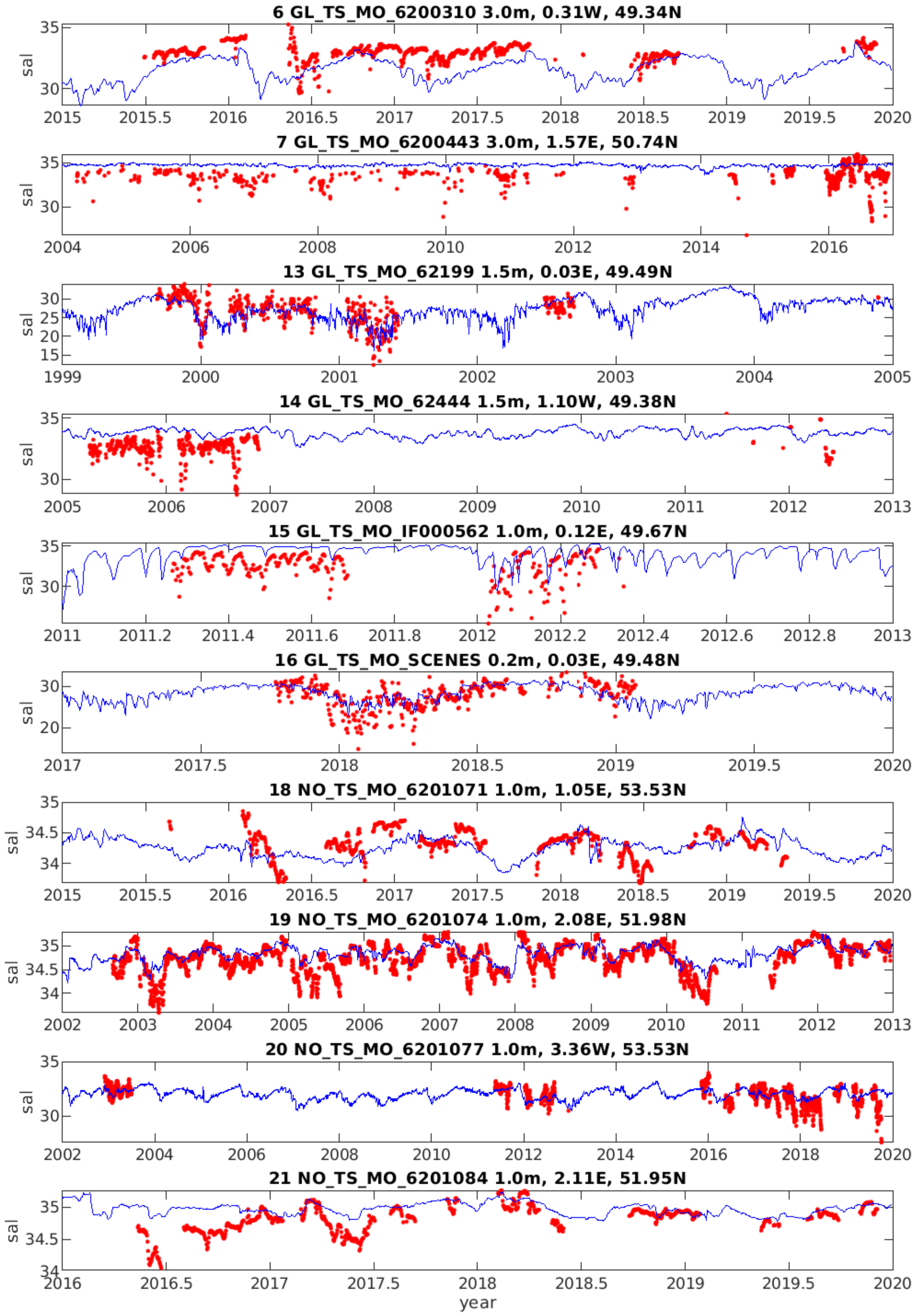

Figure 25: Comparison of daily mean V5 salinities with CMEMS observations. The titles contain: numbers referring to locations in Figure 9, names from the CMEMS data files and depths, longitudes and latitudes of the observations. The blue line is V5 and the red dots the observations.

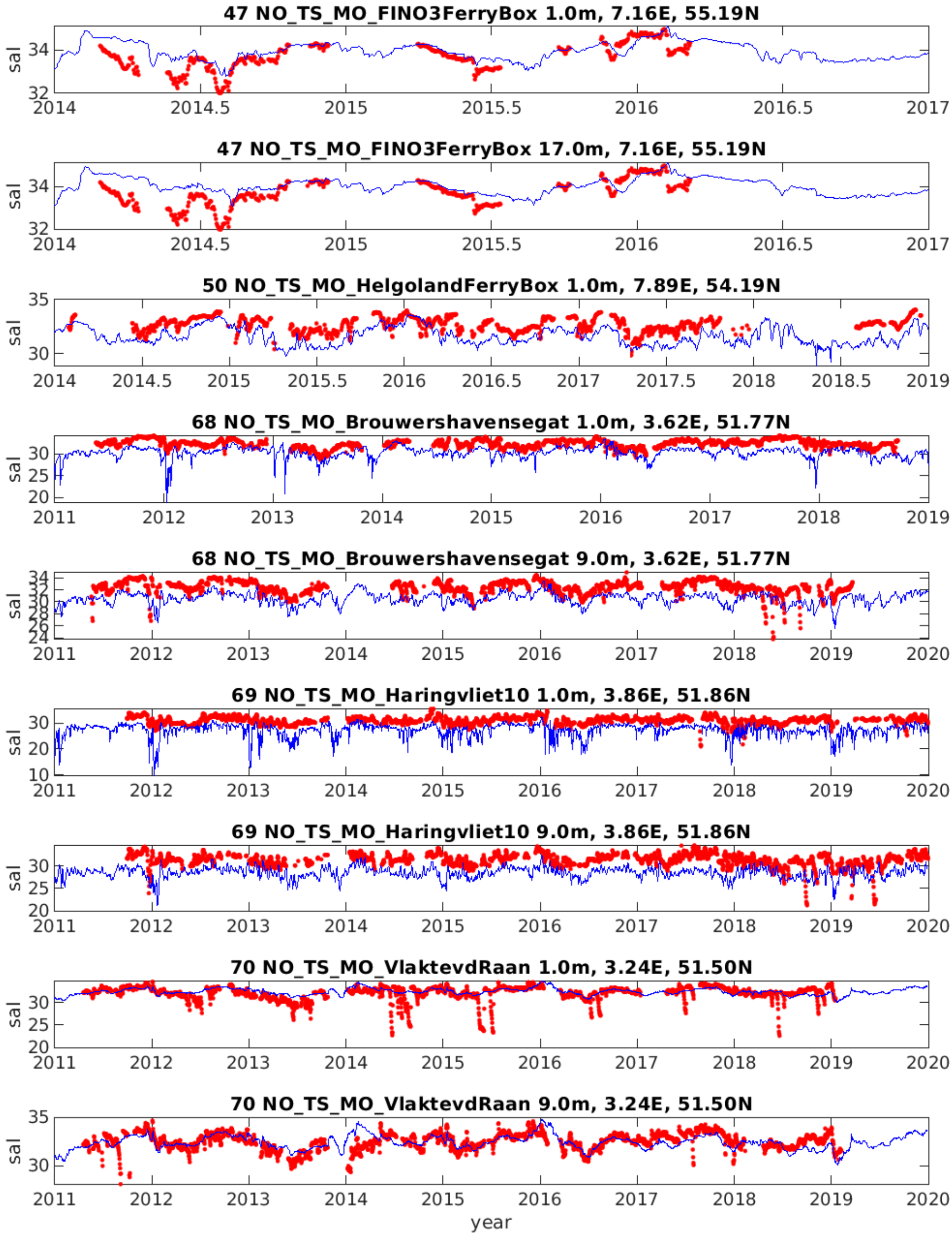

Figure 25, continued.

Table 4: Mean bias (V5 – observation), root-mean-square-difference (RMSD) and correlation coefficient for L4, E1, Cypris and CMEMS moorings daily mean salinities compared to V5.

no	mooring name	longitude	latitude	depth (m)	mean bias	RMSD	corre-lation
-	L4	4.22°W	50.25°N	0.0	0.11	0.35	0.06
-	L4	4.22°W	50.25°N	2.0	0.11	0.24	0.47
-	L4	4.22°W	50.25°N	45.0	0.01	0.14	0.31
-	E1	4.37°W	50.03°N	0.0	-0.07	0.22	0.05
-	E1	4.37°W	50.03°N	10.0	-0.08	0.20	0.01
-	E1	4.37°W	50.03°N	70.0	-0.08	0.15	0.24
-	Cypris	4.83°W	54.09°N	0.0	0.12	0.18	0.87
6	GL_TS_MO_6200310	0.31°W	49.34°N	3.0	-1.03	1.30	0.42
7	GL_TS_MO_6200443	1.57°E	50.74°N	3.0	1.20	1.64	0.25
13	GL_TS_MO_62199	0.03°E	49.49°N	1.5	-0.60	2.32	0.80
14	GL_TS_MO_62444	1.10°W	49.38°N	1.5	1.27	1.55	-0.05
15	GL_TS_MO_IF000562	0.12°E	49.67°N	1.0	1.93	2.39	0.58
16	GL_TS_MO_SCENES	0.03°E	49.48°N	0.2	0.27	2.33	0.72
18	NO_TS_MO_6201071	1.05°E	53.53°N	1.0	-0.05	0.25	0.20
19	NO_TS_MO_6201074	2.08°E	51.98°N	1.0	0.12	0.24	0.75
20	NO_TS_MO_6201077	3.36°W	53.53°N	1.0	0.17	0.82	0.44
21	NO_TS_MO_6201084	2.11°E	51.95°N	1.0	0.17	0.24	0.60
47	NO_TS_MO_FINO3FerryBox	7.16°E	55.19°N	1.0	0.31	0.53	0.74
47	NO_TS_MO_FINO3FerryBox	7.16°E	55.19°N	17.0	0.40	0.65	0.60
50	NO_TS_MO_HelgolandFerryBox	7.89°E	54.19°N	1.0	-1.05	1.19	0.72
68	NO_TS_MO_Brouwershavensegat	3.62°E	51.77°N	1.0	-1.95	2.23	0.52
68	NO_TS_MO_Brouwershavensegat	3.62°E	51.77°N	9.0	-1.91	2.19	0.50
69	NO_TS_MO_Haringvliet10	3.86°E	51.86°N	1.0	-3.55	4.22	0.46
69	NO_TS_MO_Haringvliet10	3.86°E	51.86°N	9.0	-2.70	3.08	0.41
70	NO_TS_MO_VlaktevdRaan	3.24°E	51.50°N	1.0	0.34	1.50	0.42
70	NO_TS_MO_VlaktevdRaan	3.24°E	51.50°N	9.0	-0.07	0.80	0.50

Comparison of hourly surface salinity fields against EN4 mooring data (Figure 26) shows RMS differences at the lower range of those for individual moorings above.

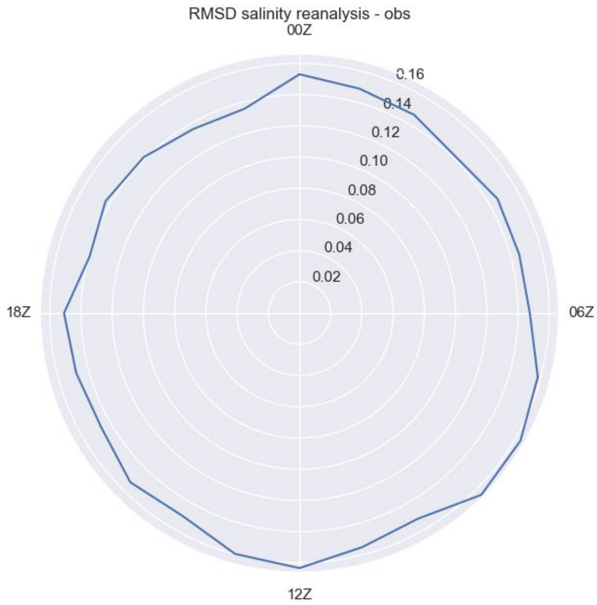

Figure 26 RMSD surface salinity (PSU), reanalysis minus EN4 in situ observations, plotted against time of day

IV.2.3 Multi-Model Ensemble mean

The salinity fields of AMM7 V5 at 0, 10, 30, 75, 300, 750 and 2000 m depth are compared to the MME MYP ensemble mean salinity (Figure 25). In the upper layers (0, 10, 30 m), there are strong positive biases in the Norwegian Trench, indicating that the Baltic outflow is too salty in AMM7 V5. Large negative biases occur along the coasts in the Southern North Sea and off western Scotland, likely due to differences in river discharges. Areas with positive bias occur in the English Channel and in the Irish Sea. The area around the Faeroe Islands is characterized by fresh biases. At 2000 m depth, AMM7 V5 overestimates the ensemble salinity. At the sea bottom, the same pattern of positive and negative biases as in the surface layer occurs close to the coasts. There are negative biases along distinct bathymetric features, such as the Northwest Shelf edge.

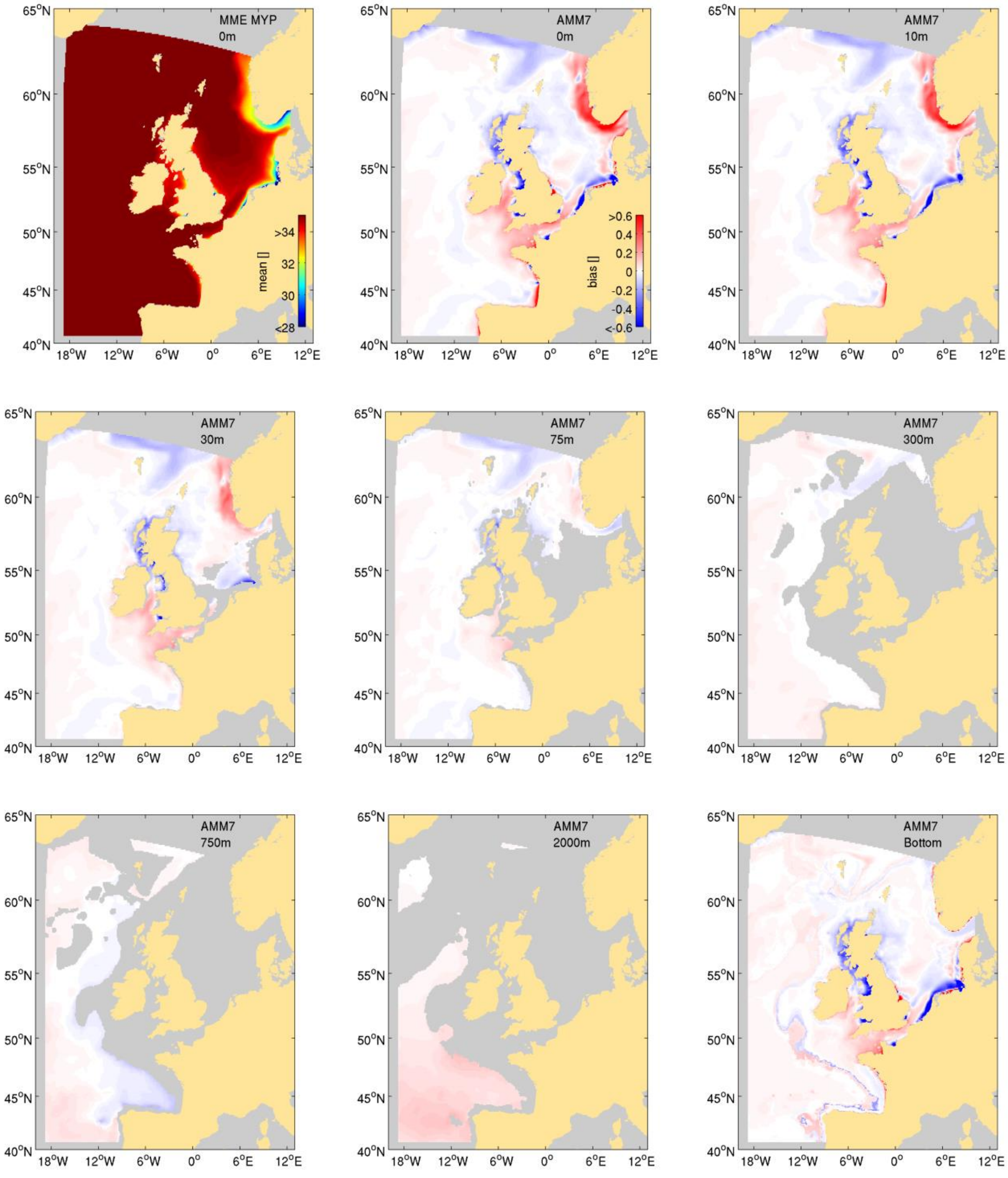

Figure 27 Bias (AMM7 V5 – MME MYP) between AMM7 V5 salinity (1993-2019) and the MME MYP mean at different depth levels. The upper left panel shows the MME MYP mean salinity at the surface. The lower right panel shows the bias at the bottom.

The monthly mean salinity biases are higher near the surface (0, 10 m), varying between -0.24 and 0.24 (Figure 26). The highest biases cannot be clearly assigned to a specific season. With increasing depth, variability decreases. Salinity biases in 30 and 75 m depth are varying between -0.08 and 0.08. In 300 and 750 m depths, AMM7 V5 underestimates the ensemble salinity over most of the reanalysis period. In contrast, the salinity biases in 2000 m depth show consistently positive values. The AMM7 V5 salinity in the bottom layer is slightly negative for most of the reanalysis period, which might be due to regions with large negative biases along the distinct bathymetric features and close to river mouths (Figure 25).

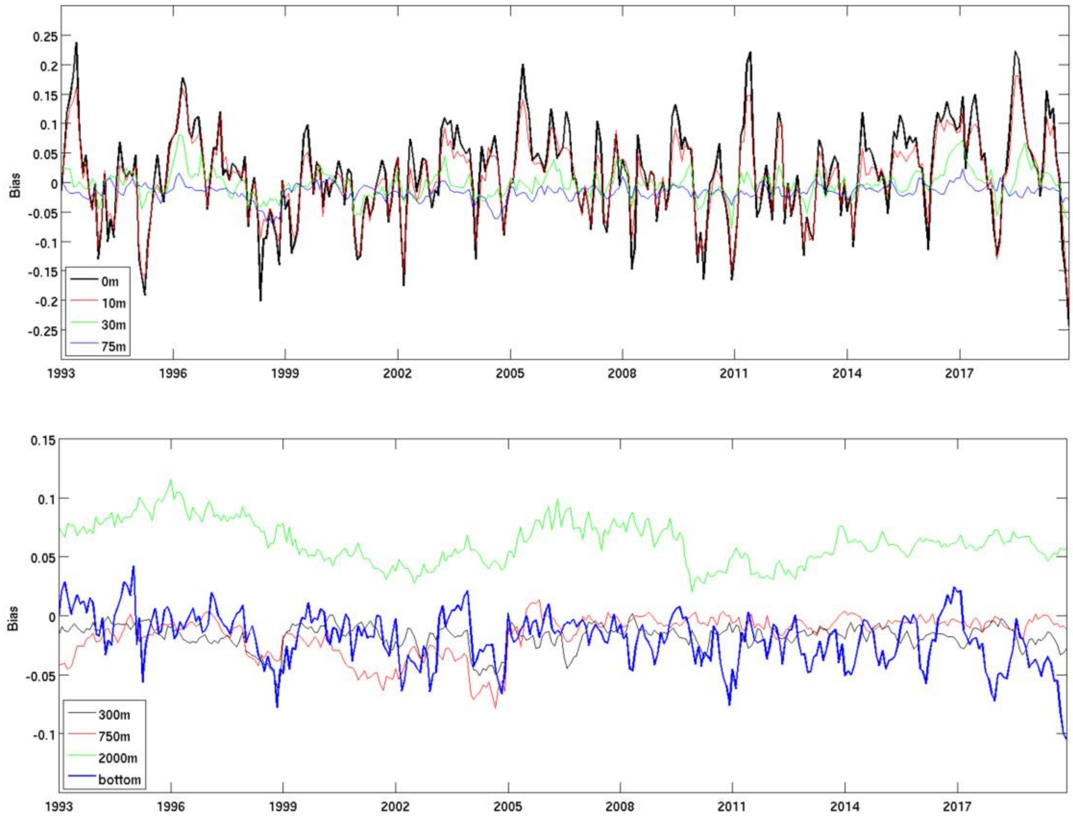

Figure 28 Monthly mean biases (AMM7 – MME MYP) for model salinity compared to the MME MYP mean, for different depth layers averaged over the model domain. Note, that the ordinates have different values in both panels.

IV.2.4 Salinity for Interim updates

Quality of interim is assessed against mooring data. Figure 29 and Table 5 compare INT salinity against observations at various depths. Many of the RMSD values are less than 1.2, the EAN value for the Shelf. Some RMSD values are much larger. The time series show that there is noise in the observations with perhaps some bad data included in the statistics. A comparison of maps of INT monthly means against the RAN climatology (not shown) do not reveal any problems with the INT salinity.

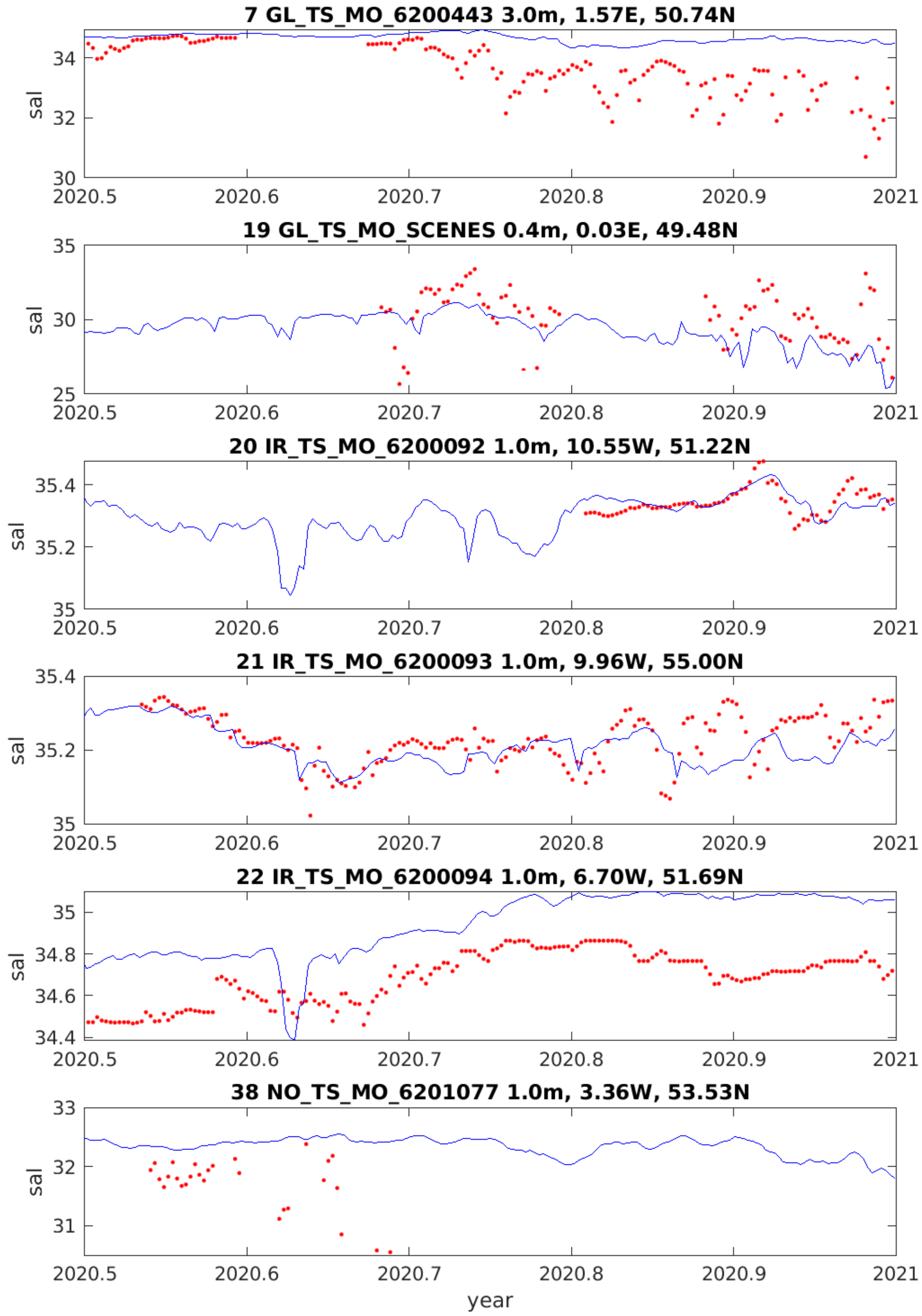

Figure 29: Comparison of daily mean V5-INT salinity with CMEMS observations. The titles contain names from the CMEMS data files and depths, longitudes and latitudes of the observations. The blue line is V5-INT and the red dots are observations. Only CMEMS observations with "good data" quality flags are included.

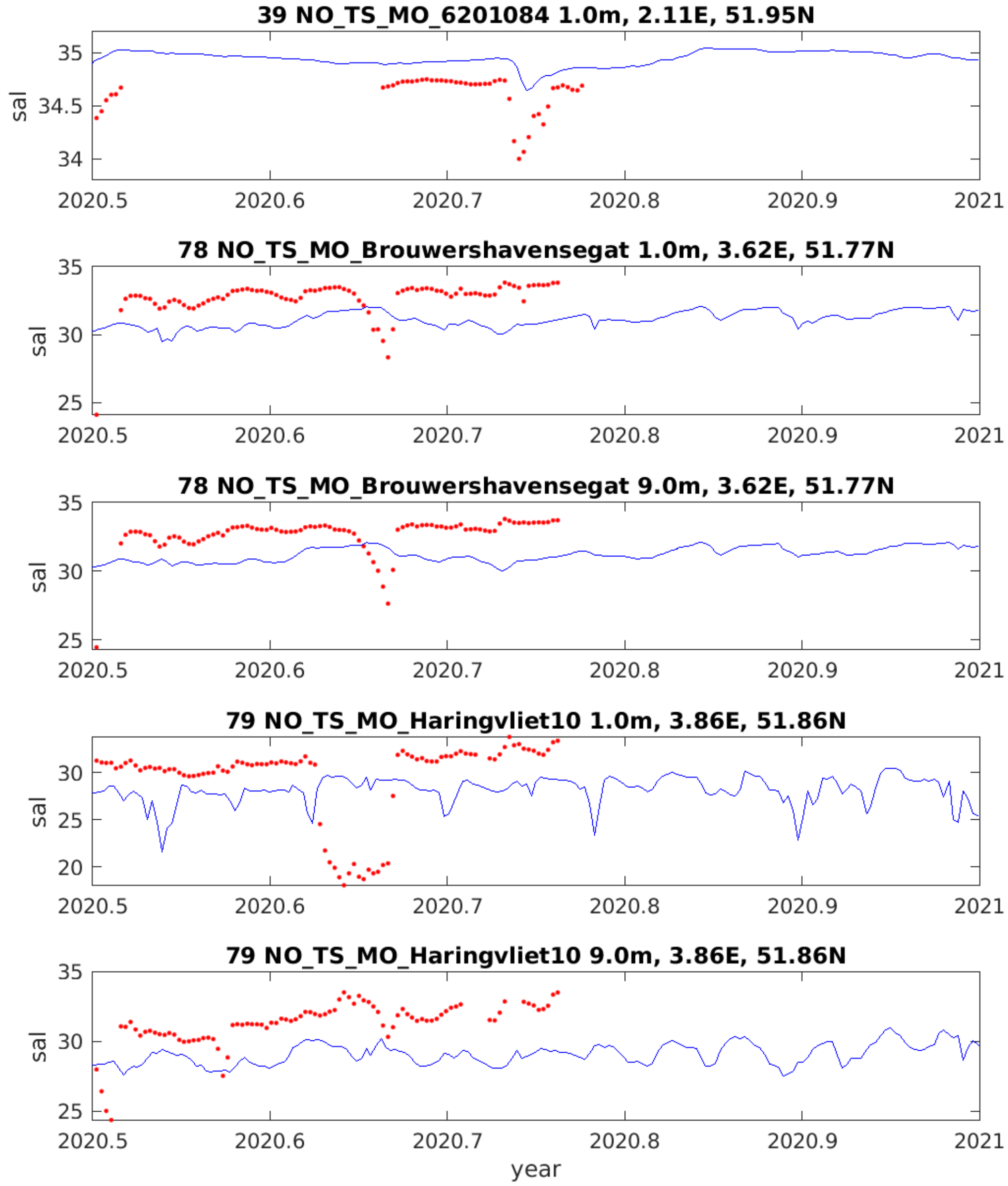

Figure 29: continued

Table 5: Mean bias (V5-INT – observation), root-mean-square difference (RMSD) and correlation coefficient for the CMEMS moorings daily mean salinities compared to V5-INT.

no	mooring name	longitude	latitude	depth (m)	mean bias	RMSD	correl-ation
7	GL_TS_MO_6200443	1.57°E	50.74°N	3.0	1.02	1.29	0.63
19	GL_TS_MO_SCENES	0.03°E	49.48°N	0.4	-1.21	1.97	0.54
20	IR_TS_MO_6200092	10.55°W	51.22°N	1.0	0.00	0.03	0.66
21	IR_TS_MO_6200093	9.96°W	55.00°N	1.0	-0.02	0.06	0.52
22	IR_TS_MO_6200094	6.70°W	51.69°N	1.0	0.26	0.27	0.79
38	NO_TS_MO_6201077	3.36°W	53.53°N	1.0	2.55	3.62	-0.28
39	NO_TS_MO_6201084	2.11°E	51.95°N	1.0	0.36	0.71	0.13
78	NO_TS_MO_Brouwershavensegat	3.62°E	51.77°N	1.0	-1.66	2.44	0.11
78	NO_TS_MO_Brouwershavensegat	3.62°E	51.77°N	9.0	-1.49	2.39	0.11
79	NO_TS_MO_Haringvliet10	3.86°E	51.86°N	1.0	-1.46	4.97	-0.28
79	NO_TS_MO_Haringvliet10	3.86°E	51.86°N	9.0	-2.36	2.75	0.46

IV.3 Currents

NOAA AOML (Atlantic Oceanographic and Meteorological Observatory) make available a 30-year climatology of near-surface current from satellite-tracked drifting buoy data (Laurindo et al., 2017). The zonal and meridional velocities are provided on a ¼ degree grid and are taken to represent currents at 15 m depth. They are used here as a reference for the reanalysis, averaged over the whole period and also averaged by month.

V5 Mean current speed (Figure 30) shows overall that the main features of the near-surface flow are represented. The slope current on the northern edge of the Shetland shelf is well defined and North Atlantic current to the north of the British Isles are well delineated in V5. In the reanalysis, the slope current has a slightly stronger core but is narrower than the NOAA climatology. This is seen in the differences plot (Figure 30). Other features defined by the underlying bathymetry can be seen in both reanalysis and climatology, for instance along the western edge of the North-West Shelf, and structures in the North Atlantic Current through the waters between Iceland and the British Isles. The largest differences off the shelf are in the West European Basin to the north-east of Spain, where the reanalysis has stronger near-surface currents. In the Celtic Sea, reanalysis currents look to be weaker than the climatology. Similar features are seen in the V4 reanalysis (Figure 31).

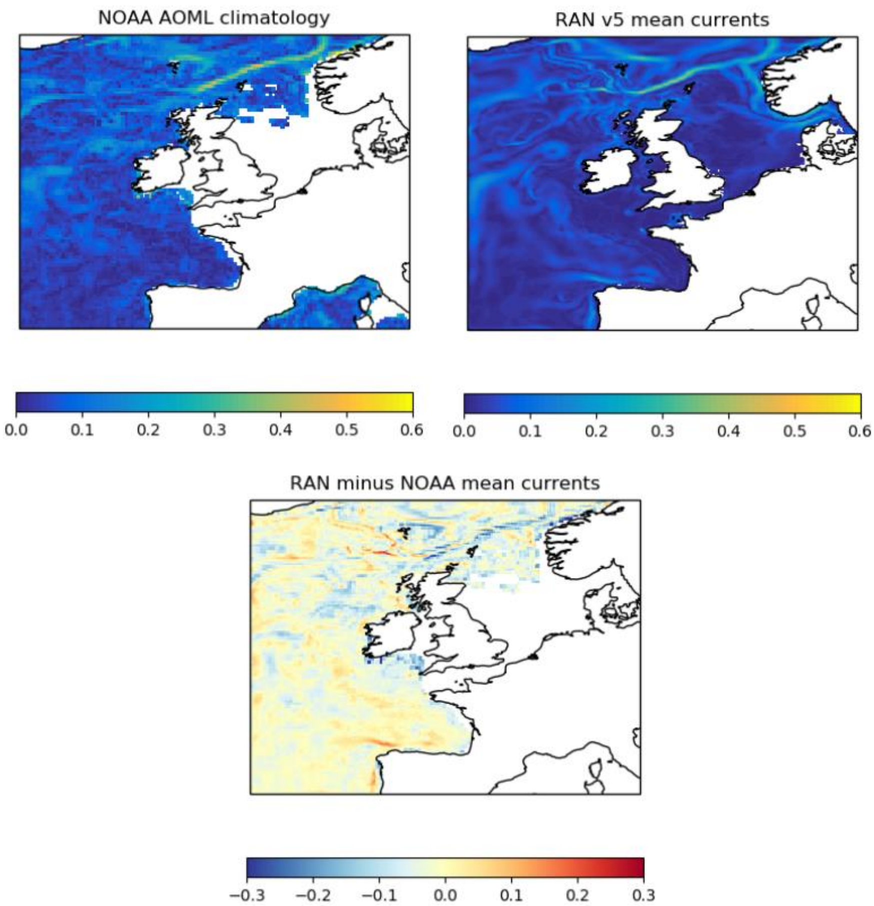

Figure 30: Mean current speed (m/s) at 15 m depth for NOAA AOML climatology, AMM7 V5 RAN 1993-2019 and the difference (RAN minus NOAA).

An assessment is provided of the performance of the V5 reanalysis in simulating tide amplitude and phase. The hourly Sea Surface Height (SSH) fields are not provided as a reanalysis product, but their assessment here gives confidence in the overall dynamical performance of the model. Hourly SSH was analysed against tide gauges for the dominant tidal constituents over the North West Shelf, for the period 1993-2017.

Some quantitative validation is possible using drifter data available from published sources (Bailly du Bois et al, 2011, Badewein et al, 2017, Carrasco et al, 2017 & 2018, Meyerjürgens et al 2019). These provide location data for drifting buoys for short periods in March 2007, Summer 2015, June 2018 and various months in 2017. The majority of these are in the German Bight. The 2007 data is just North of Cherbourg. Currents are estimated from the shift in the buoy locations over 25-hour periods, and compared against reanalysis currents for the same 25-hour periods. The choice of 25 hours instead of 24 acts to reduce any residual signal from tides.

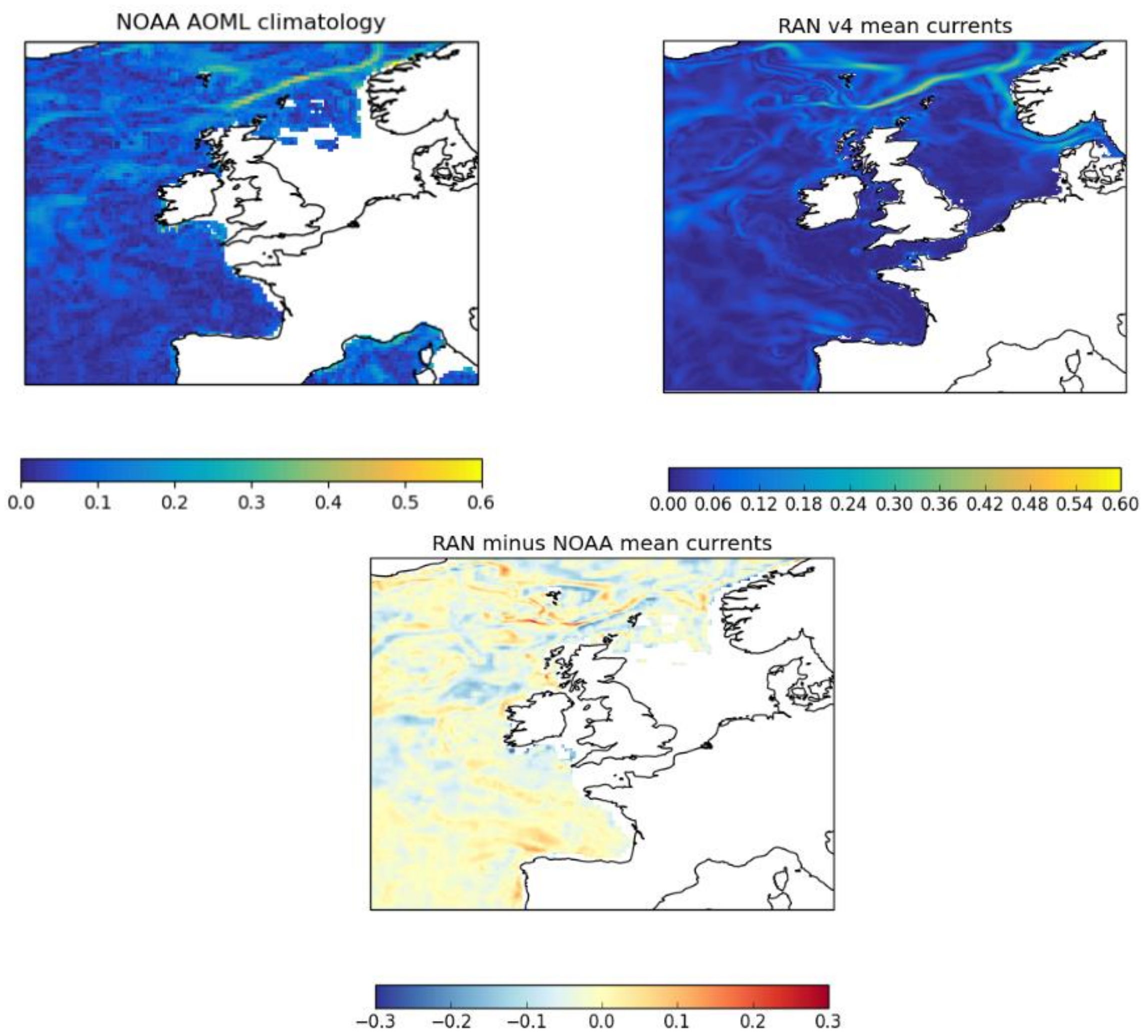

Figure 31: Mean current speed (m/s) at 15 m depth for NOAA AOML climatology, AMM7 V4 RAN 1992-2018 and the difference (RAN minus NOAA).

Figure 32 shows a scatter plot of zonal and meridional (U and V) components of current, drifter vs V5 reanalysis, for all the data. Statistics for V4 and V5 are in Table 4. Overall there is a positive correlation between drifters and reanalysis (for V5, 0.55 for U and 0.75 for V). The statistics for V5 are slightly improved over those for V4.

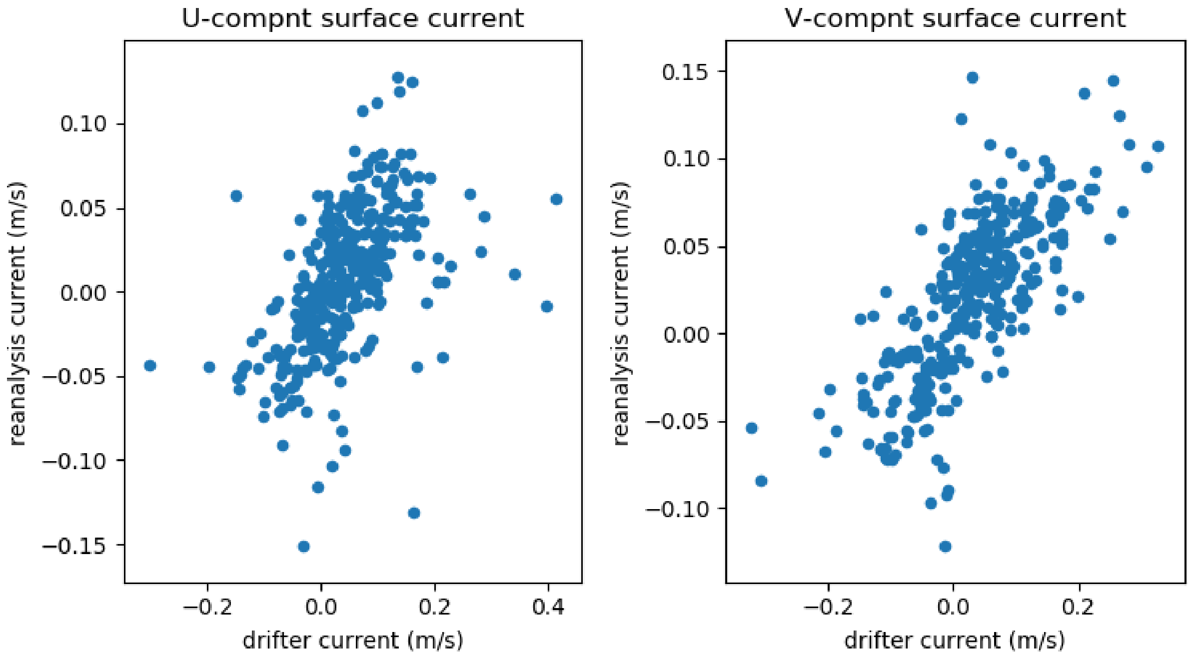

Figure 32: Scatter plot of 25-hour mean currents, drifter vs AMM7 V5 reanalysis, U and V components

Table 6: Statistics for current, reanalysis (V4 and V5) minus drifter 25-hour means

	AMM7 V4 minus Drifters		AMM7 V5 minus Drifters	
(m/s)	U	V	U	V
mean	-0.033	-0.013	-0.037	-0.008
rmsd	0.079	0.067	0.079	0.065
correlation	0.51	0.73	0.55	0.75
RMS vector wind difference	0.104		0.102	

Hourly surface currents are validated against estimates from radar (CMEMS product INSITU_GLO_UV_L2_REP_OBSERVATIONS_013_044) and RMS vector differences by hour are plotted in Figure 33. RMSD values are consistent with validation of the daily fields against drifters. The spike at 00Z is likely due to the increased volume of data recorded at that time.

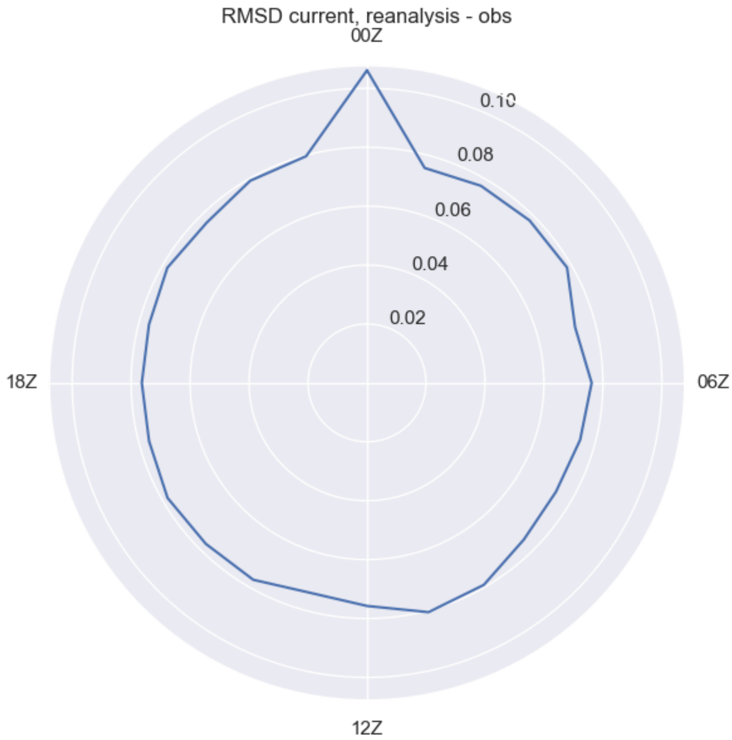

Figure 33 RMS vector current differences (m/s), reanalysis minus radar estimates, plotted against time of day

IV.3.1 Currents for Interim updates

It is difficult to assess the quality of the INT currents without extensive observation data. It is though possible to check for gross errors by comparing mean INT currents for July-December 2020 against RAN currents for July-December 2019. Figure 34 shows the Vector RMSD for the monthly mean surface currents. There are differences in the deeper Atlantic. This can be expected when comparing different years. On the Shelf, there is generally close agreement.

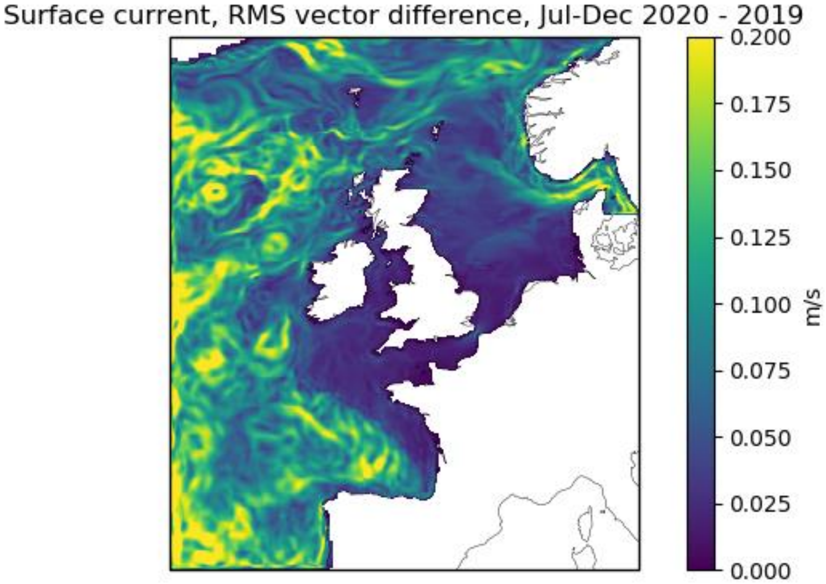

Figure 34 RMS vector difference in monthly means, surface current for July-Dec 2020 (INT) minus July-Dec 2019 (RAN)

IV.4 Tidal analysis

An assessment is provided of the performance of the V5 reanalysis in simulating tide amplitude and phase. Tides for the interim monthly updates are not assessed due to the short length of the run for deriving harmonic information. The hourly Sea Surface Height (SSH) fields are not provided as a reanalysis product, but their assessment here gives confidence in the overall dynamical performance of the model. Hourly SSH was analysed against tide gauges for the dominant tidal constituents over the North West Shelf, for the period 1993-2017. Observations are tide gauge data from National Oceanography Centre (NOC) Marine Data Products and the British Oceanographic Data Centre (BODC). V5 is compared against V4. Only plots of M2, S2 and K2 are presented for the sake of brevity. Figure 35 compares V5 and V4 against observations for amplitude and phase for tidal component M2. Figure 36 gives a spatial map of the relative errors between both versions. There is improvement in amplitude along the eastern coast of the UK, although phase is very slightly worse in the same locations.

Figure 37 and Figure 38 show the spatial map and amplitude/phase comparison for component S2. Here the improvements in amplitude are in the Bristol Channel, southern Irish Sea, around the Channel Islands and also off North-East Scotland.

For K2 the impact of V5 over V4 is mixed, in both amplitude and phase (Figure 39 and Figure 40).

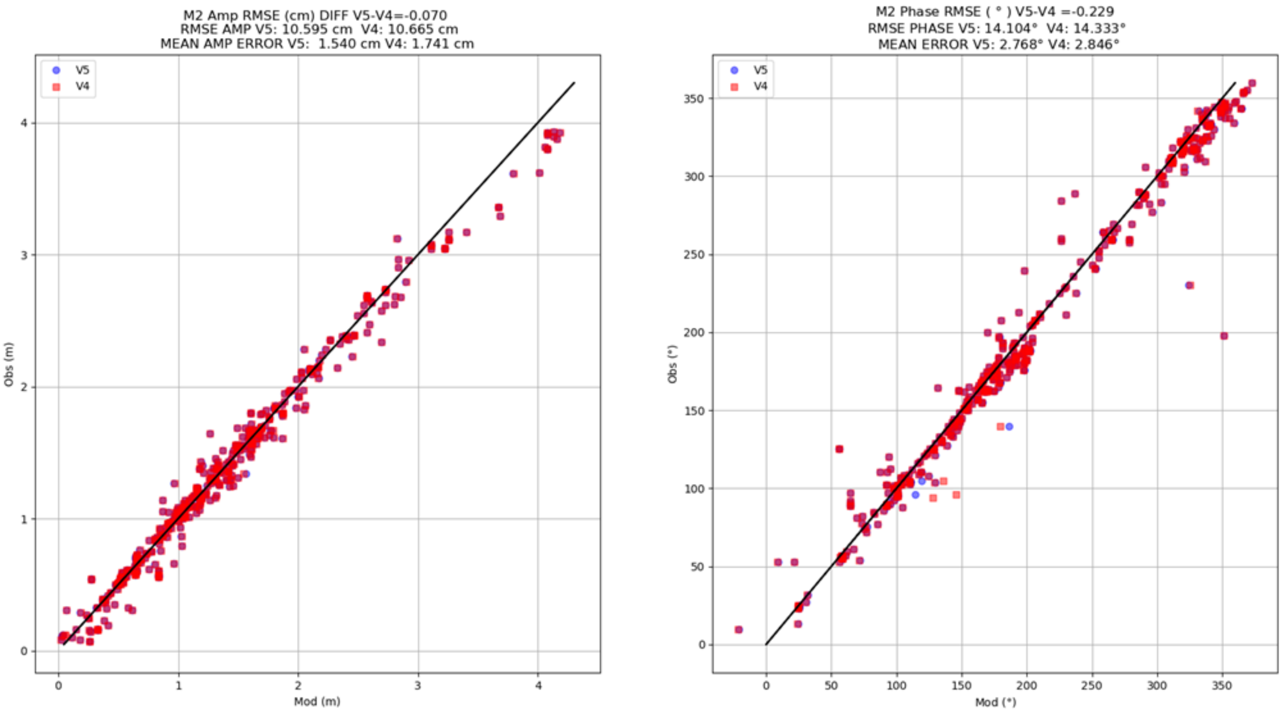

Figure 35: M2 elevation, V5 (blue) vs V4 (red). Left plot: Amplitude. Right plot: Phase.

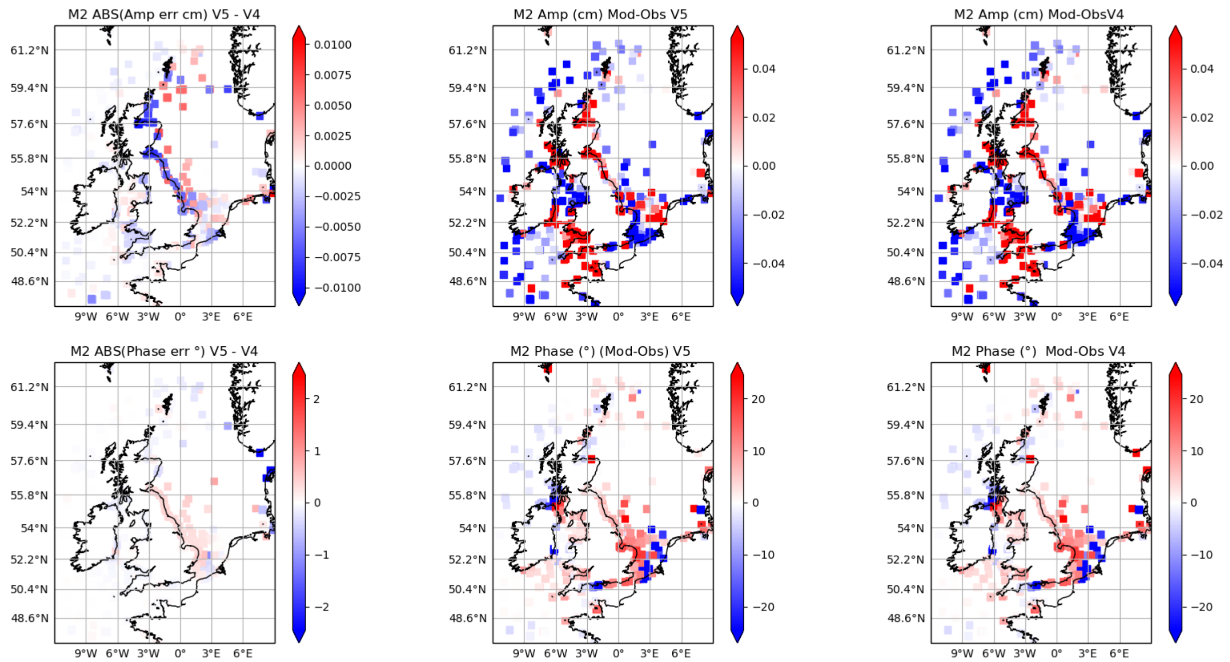

Figure 36: Spatial comparison of M2 amplitude (top row) and phase (bottom row) errors compared to observations between V5 and V4. Left column is a difference of the absolute error (V5-V4), blue=> V5 improvement. Middle column is V5 Error, and right column is V4 error

.

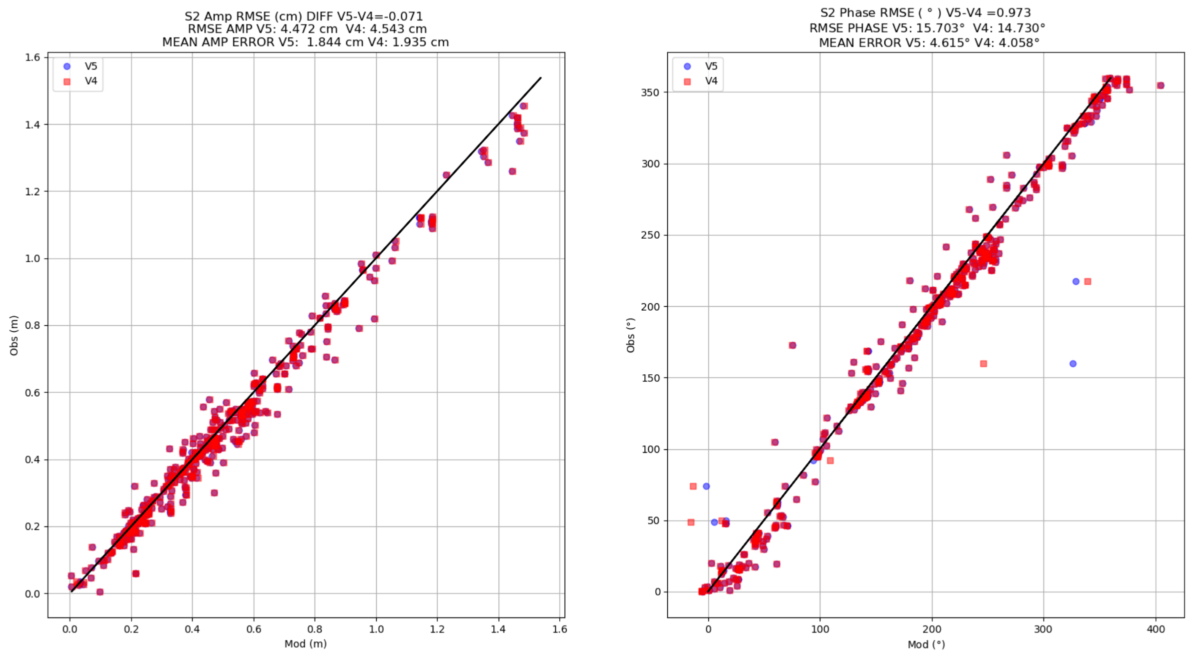

.

Figure 37: S2 elevation V5 (Blue) Vs. V4 (Red). Amplitude left and phase right

.

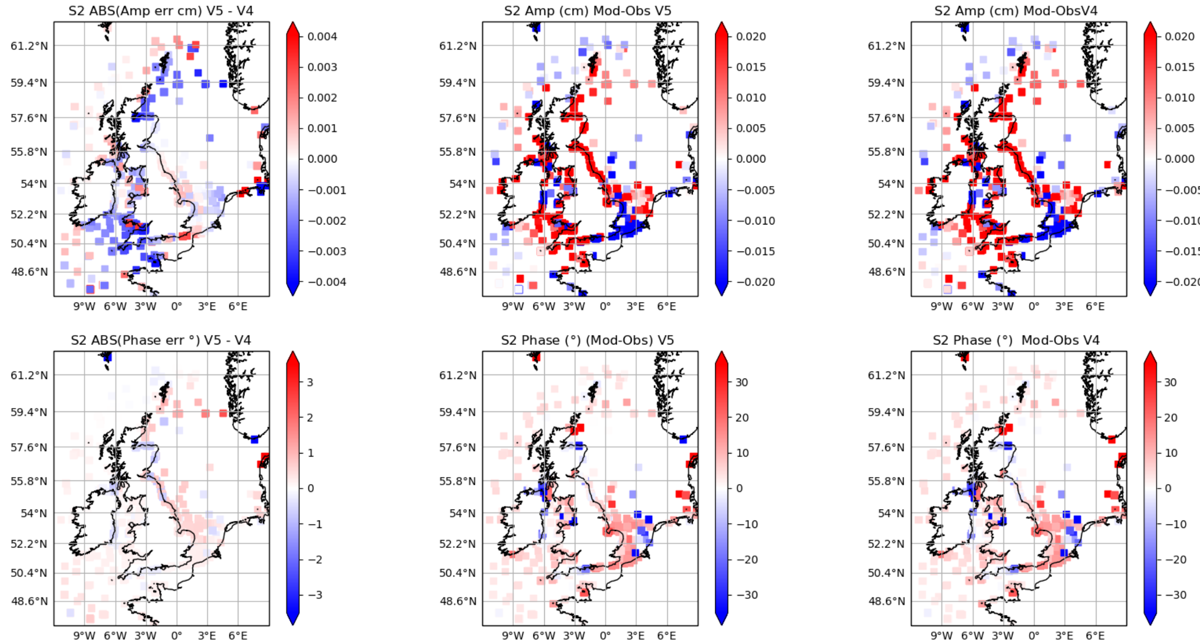

Figure 38: Spatial comparison of S2 amplitude (top row) and phase (bottom row) errors compared to observations between V5 and V4. Left column is a difference of the absolute error (V5-V4), blue=> V5 improvement. Middle column is V5 Error, and right column is V4 error

.

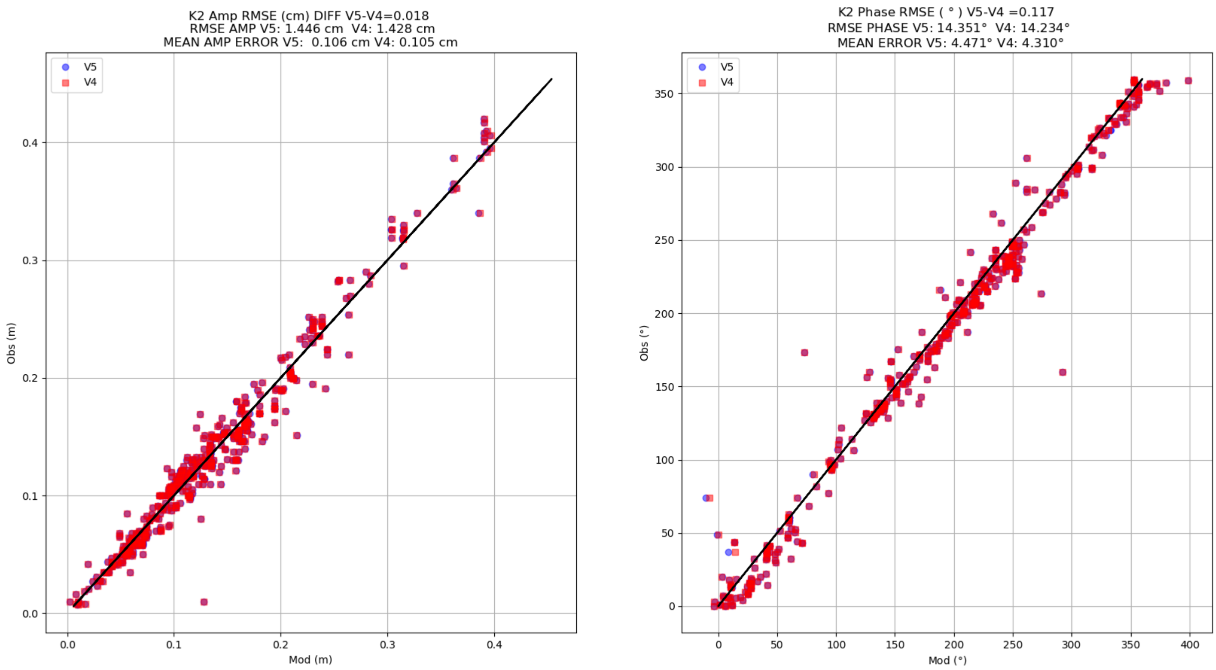

Figure 39: K2 elevation V5 (Blue) Vs. V4 (Red). Amplitude left and phase right

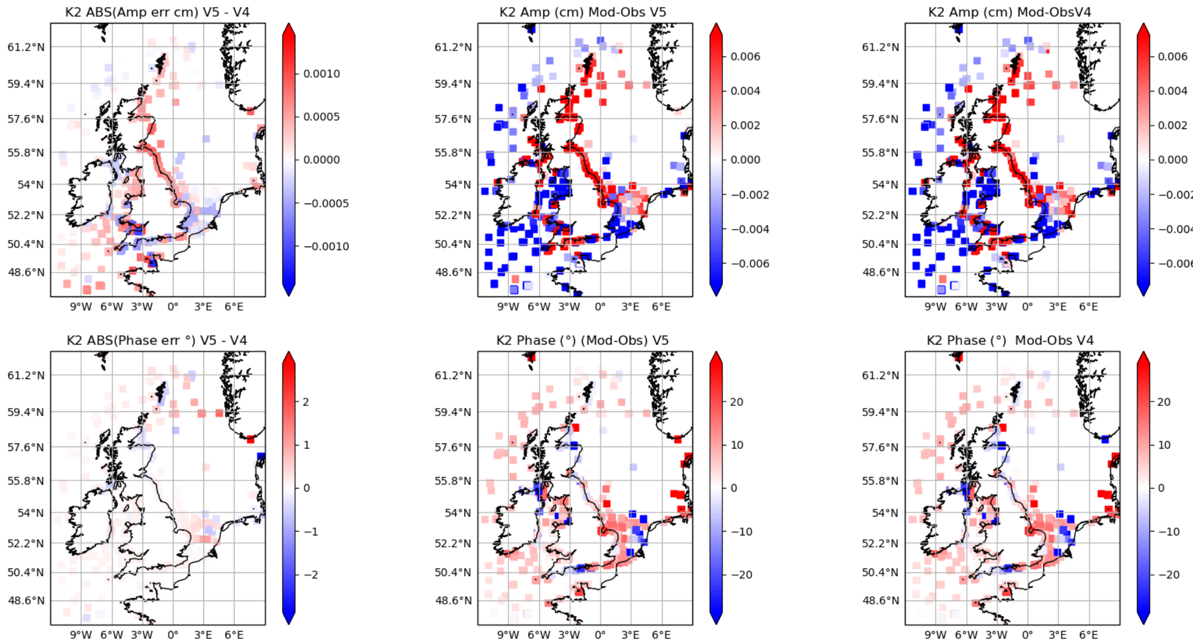

Figure 40: Spatial comparison of K2 amplitude (top row) and phase (bottom row) errors compared to observations between V5 and V4. Left column is a difference of the absolute error (V5-V4), blue=> V5 improvement. Middle column is V5 error, and right column is V4 error.

Statistics for some of the principal constituents are summarised in Table 7. Both the phase and amplitude have improved for the dominant constituents.

Table 7: RMSD and Bias, V4 and V5 minus observations, for amplitude and phase of various tidal components.

	Amplitude (cm)				Phase (°)			
	RMSD		Bias		RMSD		Bias	
	V4	V5	V4	V5	V4	V5	V4	V5
M2	10.66	10.59	1.74	1.54	14.33	14.10	2.85	2.77
S2	4.54	4.47	1.93	1.84	14.73	15.70	4.06	4.61
K2	1.43	1.45	0.10	0.11	14.23	14.35	4.31	4.47
N2	3.50	3.52	1.01	1.04	25.92	26.08	4.33	4.39
O1	1.81	1.83	-1.27	-1.29	20.13	20.17	-3.07	-3.00
K1	1.78	1.80	0.54	0.54	16.54	16.88	-4.48	-4.88
P1	0.72	0.73	0.31	0.29	17.86	17.78	0.91	0.43

IV.5 Mixed layer depth

The V5 reanalysis outputs a modified version of the Kara Mixed Layer Depth (MLD) (Kara et al. 2000) which uses a reference depth at 3 m instead of 10 m and a delta T of +0.8K. We compare the V5 MLDs to observed MLDs calculated from the quality controlled temperature and salinity profile database EN4 (Good et al. 2013) using the same algorithm employed in the V5 reanalysis.

Each EN4 MLD is calculated from measurements taken over the duration of the profile observation and so corresponds to MLD conditions at that time. Ideally, we would compare the EN4 MLD to the V5 MLD calculated at the observation time. However, these data are not available for post-processing validation. We compare the observations to daily (25-hour) mean V5 MLDs, since this removes most of the tidal variation from the V5 MLDs and avoids introducing errors from mis-matched observation/model times. For each EN4 MLD, we extract a corresponding V5 MLD at the nearest model grid point and on the date of the observation. By using reanalysis data only for the locations and the days of observations, we minimise potential analysis biases due to gaps in space and time in the sparse observations.

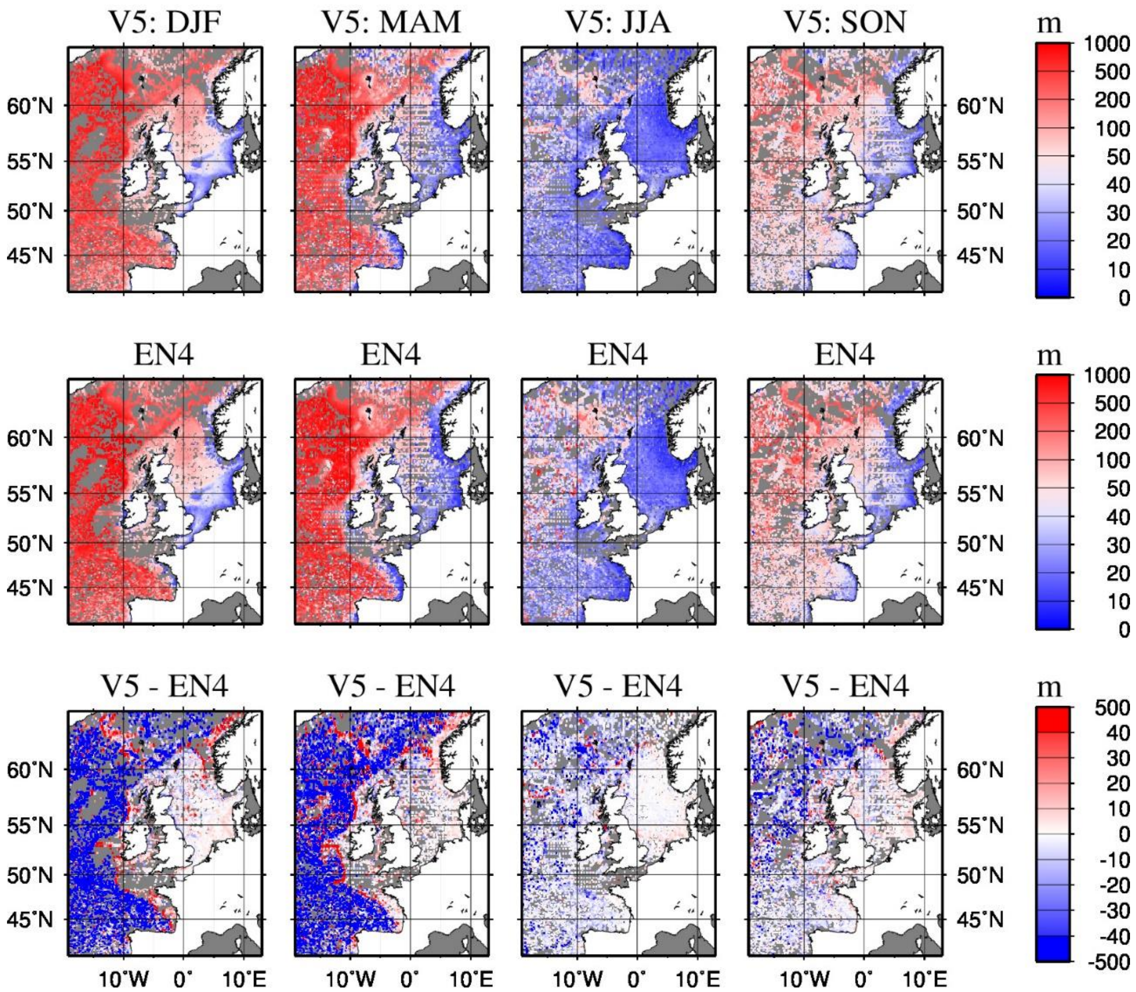

Figure 41: Seasonal mean MLD for the reanalysis (V5, top), derived from EN4 profiles (middle) and the mean bias (bottom) for column 1: December, January and February (DJF); column 2: March, April and May (MAM); column 3: June, July and August (JJA); and column 4: September, October and November (SON).

Seasonal mean MLDs for 1993 to 2019 are calculated from co-located reanalysis and observed data (Figure 41). The V5 MLDs show good spatial agreement with the EN4 MLDs on seasonal timescales, capturing the deep permanent thermocline off-shelf in winter and spring and the transition to seasonal MLD for summer. In the winter and spring, V5 underestimates the MLD in the deeper ocean by an average of ~89 m, reducing to ~22 m during summer and ~19 m in autumn. Biases are generally smaller on the shelf, reflecting the shallower mixed depths on the shelf. They range from shelf-mean bias of ~3 m too deep in winter to ~1 m too shallow in summer.

When averaged over the NWS region (depths < 200 m), the V5 MLDs capture the seasonal signal displayed by EN4 MLDs (Figure 42). Mean bias is on average less than 0.5 m, with V5 MLD being generally too shallow compared to EN4 MLD. Root Mean Square (RMS) differences average ~15 m. Biases and RMS differences are smallest in the summer months (June to August) and increase in the stratification onset period during spring (Figure 43). Correlation coefficients (Figure 42) between NWS EN4 and V5 MLDs for each month are variable, ranging from 0.2 to greater than 0.9, with an average of ~0.8, showing fair spatial correlation on monthly time scales.

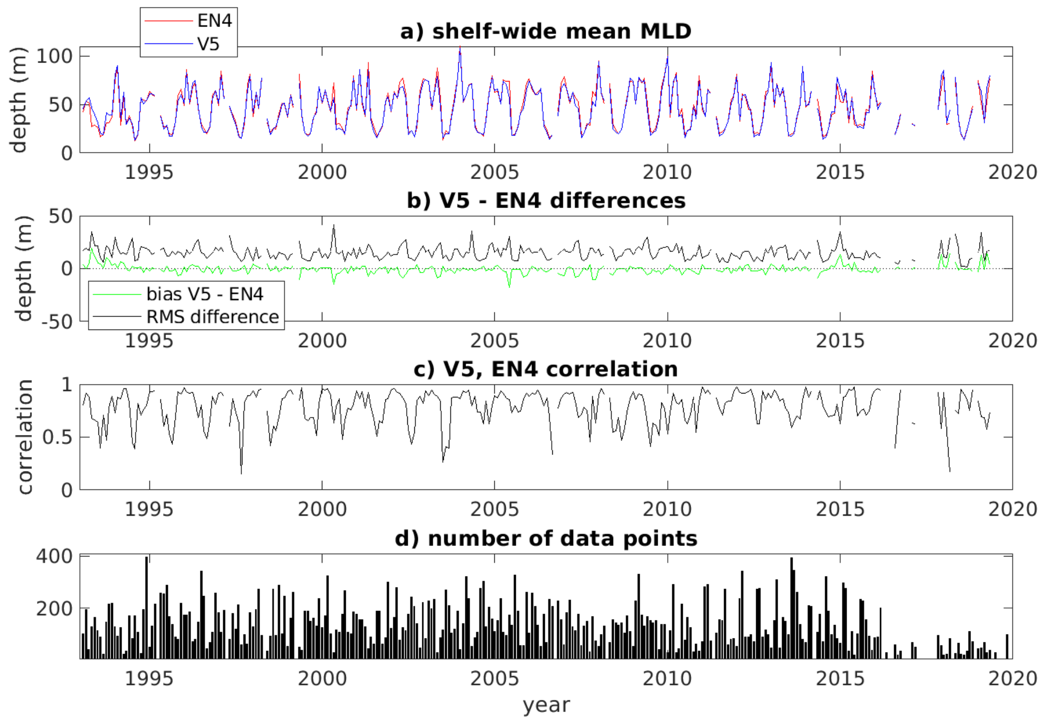

Figure 42: Time series of a) monthly mean MLD integrated over the NWS from the reanalysis (V5) and derived from EN4 data; b) the bias (reanalysis minus observation) and RMS difference; c) correlation between the reanalysis and observations and d) the number of data points.

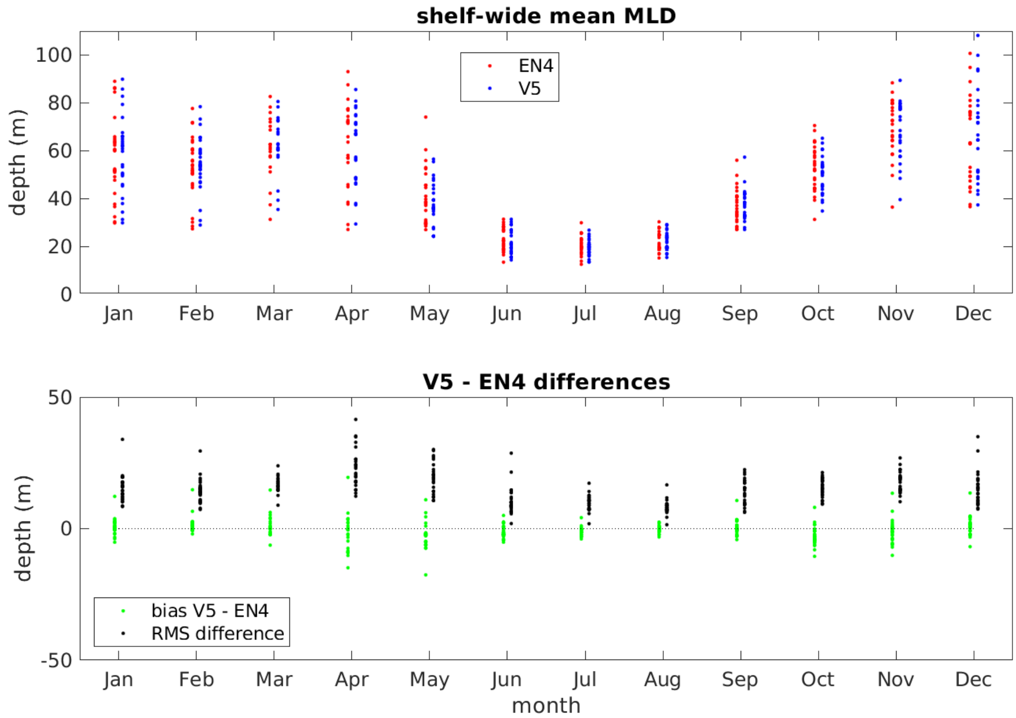

Figure 43: Monthly mean MLD integrated over the NWS from the reanalysis (V5) and derived from EN4 data, plotted as an annual cycle with one data point for each month during 1993 to 2019 (top), and the corresponding mean biases and RMS differences (bottom).

A similar comparison for hourly MLD fields is shown, by hour, in Figure 44. RMSD values vary between 20 m and 25 m, slightly higher than for the longer period means.

MLD isn't assessed for INT because of the small number of suitable mooring data for this short period.

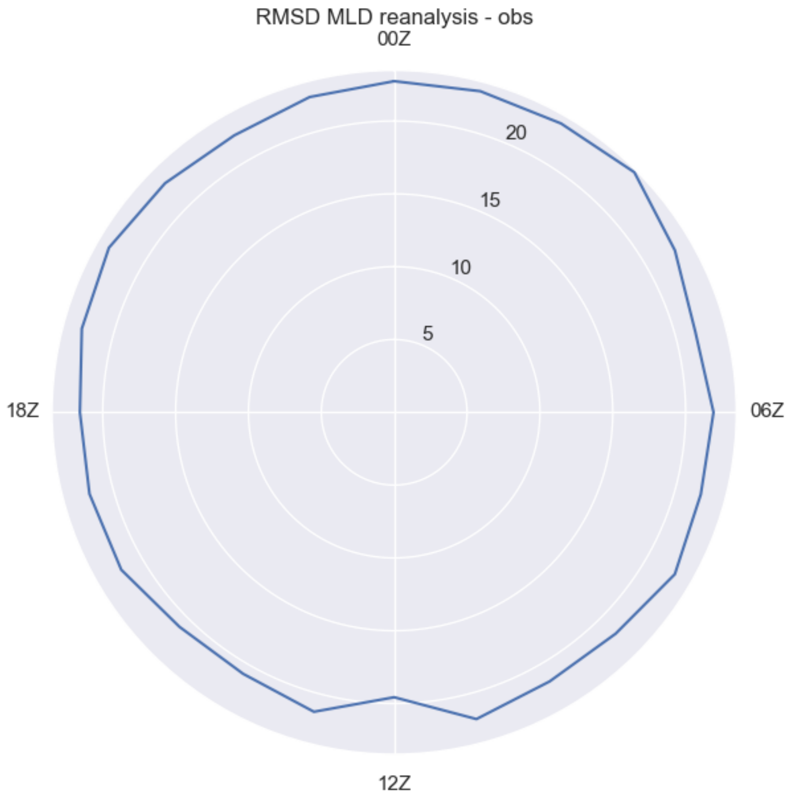

Figure 44 RMSD mixed layer depth (m), reanalysis minus estimates from EN4 profiles, plotted against time of day

V SYSTEM'S NOTICEABLE EVENTS, OUTAGES OR CHANGES

Baltic boundary conditions (temperature, salinity and currents) were taken from BALTICSEA_REANALYSIS_PHY_003_011. Baltic boundary conditions weren't available for the last 6 months of 2019, and so values from 2018 were used.

V5.1 Interim monthly updates were added.

RAN was rerun for Oct 2018 to Dec 2019 to take advantage of now available Baltic RAN boundary conditions (and PFT chlorophyll observations for the biogeochemistry).

RAN was extended for the period Jan-June 2020, using Baltic boundary conditions from the NRT product BALTICSEA_ANALYIS_FORECAST_PHY_003_006.

The quality of the RAN rerun (Oct 2018-Dec 2019) and extension was assessed and was found to be consistent with the quality assessment in this document.

Hourly fields of surface temperature, salinity, currents, and of sea surface height and mixed layer depth, are added to the catalogue in December 2021.

VI QUALITY CHANGES SINCE PREVIOUS VERSION

The current version V5 of the reanalysis (NWSHELF_MULTIYEAR_PHY_004_009) is here compared to the previous version V4.

Validation shows mixed impacts relative to V4. For surface and near-surface temperature (IV.1), biases in V4 and V5 are similar. For 30-80m depth, V5 has increased RMSD during the summer months. The generally cold bias of V4 for the Norwegian Sea has been reduced, and for the deeper ocean South of 50ºN the warm bias of V4 becomes a slightly cold bias in V5. The cold bias in the southern Irish Sea and the warm bias in the southern North Sea are both larger. For the layer 800-2000m, V5 has overall improved bias. Below 2000m (Bay of Biscay and further out into the Atlantic) there is a shift to a warm bias in V5 which is confirmed in the comparison against other members of the multi-model ensemble.

For salinity (IV.2), the fresh bias above 80 m in the Norwegian Sea that occurred in V4 persists in V5. However, V5 has improved on the isolated regions of fresh biases west of 10°W that occurred in V4. V5 is too salty in the Irish and Celtic Seas and shallower than 30 m in the Norwegian Trench with increased biases from V4. The Bay of Biscay deeper than 2000 m is also too salty in V5.

In 2021 the reanalysis was extended to add January to June 2020. It will continue to be extended every 6 months. The period October 2018 to December 2019 was also rerun, replacing a climatology on the Baltic boundary with values from the Baltic reanalysis when they became available (consistent with what was used for 1993-2018), and from the Baltic NRT product BALTICSEA_ANALYSISFORECAST_PHY_003_006 for January to June 2020.

The quality of this 2018/19 rerun and 2020 extension was assessed and was found to be similar to previous years. Further extensions will be assessed in the same way.

VII ACKNOWLEDGEMENTS

We would like to thank and acknowledge:

Nico Bruneau (NOC), initial testing and tuning of NEMO

Sonja Van Leeuwen (NIOZ), Helen Powley & Yuri Artioli (PML), for providing the rivers dataset

ECMWF reanalysis team for the ERA5 atmospheric forcing,

BALTIC MFC for providing boundary conditions on the Baltic boundary,

Simon Good, Mark Worsfold, Rachel Killick, Chris Atkinson (Met Office) for assistance with observation datasets,

Rob King, James While, Matt Martin (Met Office) for assistance with setting up the reanalysis system and the data assimilation,

Jonathan Tinker (Met Office) for advice through the project and for review of this document.

VIII REFERENCES

Atkinson, C. P., N. A. Rayner, J. J. Kennedy, and S. A. Good (2014), An Integrated Database of Ocean Temperature and Salinity Observations, J. Geophys. Res. Oceans, 119, 7139-7163, https://doi.org/10.1002/2014JC010053

Badewien, Thomas H; Braun, A, Butter, M, Chojnowski, M J; Götz, , Herold, J-M, Jeuk, J, Meyerjürgens, J, Müller, J, Weil S-S (2017): Track of GPS-Drifter ICBM_E1703_015 in the southern North Sea. Institute for Chemistry and Biology of the Marine Environment, Carl-von-Ossietzky University of Oldenburg, Germany, PANGAEA, https://doi.org/10.1594/PANGAEA.873950

Bailly du Bois, P, Dumas, F; Solier, L; Voiseux, C (2011): DISPRO drifter 72878 trackline. PANGAEA, https://doi.org/10.1594/PANGAEA.762193

Bloom S.C., Takacs, L.L., Da Silva A.M., Ledvina, D., (1996) Data assimilation using incremental analysis updates, Monthly Weather Review, 124, 1256-1271.

Carrasco, R, Horstmann, J (2017): Track of GPS-Drifter HE445/DRIFT-1 in the German Bight. Helmholtz-Zentrum Geesthacht Centre for Materials and Coastal Research, PANGAEA, https://doi.org/10.1594/PANGAEA.874383

Carrasco, R, Floeter, J, Horstmann, J (2017): Track of GPS-Drifter from HEINCKE cruise HE490, Drifter 1. Helmholtz-Zentrum Geesthacht Centre for Materials and Coastal Research, Institut für Hydrobiologie und Fischereiwissenschaften, Universität Hamburg, PANGAEA, https://doi.org/10.1594/PANGAEA.882324

Carrasco, R, John, U, Henkel, R, Horstmann, J (2018): North Sea surface drifter data from Heincke cruise HE513, Drifter 17. Helmholtz-Zentrum Geesthacht Centre for Materials and Coastal Research, Alfred Wegener Institute, Carl von Ossietzky University Oldenburg, PANGAEA, https://doi.org/10.1594/PANGAEA.896383

Flather, R. A., (1976): A tidal model of the northwest European continental shelf. Memoires de la Societe Royale de Sciences de Liege, 6, 141-164.

Flather R. A. (1981). "Results from a model of the north east Atlantic relating to the Norwegian Coastal Current". The Norwegian Coastal Current (Proceedings from the...symposium, Geilo, 9-12 September 1980). Bergen: Bergen University, 2, 427-458

Good S.A., Martin M.A., and Rayner N.A., (2013) EN4: quality controlled ocean temperature and salinity profiles and monthly objective analyses with uncertainty estimates, JGR: Oceans, 118, 6704-7616. doi:10.1002/2013JC009067

Hersbach, H, Bell, B, Berrisford, P, et al. The ERA5 global reanalysis. Q J R Meteorol Soc. 2020; 146: 1999– 2049. https://doi.org/10.1002/qj.3803

Holt, J., S. Hughes, J. Hopkins, S. L. Wakelin, N. Penny Holliday, S. Dye, C. González-Pola, S. S. Hjøllo, K. A. Mork, G. Nolan, R. Proctor, J. Read, T. Shammon, T. Sherwin, T. Smyth, G. Tattersall, B. Ward, and K. H. Wiltshire (2012), Multi-decadal variability and trends in the temperature of the northwest European continental shelf: A model-data synthesis, *Progress in Oceanography*, *106*, 96-117.

Huthnance, J. M., (1984): Slope Currents and “JEBAR”. J. Phys. Oceanogr., 14, 795–810.

Kara, A. B., P. A. Rochford, and H. E. Hurlburt (2000), An optimal definition for ocean mixed layer depth, J. Geophys. Res., 105(C7), 16803–16821, doi:10.1029/2000JC900072.

Large W, Yeager S (2004) Diurnal to decadal global forcing for ocean and seaice models: the data sets and climatologies. Technical Report TN-460+STR, NCAR, 105

Large, W., Yeager, S., (2009): The global climatology of an interannually varying air-sea flux data set. Clim. Dynamics, 33:341–364, DOI 10.1007/s00382-008-0441-3

Lenhart, H-J., Mills, D., Baretta-Bekker, H., van Leeuwen, S., van der Molen, J., Baretta, J.W., Blaas, M., Desmit, X., Kühn, W., Lacroix, G., Los, H.J., Ménesguen, A., Neves, R., Proctor, R., Ruardij, P., Skogen, M.D., Vanhoutte-Brunier, A., Villars, M.T., Wakelin, S.L., Predicting the consequences of nutrient reduction on the eutrophication status of the North Sea, Journal of Marine Systems, Volume 81, 2010, Pages 148-170, ISSN 0924-7963, https://doi.org/10.1016/j.jmarsys.2009.12.014

Laurindo, L., A. Mariano, and R. Lumpkin, 2017: An improved near-surface velocity climatology for the global ocean from drifter observations Deep-Sea Res. I, 124, pp.73-92, doi:10.1016/j.dsr.2017.04.009 .

MacLachlan, C., Arribas, A., Peterson, D., Maidens, A., Fereday,D., Scaife, A.A., Gordon, M., Vellinga, M., Williams, A., Comer, R.E., Camp, J., and Xavier, P., (2014): Global Seasonal Forecast System 5 (GloSea5): a high resolution seasonal forecast system, Q. J. Roy. Meteor. Soc.

Madec G., Delecluse P., Crépon M., Lott F., (1996) Large-Scale Preconditioning of Deep-Water Formation in the Northwestern Mediterranean Sea. Journal of Physical Oceanography, 26(8), 1393-1408.

Madec, G. and the NEMO team (2016) NEMO ocean engine. Note du Pôle de modélisation, Institut Pierre-Simon Laplace (IPSL), France, No 27 ISSN No 1288-1619.

Merchant C.J., Embury O., Roberts-Jones J., Fiedler E., Bulgin C.E., Corlet G.K., Good S., McLaren A., Rayner N., Morak-Bozzio S., Donlon C., (2014) Sea surface temperature datasets for climate applications from Phase 1 of the European Space Agency Climate Change Initiative (SST CCI), Geoscience Data Journal, Vol. 1 , Issue 2: 179-191. DOI: 10.1002/gdj3.20

Meyerjürgens, J., Badewien, T.H., Zielinski, O., Braun, A., Butter, M. (2019): Track of GPS-Drifter North_Sea_Drifter1 in the German Bight, Southern North Sea. Institute for Chemistry and Biology of the Marine Environment, Carl-von-Ossietzky University of Oldenburg, Germany, PANGAEA, https://doi.org/10.1594/PANGAEA.897989

Mogensen, K. S., Balmaseda, M. A., and Weaver, A.: The NEMOVAR ocean data assimilation system as implemented in the ECMWF ocean analysis for System 4, ECMWF Tech. Memo. 668., 2012.

Siddorn, J., Furner R. (2013): An analytical stretching function that combines the best attributes of geopotential and terrain-following vertical coordinates, Ocean Modelling, 66, 1-13

Siddorn, J., Furner R. (2013): An analytical stretching function that combines the best attributes of geopotential and terrain-following vertical coordinates, Ocean Modelling, 66, 1-13

Siddorn, J., Furner R. (2013): An analytical stretching function that combines the best attributes of geopotential and terrain-following vertical coordinates, Ocean Modelling, 66, 1-13

Sterlini, P., D. Le Bars, H. de Vries, and N. Ridder (2017), Understanding the spatial variation of sea level rise in the North Sea using satellite altimetry, JGR Oceans, 122, 6498-6511, doi:10.1002/2017JC012907

Smyth, T.J., Hardman-Mountford, N., Frost, M., Fishwick, J.R. (2011) Temperature and salinity from time series station L4 in the western English Channel from 1988 to 2011. Plymouth Marine Laboratory, doi:10.1594/PANGAEA.757204

Smyth, T.J., Hardman-Mountford, N., Frost, M., Fishwick, J.R. (2012) Temperature and salinity profiles at 10 m depth resolution from time series station E1 in the western English Channel from 1903 to 2011. doi:10.1594/PANGAEA.775761

Umlauf, L., Burchard, H., (2003). A generic length-scale equation for geophysical turbulence models. Journal of Marine Research 61, 235–265.

Vörösmarty, J., P. Green, J. Salisbury, R. B. Lammers (2000) Global Water Resources: Vulnerability from Climate Change and Population Growth. Science 289, 284-288; DOI: 10.1126/science.289.5477.284.

Young, E. F., Holt, J. T.: Prediction and analysis of long-term variability of temperature and salinity in the Irish Sea.(2007) JGR Oceans, 112, C1, 1-18, doi:10.1029/2005JC003386,

Zalesak, S. T., (1979) Fully Multidimensional Flux-Corrected Transport Algorithms for Fluids, J. Comput. Phys., 31, 335–362.